INERT GAS DILUTION EFFECT ON FLAMMABILITY LIMITS OF HYDROCARBON MIXTURES

A Dissertation

by

FUMAN ZHAO

Submitted to the Office of Graduate Studies of
Texas A&M University
in partial fulfillment of the requirements for the degree of

DOCTOR OF PHILOSOPHY

December 2011

Major Subject: Chemical Engineering

INERT GAS DILUTION EFFECT ON FLAMMABILITY LIMITS OF HYDROCARBON MIXTURES

A Dissertation

by

FUMAN ZHAO

Submitted to the Office of Graduate Studies of
Texas A&M University
in partial fulfillment of the requirements for the degree of

DOCTOR OF PHILOSOPHY

Approved by:

Chair of Committee,	M. Sam Mannan
Committee Members,	Kenneth R. Hall
	Zhengdong Cheng
	Debjyoti Banerjee
Head of Department,	Charles Glover

December 2011

Major Subject: Chemical Engineering

ABSTRACT

Inert Gas Dilution Effect on Flammability Limits of

Hydrocarbon Mixtures. (December 2011)

Fuman Zhao, B.S., University of Tianjin;

M.S.; M.S., Texas A&M University

Chair of Advisory Committee: Dr. M. Sam Mannan

Flammability limit is a most significant property of substances to ensure safety of chemical processes and fuel application. Although there are numerous flammability literature data available for pure substances, for fuel mixtures these are not always available. Especially, for fuel mixture storage, operation, and transportation, inert gas inerting and blanketing have been widely applied in chemical process industries while the related date are even more scarce.

Lower and upper flammability limits of hydrocarbon mixtures in air with and without additional nitrogen were measured in this research. Typically, the fuel mixture lower flammability limit almost keeps constant at different contents of added nitrogen. The fuel mixture upper flammability limit approximately linearly varies with the added nitrogen except mixtures containing ethylene. The minimum added nitrogen concentration at which lower flammability limit and upper flammability limit merge together is the minimum inerting concentration for nitrogen, roughly falling into the range of 45±10 vol % for all the tested hydrocarbon mixtures.

Numerical analysis of inert gas dilution effect on lower flammability limit and upper flammability limit was conducted by introducing the parameter of inert gas dilution coefficient. Fuel mixture flammability limit can be quantitatively characterized using inert gas dilution coefficient plus the original Le chatelier's law or modified Le Chatelier's law.

An extended application of calculated adiabatic flame temperature modeling was proposed to predict fuel mixture flammability limits at different inert gas loading. The modeling lower flammability limit results can represent experimental data well except the flammability nose zone close to minimum inerting concentration.

Le Chatelier's law is a well-recognized mixing rule for fuel mixture flammability limit estimation. Its application, unfortunately, is limited to lower flammability limit for accurate purpose. Here, firstly a detailed derivation was conducted on lower flammability limit to shed a light on the inherent principle residing in this rule, and then its application was evaluated at non-ambient conditions, as well as fuel mixture diluted with inert gases and varied oxygen concentrations. Results showed that this law can be extended to all these conditions.

ACKNOWLEDGEMENTS

I would like to acknowledge and thank my dissertation advisor and committee chair, Dr. M. Sam Mannan, for his guidance, advice, and encouragement throughout this research project. Also, I appreciate the sharing of his experience in research and industries, which has been shedding me with numerous lights on engineering and life. I will always remember the scholarly and familial environment that he created in my graduate education in Mary Kay O'Connor Process Safety Center.

I would like to express my appreciation to my committee members, Dr. Kenneth R. Hall, Dr. Zhengdong Cheng, and Dr. Debjyoti Banerjee for their supports, counsels, suggestions, availabilities and commitments.

I thank Dr. Hans J. Pasman and Dr. William J. Rogers for their friendly, insightful, detailed directions and comments of my research and experiment conductions.

A special thank you goes to my family for their love, support, encouragement, and patience. It is to you that I dedicate this dissertation and to whom I owe all that I have achieved.

To the colleagues in Mary Kay O'Connor Process Safety Center and many friends who helped and encouraged me throughout my scholastic pursuits, your efforts and kindness will always be remembered and appreciated.

TABLE OF CONTENTS

Page

CHAPTER Page

CHAPTER Page

CHAPTER Page

Page

LIST OF FIGURES

FIGURE Page

FIGURE Page

FIGURE Page

FIGURE Page

FIGURE Page

LIST OF TABLES

TABLE Page

CHAPTER I

INTRODUCTION

Flammable or combustible substances are prevalent in today's chemical and petrochemical industries. Accurate data on flammability limits are significant for safety processes. Flammability limits describe the composition of gas that can form propagating flames, and they are often provided with material safety data (MSDS) sheets. In industry, fire generally happens in the vapor or gas phase with a certain concentration in air. Compared with other fire safety properties, e. g, flash point, minimum ignition energy (MIE), autoignition temperature (AIT), flammability limit attract more attention from our engineers, and it is the most important safety specification that must be considered in assessing the overall flammability hazard potential of chemical substances in chemical process industry.

1.1 Motivations

The flammability limits are the most important safety specification that must be taken into account for assessing the overall fire and explosion hazard potential of chemical substances in storage, processing, and handling. Normally, the flammability data for pure fuels in ambient conditions are available in the literature, but for fuel mixtures, the flammability data are often inconsistent and deficient, especially

---

This dissertation follows the style of Journal of Hazardous Materials.

inadequately matched to the conditions of interest. Some of these conditions are the different initial temperature and pressure, varied oxygen concentrations, and dilution with inert gas. Obviously, with the many different combinations of gaseous fuel mixtures and diluents that may be encountered in numerous practical situations using inert gas purging, blanketing and inerting, it would be clearly valuable to have research in this area. Also, it is very important to develop guidelines to predict their lower flammability limits and upper flammability limits for fuel mixtures diluted with different inert gases based on knowledge the flammability limits of the individual combustibles and inert gas dilution capacities.

When processing flammable substances, ignitable fuel-air mixtures can develop in the vapor space above the liquid in storage tanks. There are a large variety of cases where internal gas explosion may occur, which are caused by uncontrolled leaks, or simply by accidental purging with air without inerting systems or tank inert blanketing system fails. The subsequent explosion can result in significant consequences. The most famous internal tank explosion case is the 1996 TWA Flight 800 disaster in which the center fuel tank exploded shortly after takeoff and resulted in the deaths of 230 people [1]. To effectively prevent fire or explosion taking place in fuel storage tanks with large volumes of flammables, inert gas blanketing treatment in storage or processing tanks has been recommended by the Federal Aviation authority (FAA) and the National Transport Safety Board (NTSB), and the inert gas dilution effect on flammability, thereby, has been recognized as an significant safety issue in the chemical process industries.

Recently some new concepts of fire suppression systems have been developed to prevent depletion of the stratospheric ozone layer. For many years, Halon 1301 was popularly recommended to be used as the effective fire suppressants for high-value assets. But, in 1989, the Montreal Protocol determined that halon possesses the potential to deplete the ozone layer, and the U.S. Environmental Protection Agency subsequently banned its manufacture in 1994some halon alternatives as clean fire-extinguishing agents have been developed. The clean agents are classified into two types: halocarbon agents and inert gas agents, in which the inert gas agents, mostly including nitrogen, carbon dioxide, and argon, are of interest, because they are not only non-ozone-depleting but also non-toxic and non-pyrolytic gases.

1.2 Objectives

In this research, nitrogen dilution effect on the lower flammability limit (LFL) and upper flammability limit (UFL) of low-carbon hydrocarbons (methane, ethane, propane, n-butane, ethylene, and propylene) and their binary mixtures were measured at ambient conditions. Because Le Chatelier's law is a well-recognized principle for fuel mixture flammability estimation, its applicability was verified by comparing its predictions with experimental measurements. In the case of additional nitrogen added to hydrocarbon mixture/air mixtures, modification of Le Chatelier's law was conducted on the numerical basis through the introduction of a new parameter, inert gas dilution coefficient. Next, a theoretical derivation of Le Chatelier's law was conducted with the assumption of constant flame temperature. Moreover, Le Chatelier's law's applicability was verified at

other conditions, e.g., at non-ambient conditions, fuel mixture with inert gas dilution and at different oxygen content. Finally, an adiabatic flame temperature was constructed and used to quantify inert gas dilution effect on fuel mixture flammability. Specifically, the objectives of this research are four-fold: (i) collecting experimental flammability data, and verifying the applicability of Le Chatelier's law on LFL and UFL with and without inert gas dilution; (ii) conduct the modification of Le Chatelier's law on a numerical basis; (iii) adiabatic flame temperature modeling on flammability limits with inert gas dilution; and (iv) deriving Le Chatelier's law and evaluating its application on a theoretical basis, where heat losses is considered as a general case.

1.3 Organization of dissertation

The first chapter of this dissertation presented the gap between the existing flammability data and the needs of the chemical industry. It has been an accepted fact that process hazards arouse a high intention to generate more flammability data of fuel mixtures to protect and preserve health and safety. Following that discussion, the objectives of this work were presented.

Some background on flammability properties, experimental methods to college flammability data and flammability modeling were presented in the second chapter.

Chapter III covered the experimental equipment and method. Here flammability apparatus setup, its schematic configuration, experimental procedure, and flammability estimation criterion were discussed.

Experimental results were presented in the fourth and fifth chapters. In the fourth chapter, binary hydrocarbon mixture LFLs and UFLs without addition of inert gases were collected. Comparison of experimental data with predictions using Le Chatelier's law was made, and modification of this rule was conducted based on the numerical data analysis. Chapter V focused on binary hydrocarbon mixture LFL and UFL diluted with nitrogen, where a variable of inert gas dilution effect, the inert gas dilution coefficient, was defined for each pure hydrocarbon based on the experimental data. By combining the parameter of inert gas dilution coefficient, Le Chatelier's law, or the modified Le Chatelier's law, fuel mixture flammability limit can be quantitatively characterized using pure hydrocarbon flammability data.

Chapter VI talked about flammability modeling on binary hydrocarbon mixtures with additional nitrogen. The applied criterion is the calculated adiabatic flame temperature (CAFT).

A theoretical deviation of Le Chatelier's mixing rule was performed in Chapter VII base on the combustion mechanisms at LFL and UFL. Primarily, this rule has been admitted to work well on LFL estimation for fuel mixture in air at ambient condition. By using the same reaction mechanisms and assumptions, the application of Le Chatelier's law was verified valid for fuel mixtures with inert gas dilutions, and at varied oxygen conditions. Furthermore, it was proven feasible to be applied to at non-ambient conditions.

Finally, this dissertation wrapped with Chapter VIII, which including the conclusions from this research, and some recommendations for future work.

CHAPTER II

BACKGROUND

2.1 Definition of flammability limits

Flammability limit, sometimes referred to as explosion limit [2], “is referred to the concentration range in which a flammable substance can produce a fire or explosion when an ignition source (such as a spark or open flame) is present”. The concentration in air is generally expressed as percentage fuel by volume in the vapor phase. Specifically, flammability limit is categorized as two types: (i) the upper flammable limit (UFL) above which the fuel is too rich (oxygen in lean) to burn; (ii) the lower flammability limit (LFL) below which the oxygen is in excess and fuel becomes too lean to be ignited.

2.2 Dependences of flammability limits

Flammability limit is not constant. As with most aspects of flammability, the evaluation of flammability limits is not absolute, but rather depends on the details of the test apparatus, detection criteria, and experimentally internal and external conditions. In practice, flammability limits are affected by a variety of factors including temperature, pressure, dilution of inert gases, varied oxygen concentrations, flammability apparatus size and configuration, flammability detection criteria, direction of flame propagation, and others [3].

2.2.1 Flammability limit vs. temperature

Research on combustible gases or vapors by Zabetakis [4] indicated that the flammability limit of most fuels is not stable at varied external temperature. With external temperature going up, flammability zone becomes wider. Specifically, the LFL declines continuously and UFL keeps climbing up. By using the hydrocarbon flammability limit data, Zabetakis generated two equations on LFL (Eq. (2-1)) and UFL (Eq. (2-2)) to quantify the temperature impact on flammability limit.

$$\frac{LFL_T}{LFL_{25}} = 1 - 0.000784(T - 25) \tag{2-1}$$

$$\frac{UFL_T}{UFL_{25}} = 1 + 0.000721(T - 25) \tag{2-2}$$

where, LFL_{25} and UFL_{25} are flammability limits at room temperature (25 ºC). LFL_T and UFL_T are flammability limits at another temperature T (ºC). The predicted temperature effect on the LFL is very similar to the measured data. For UFL, however, there are substantial discrepancies. Even the higher alkanes (hexane, heptane, and octane) do not follow the general relationship. One reason that nonlinearities arise is due to cool-flame ignitions with some gases at some temperatures, and not at others [5].

The data may also be fairly well correlated by the modified Burgess-Wheeler law, suggested by Zabetakis, Lambiris and Scott for the effect of temperature on the LFL and UFL of hydrocarbons in the absence of cool flames, which is expressed by Eq. (2-3) and Eq. (2-4) [4], where ΔH_C is the net heat of combustion (kcal/mole) and T in ºC.

$$LFL_T = LFL_{25} - \frac{0.75}{\Delta H_C}(T - 25) \quad (2\text{-}3)$$

$$UFL_T = UFL_{25} + \frac{0.75}{\Delta H_C}(T - 25) \quad (2\text{-}4)$$

2.2.2 Flammability limit vs. pressure

Melhem computed flame temperatures for several gases as the function of concentration and pressure, and observed that increasing pressures raises the flame temperature for fuel-rich mixtures, but not for lean ones [6]. Thus, if the flame temperature is assumed to be constant at the flammability limits, then the UFL will rise with increasing pressure, but the LFL will not change. Practically, raising the initial pressures of the fuel-air mixture can generally broaden its flammability limit range, where pressure has a slight effect on LFL except at a low pressure less than 50 mmHg absolute, while the UFL increases dramatically as the initial pressure increases [7]. With respect to hydrocarbons, the initial pressure on LFL and UFL can be represented by formulas Eq. (2-5) and Eq. (2-6) [8], where LFL_{1atm} and UFL_{1atm} are flammability limits at 1 atmospheric pressure; LFL_P and UFL_P are flammability limits at pressure P (atm absolute).

$$LFL_P = LFL_{1atm} - 0.31 \ln P \quad (2\text{-}5)$$

$$UFL_P = UFL_{1atm} + 8.9 \ln P \quad (2\text{-}6)$$

At a certain pressure range, some compounds are capable of slow reaction, which results in cool flame at the concentrations outside the normal flammability limits. For hexane combustion in air at initial temperature 150 °C, before pressure reaches up to 4.1, there is only one range of flammable mixture for normal flame; while at the pressure of 4.1 atm, cool flame occurs, and its range is located with mixtures of composition between 11 and 22% of hexane, and wider at a higher pressure [9].

2.2.3 Flammability limit vs. oxygen and inert gases

Flammability limit is not constant at varied oxygen and/or inert gas concentrations. A typical way to represent the flammability limit of a gas or vapor is by the triangle diagram. Typically, concentrations of fuel, oxygen, and inert gas are plotted on the three axes in vol % [10]. Each point in the triangular area and on the edges represents a 100 vol% mixture composed of fuel, oxygen, and inert gas. The zone enclosed by flammability line represents all mixtures that are flammable. The fuel mixtures lying outside this zone are non-flammable.

LFLs in a variety of oxygen concentrations are almost same as in air. Since the LFL is a fuel-lean condition, excess oxygen is available at 21% and any further excess oxygen is simply acting as a diluent. The molar heat capacities of oxygen and nitrogen are similar, and consequently the LFL value is not changed by going to a 100% oxygen atmosphere; however, UFL increases sharply with increasing oxygen concentrations. The same tendency can be identified with varied nitrogen amount added. Besnard

provided some excellent examples for the influences of different inert gases on the flammability limits [11]. Most inert gas inerting effect is dependent on the heat capacity, and the effect is mainly on the UFL except chemical $C_2H_2F_4$, because it is a typical chain reaction inhibitor . All of the inert additives are able to make a mixture non-flammable if added in sufficient quantities. These are very high amounts, whereas much lower concentrations are sufficient when using many halogen-containing gases.

2.2.4 Flammability limit vs. apparatus size and shape

Two hundred years of flammability limit experiments indicated that experimental flammability limits are sensitive to the size and configuration of flammability testing apparatus [12]. Coward and Jones [13] used a cylindrical vertical tube of 5 cm I.D. to measure the flammability limits for a variety of gases and vapors. However, Zabetakis [3] later suggested that a tube with the diameter of 5 cm is too small for accurate measurement of the flammability of some flammable halogenated hydrocarbons because of its quenching effect. An experimentally determined lower flammability limit of a methane/air mixture in 24 mm diameter tube was 4.90±0.03% by volume, compared with the earlier measured flammability limit of 5.1-5.2% in a standard tube [14]. Takahashi [15] evaluated the flammability limit variations with the apparatus of different geometries, e.g., different sizes and shapes. The observed results can be summarized as: (i) the flammability limits are highly dependent on the reactor wall quenching effect if the cylindrical reactors have small diameters but a large heights; (ii) for cylindrical reactors with small heights, the flammability limits are affected by a bunch of factors

including the tendency of hot gas accumulation at the vessel top, unburnt gas heating, incipient flame self-heating, and also the quenching effect of the reactor walls; (iii) When the reactor size is large enough, the experimental flammability limits get close to those obtained from open space.

2.2.5 Flammability limit vs. flame propagation direction

Experimental flammability limit varies with different flame propagation directions. When same criterion is applied to cylindrical combustion chambers, Several previous work [16, 17] had demonstrated that the flammability limit is wider for upward than for downward flame propagation. The obvious reason is that when fuel concentration gets close to flammability limit, flame cannot travel downward because buoyancy creates an upward convective current; while upward propagation can remain possible since buoyancy aids propagation. Without buoyancy effect, the flammability limit at horizontal flame propagation lies between the upward and downward flammability limits [12]. For fundamental combustion chemistry studies, downward propagation is preferred precisely because the extra effects of buoyancy do not come into play, but for industrial interest, upward flame propagation is recommended [7]. Table 2.1 lists some hydrocarbon flammability limit data at different flame propagation direction conditions. Normally, the UFL values are much more affected by the direction than the LFL values, in which the differences are mostly within experimental data scatter [18].

Table 2.1. Effect of flame propagation direction on flammability limits (25 °C and 1 atm) [18].

Mixture	**Direction**	**LFL** (vol%)	**UFL** (vol%)
methane/air	Upward	5.35	14.85
	Horizontal	5.40	13.95
	Downward	5.95	13.35
pentane/air	Upward	1.42	8.0
	Horizontal	1.44	7.45
	Downward	1.48	4.64
benzene/air	Upward	1.45	7.45
	Horizontal	1.46	6.65
	Downward	1.48	5.55

2.3 Flammability limit testing

As discussed above, there are a lot of parameters that influence the experimental flammability limit. Even at same testing conditions, the testing results are not consistent because of the different detection criteria (e.g., flame propagation, relative pressure rise), or even the different definitions of flammability from author to author, for example, Zabetakis [3] defined flammability limit as the fuel concentrations where the flame is capable of propagating from the ignition source through the mixture; While Conrad et al. [19] defined the flammability limit as the fuel concentration beyond which the fuel-air mixture is not ignitable.

2.3.1 Bureau of Mines method

U.S. Bureau of Mines flammability tube [13] is one of the best known experimental apparatus for measuring flammability limits of premixed gases by using the visual flame detection criterion. This flammability tube contains of a 50 mm I.D. glass tube, 1.5 m long. For a mixture to be declared flammable, propagation has to occur at least the distance of 75 cm with the half half way up the tube ; if only a shorter propagation distance is observed, this is deemed to occur due to localized heating from the igniter, and is not considered representative of the substance. The flammability limit is experimentally estimated by determining the related limiting mixture compositions at the flammable and non-flammable conditions [20], as is indicated in Eqs. (2-7) and (2-8).

$$LFL_{T,P} = \frac{1}{2}(C_{g,n} + C_{l,f}) \tag{2-7}$$

$$UFL_{T,P} = \frac{1}{2}(C_{g,f} + C_{l,n}) \tag{2-8}$$

where $LFL_{T,P}$, $UFL_{T,P}$ are lower flammability limit and upper flammability limits at the specific temperature, T, and pressure, P; $C_{g,n}$, $C_{l,n}$ are greatest concentration and least concentration of fuel in oxidant that are nonflammable; $C_{l,f}$, $C_{g,f}$ are greatest concentration and least concentration of fuel in oxidant that are flammable.

By using this experimental methodology, the U.S. Bureau of Mines generated a large body of flammability limit data for pure gas as well as some gas mixtures. Much of

the work was done and summarized by Coward and Jones [13], Zabetakis et al. [4], and Kuchta et al. [5] through Bureau of Mines Bulletin publications.

2.3.2 ASTM methods

The American Society for Testing and Materials (ASTM) adopted three closed vessel methods to measure flammability limits of gases and vapors.

ASTM E681 [21]: It uses a 5 L glass flask to determine the flammability limits of substances in air with a high voltage central spark as the ignition source. The affordable testing conditions is 1 atm or lower pressure and at temperature below 150 ºC. The flammability detection criterion is visual observation, through which the outward and upward flame propagation from the ignition source is noted. The concentration of the flammable component is varied between trials until the composition that will just sustain propagation of the flame is determined. The final obtained flammability limit data are calculated based on Eq. (2-7) and Eq. (2-8) for LFL and UFL, respectively.

ASTM E918 [22]: It consists of a metal pressure vessel with a minimum volume of 1 L and a minimum inside diameter of 76 mm, an insulated chamber equipped with a source of controlled-temperature inert gas, and an ignition device with appropriate power supply. The applied criterion of flame propagation is defined as the combustion reaction that produces at least a 7% rise of initial absolute. The final obtained flammability limit data are calculated based on Eq. (2-7) and Eq. (2-8) for LFL and UFL, respectively. The tests using this method cover the determination of LFL and UFL

of combustible vapor-oxidant mixtures at temperature up to 200 ºC and initial pressures up to as much as 1.38 Mpa (200 psia).

ASTM E2079 [23]: This testing method covers the determination of the limiting oxygen (oxidant) concentration (LOC) of mixtures at a specified initial pressure and initial temperature. It requires a 4 L or larger near-spherical vessel placed in a heating oven with a 10 J or greater ignition source, and 7% total pressure rise criterion at varying oxygen contents. The purpose of the test is solely to establish LOC, so various concentrations of oxygen are supplied by trial-and-error until the minimum value is found.

2.3.3 ASHRAE method

The ASHRAE (American Society of Heating, Refrigerating and Air-Conditioning Engineers) method [24] was developed specifically to accommodate halogenated compounds that may be difficult to ignite in smaller vessels. The explosion vessel is a 12 liter spherical glass flask and is equipped with a pair of tungsten electrodes for ac electric discharge together with a fan for gas mixing. Determination criterion of the flammability limit by using ASHRAE method is that if the flame moves upward and outward from the ignition point to reach an arc of the vessel wall which subtends an angle equal to or larger than 90º as measured from the ignition point, the fuel mixture is treated as a flammable one.

2.3.4 European methods

In European, the current standard methods for flammability limit determination are DIN 51649 [25] and EN 1839 [25] (subdivided into EN 1839-T and EN 1839-B). The DIN 51649 test method uses a 6 cm diameter, 30 cm tall glass cylinder opened at the top with a spark igniter (0.5 s, 10 W) at the bottom. The criterion for flammability is any visual sign of flame detachment from the ignition source. The EN 1839-T method uses an 8 cm wide, 30 cm tall, open top glass cylinder, with spark igniter at the bottom (0.2 s and 10 W). The criterion for flammability is propagation of flame 10 cm vertically above the igniter or 12 cm in the horizontal direction at any point of the flame path. EN 1839-B allows the use of a cylinder or spherical vessel of at least 5 L and an exploding fuse wire (0.2 s, 10-20 J) in the center. The criterion for flammability is a 5% minimum pressure rise after ignition.

2.3.5 Counterflow burner method

Counterflow burner method uses a new conceptual and indirect way to experimentally estimate flammability limits. The counterflow burner was configured by two gas jets of premixed fuel and oxidizer, which are released from opposing nozzles against each other. When the premixed combustible is ignited, it produces twin and planar flames. Estimation of flammability limit is to measure the relationship of fuel concentration *v.s.* average gas exiting velocity defined as the stretch rate here. Specifically, by plotting the fuel concentration as a function of stretch rate, the fuel

concentration at the intercept can be treated as the flammability limit through extrapolating linearly the plotted line to a stretch rate of zero [26].

2.4 Flammability test standardization and correlation

In general, it has been shown that data determined using European methods correspond to a wider fuel-concentration flammability range over which a fuel-air mixture is considered flammable than those methods applied in USA. An example of hydrogen, ethylene, methane and ammonia LFL and UFL is listed in Table 2.2 [4, 25, 27-28]. The discrepancies between flammability data determined using different methods have been pointed out as evidence that fundamental flammability limits may not exist because the numerous other variables that affect the measured flammability limit make it difficult to show experimentally whether or not a fundamental flammability limit exists [29, 30]. Therefore, although many attempts have been made to standardize the measurement methods to improve compatibility of flammability data, no standard method for that measurement has been estimated yet.

Due to different test methods giving rise to different results, it would be useful to quantify the correlation and conversion of flammability limits obtained using different test methods. There is little work done in this area. One practical experience is from De Smedt [2], who made a comparison between two internationally accepted methods: glass tube in accordance with DIN 51649 and 20 L spherical vessel with 7% pressure rise criterion similar to ASTM E918. The correlation results for the experimental

flammability limits of hydrocarbons at ambient conditions can be approximated as Eq. (2-9) and Eq. (2-10).

Table 2.2. LFL and UFL of methane, hydrogen, ethylene and ammonia in air at ambient conditions [4, 25, 27-28].

Fuel/air	**BMs*** (vol%)	**ASTM E681** (vol%)	**ASHRAE** (vol%)	**DIN 51649** (vol%)	**EN 1839-B** (vol%)
LFL(CH_4/air)	5.0	3.8	4.9	4.2	4.9
UFL(CH_4/air)	15.0	16.9	15.8	16.6	16.9
LFL(H_2/air)	4.0	3.75	4.5	3.8	4.2
UFL(H_2/air)	75.0	75.1	75.0	75.8	77.0
LFL(C_2H_4/air)	2.7	2.15	2.74	2.3	2.6
UFL(C_2H_4/air)	36.0	33.3	31.5	33.0	27.4
LFL(NH_3/air)	15.0	13.3	15.2	14.3	14.2
UFL(NH_3/air)	28.0	32.9	30.0	31.7	39.4

$$LFL_{7\%} = 1.03LFL_{DIN} + 0.11 \tag{2-9}$$

$$UFL_{7\%} = 0.98UFL_{DIN} - 0.76 \tag{2-10}$$

2.5 Flammability limit estimation

Primarily, experimental data for flammability limit are always preferred because of its unspecified property. So far, flammability limit data are still extremely deficient, and most of them focus on pure fuel at ambient conditions. To satisfy the requirements

from various industrial process operations, some empirical formulas and predicting models were developed by summarizing experimental results or theoretical derivation.

2.5.1 Empirical correlations

Bureau of Mines method [4]: Several empirical equations were generated by Bureau of Mines for hydrocarbon flammability limit estimation. Specifically, prediction of paraffin LFL at a single temperature point starts from room temperature, says, 293K, as Eq. (2-11).

$$LFL_{293K} = 0.55C_{st} \tag{2-11}$$

where, C_{st} is the fuel concentration in vol% required for stoichiometric combustion, typically found using Eq. (2-12), and n is carbon atom number in molecular formula.

$$C_{st} = \frac{100}{1+4.773(1.5n+0.5)} \tag{2-12}$$

Adding temperature dependence by using the modified Burgess-Wheeler law, LFL at different can be estimated as Eq. (2-13).

$$\frac{LFL_T}{LFL_{293K}} = 1 - \frac{C_{P,fuel-air} \times 100}{LFL_{293K} \times (-\Delta H_C)}(T - 293) \tag{2-13}$$

where, T is random temperature; ΔH_C is combustion heat release; $C_{P,fuel\text{-}air}$ is the total specific heat of fuel-air mixture, expressed as Eq. (2-14).

$$C_{P,\,fuel-air} = LFL \times C_{P,\,f} + (100 - LFL) \times C_{P,air} \tag{2-14}$$

and $C_{p,f}$ and $C_{p,air}$ are the molar heat capacities of fuel and air, respectively.

By volume, at atmospheric pressure and room temperature, the paraffin hydrocarbon UFL and LFL can be related as Eq. (2-15).

$$UFL_{293K} = 7.1\left(LFL_{293K}\right)^{0.56} \tag{2-15}$$

Moreover, a more precise correlation was proposed as Eq. (2-16) and Eq. (2-17) when cool flame is ignorable.

$$UFL_{293K} = 6.5\sqrt{LFL_{293K}} \tag{2-16}$$

$$UFL_{293K} = 4.8\sqrt{C_{st}} \tag{2-17}$$

Hilado method [31]: Hilado proposed that the LFL can in general be approximated as Eq. (2-18). He also proposed a rule for the UFL, but it does not exhibit much generality.

$$LFL = A \cdot C_{st} \tag{2-18}$$

where the constant A assumes the following values listed in Table 2.3.

Table 2.3. Values of the constant, A, for different chemicals [31].

Chemicals	A
C, H, O compounds	0.537
amines	0.692
chlorides	0.609
dichlorides	0.716
bromides	1.147
Sulfur-containing compound	0.577

Shimy method [32]: Based on former researchers' work, Shimy pointed out that flammability limit is function of constituting atoms for fuels. He gave some empirical equations to estimate the LFL and UFL separately for various chemicals at ambient conditions. The results are noted in Table 2.4. Specifically, the LFL is dependent on the numbers of carbon atoms only, while the UFL is associated with the numbers of carbon atoms, hydrogen atoms in radicals, and hydrogen atoms not in radicals.

Table 2.4. Shimy's equations for flammability limits estimation [32].

	LFL	UFL
Paraffinic hydrocarbons and olefins	$\frac{6}{nC^{a}}+0.2$	$\frac{60}{nH^{b}}+\frac{nC}{20}+2.2$
Iso-hydrocarbons	$\frac{6}{nC}+0.1$	$\frac{60}{nH}+2.3$
Benzene series	$\frac{8}{nC}$	$\frac{86}{2nH_{r}^{\ c}+nH'^{d}}$
Alcohols	$\frac{6}{nC}-0.7$	$\frac{80-2nH}{2nC}+3$

a: nC is the number of carbon atoms
b: nH is the number of hydrogen atoms
c: nH_r is the number of hydrogen atoms in radicals
d: nH′ is the number of hydrogen atoms not in radicals

Monakhov method [33]: Monakhov offered approximate methods for computing the LFL and UFL represented as Eq. (19) and Eq. (20), respectively.

$$LFL \approx \frac{100}{a\beta + b} \tag{2-19}$$

$$UFL \approx \frac{100}{c\beta + d} \tag{2-20}$$

where,

$$\beta = n_C + n_S + \frac{n_H - n_X}{4} - \frac{n_O}{2} \tag{2-21}$$

With n_C being the number of carbon atoms in the fuel molecule, n_S sulfur, n_H hydrogen, n_O oxygen, and n_X denoting any halogen (F, Cl, Br, I) atoms. The values of other constants are:

a = 8.684

b = 4.679

when $\beta \leq 7.5$,

c = 1.55

d = 0.56

when $\beta > 7.5$,

c = 0.768

d = 6.554

This relation is applicable to a wider range of fuels, including ones with oxygen, sulfur, and halogen atoms. For hydrocarbons, in some cases, the UFL of a straight-chain (or normal) compound will be known but not the values for the branched-chain isomer. For such cases, Monakhov offered an approximation as Eq. (2-22):

$$\frac{UFL_{isomer}}{UFL_{normal}} = \frac{T_{b,isomer}}{T_{b,normal}} \tag{2-22}$$

where, Tb is the boiling point (K). Considering experimental uncertainty, Monakhov pointed out hydrocarbon LFLs approximately have the same values for strait-chain compounds and branched-chain ones (Eq. (2-23)).

$$LFL_{isomer} = LFL_{normal} \tag{2-23}$$

Suzuki method [34 -36]: Suzuki estimated the flammability limits using empirical correlations based on the gross heat of combustion ($\Delta H_{c,g}$) in 10^3 kJ·mol. The correlation results are represented as Eq. (2-24) for LFL and Eq. (2-25) for UFL.

$$LFL = \frac{-3.42}{\Delta H_{c,g}} + 0.569\Delta H_{c,g} + 0.0538\Delta H_{c,g}^2 + 1.80 \tag{2-24}$$

$$UFL = 6.30\Delta H_{c,g} + 0.567\Delta H_{c,g}^2 + 23.5 \tag{2-25}$$

Another correlation developed from Suzuki includes molecular weight, critical temperature, T_c (K), and critical pressure, P_c (bar) for LFL (Eq. (2-26)).

$$LFL = \frac{-4.57}{\Delta H_{c,g}} + 0.0124MW - 0.00237T_c + 0.0205P_c - 0.46 \qquad (2\text{-}26)$$

Moller method [37]: This method developed by Moller estimates the LFL of organic compounds from a linear relation with stoichiometric concentration, C_{st} at Eq. (2-27).

$$LFL = aC_{st} + b \qquad (2\text{-}27)$$

where, values for the constants, a and b, vary by chemical classes, and are given in Table 2.5.

Table 2.5. Constants a and b for LFL estimation using Moller method [37].

Chemicals	a	b	Chemicals	a	b
Aliphatic hydrocarbon	0.45	0.12	Aliphatic monoketone	0.53	0.14
Alkene, alkyne and diene (halogen free)	0.25	0.66	Aliphatic aldehyde	0.53	0.23
Aliphatic mononitrile	0.33	0.74	Aliphatic ester from valeric up	0.45	0.12
Monobromoalkane	0.69	0.66	Aliphatic formate	0.49	0.24
Aliphatic monoamine	0.71	0.48	Aliphatic acetate	0.56	0.05
Alkoxyalcohol	0.57	0.3	Epoxyalkane	0.24	0.79
Aliphatic monoalcohol (halogen free)	0.5	0.08	Cycloalkane	0.56	0.06
Dialkanol	0.45	0.01	Benzole	0.48	0.03
Aliphatic diether (acetal/ketal)	0.47	0.1	Naphthyl	0.69	0.29
Aliphatic monoether	0.36	0.37	Monochloroalkane	0.65	0.3
Aliphatic monocarboxylic acid (halogen free)	0.32	0.63	Dichloroalkane	0.8	0.49

Dalmazzonne method [38]: Based on thermal hazard criteria used in CHETAH, Dalmazzone, Laforest, and Petit proposed that the LFL of hydrocarbons could be estimated using Eq. (2-28).

$$\frac{10\left(\frac{LFL}{100}\Delta H_c\right)^2}{\left[\frac{LFL}{100}MW + 28384\left(1-\frac{LFL}{100}\right)\right]\left[\frac{LFL}{100}n_{C+H} + 2\left(1-\frac{LFL}{100}\right)\right]} = 15.1 \qquad (2\text{-}28)$$

where MW is the molecular weight of the fuel, n_{C+H} is the number of carbon and hydrogen atoms, and the heat of combustion is given in kcal·mol^{-1}.

Funk method [39]: According to Funk, the LFL can be calculated from Eq. (2-29), where the coefficients a and b depend on the chemical class, and are listed in Table 2.6; β is oxygen coefficient for stoichiometric combustion.

$$\log(LFL) = a - b\log(\beta) \tag{2-29}$$

Table 2.6. Coefficients a and b for LFL estimation using Funk method [39].

Chemical types	LFL	UFL
Alkene	0.77815	0.73492
Alkyne and diene	0.68574	0.7756
Dichloro	1.17609	1.0299
Monochloro	1.07555	1.008
Nitrogen-containing	1.20412	1.1296
Others	0.90037	0.87024

Hshieh method [40, 41]: Hshieh related the LFL and UFL of organic and organosilicon compounds to the heat of combustion ($kJ \cdot mol^{-1}$) as Eq. (2-30), and Eq. (2-31), respectively.

$$LFL = 1145.2246\left(-\Delta H_c\right)^{-0.7972} - 0.3822 \tag{2-30}$$

$$UFL = 13514\left(-\Delta H_c\right)^{-0.81} + 6.71 \tag{2-31}$$

Miloshev method [42]: Miloshev correlated the flammability limits of hydrocarbons with the normal boiling point (°C), and obtained Eq. (2-32) and Eq. (2-33) for LFL and UFL, respectively. Values for parameters a and b are given in Table 2-7.

$$LFL = a\frac{813.1 - T_b}{b + T_b} \tag{2-32}$$

$$UFL = c\frac{813.1 - T_b}{d + T_b} \tag{2-33}$$

Table 2.7. Parameters for LFL and UFL prediction using Miloshev method [42].

Chemical types	LFL		UFL	
	a	b	c	d
Aromatics	0.45	123.9	6.21	479.5
Cyclohexanes	0.43	185.9	6.92	611
Cyclopentanes	0.42	182.6	6.82	601.9
Saturated hydrocarbons	0.4	189.2	6.87	618.5

2.5.2 Calculated adiabatic flame temperature (CAFT) modeling

Calculated adiabatic flame temperature is the temperature that is obtained when there are no combustion heat losses from the reaction system to its surroundings. Initially, this method was proposed by White [43], and then used by Hartzberg [44], Stull [45], Hansel [46], Melhem [6], Mashuga [47], and Brooks [48]. To estimate the flammability limits, a temperature threshold is assumed. Some researchers agree that this temperature is around 1550 K [49] or 1200 K [47], while others believed that this

temperature is in the range of 1000-1500 K [6]. By using Vidal's provided methodology [50], the LFL can be mathematically derived as follows. The methodology was originally presented by Shebeko at al [49], where an overall adiabatic temperature of 1600 K was used for the estimation of the LFL.

$$LFL = \frac{100}{1 + v_{ao}} \tag{2-34}$$

where v_{a0} is the number of moles of air per mole of fuel in the mixture at the LFL.

At adiabatic conditions, the enthalpy of reaction system remains constant at initial and final stages. By using energy balance equation, we have,

$$\sum_i H_{reac,i}(T_i, P) = \sum_j H_{prod,j}(T_{ad}, p) \tag{2-35}$$

where $H_{reac,i}$ and $H_{prod,j}$ are the enthalpies of the reactant i and product j; T_i is the initial temperature, T_{ad} is the adiabatic flame temperature which is equal to final temperature.

Expanding Eq. (2-35) by a given fuel $C_nH_mO_l$ reacting with air, we can get,

$$H_f^i + v_{a0}H_a^i = nH_{CO_2}^{ad} + \frac{m}{2}H_{H_2O}^{ad} - \beta H_{O_2}^{ad} + v_{a0}H_a^{ad} \tag{2-36}$$

where H is the absolute mole enthalpy; the subscript f and a are fuel and air; β is the stoichiometric coefficient of oxygen in the complete reaction; superscripts i and ad refer to the initial and final conditions, respectively. Solving v_{a0} from Eq. (2-36) and putting it into Eq. (2-34), we can get the calculated LFL as follows,

$$LFL = \frac{100}{1 + g_f \Delta H_f + g_C n + g_H m + g_O l} \quad (2\text{-}37)$$

where,

$$g_f = \frac{1}{H_a^{ad} - H_a^i}$$

$$g_C = g_f (H_C^i - H_{CO_2}^{ad} + H_{O_2}^{ad})$$

$$g_H = 0.5 g_f (H_{H_2}^i - H_{H_2O}^{ad} + 0.5 H_{O_2}^{ad})$$

$$g_O = -0.5 g_f (H_{O_2}^{ad} - H_{O_2}^i)$$

2.5.3 Structure group contribution (SGC) modeling

The theoretical concept of the SGC approach has been explained by Benson and Buss [51]. Reid [52] has mentioned that this approach is a powerful tool for predicting properties of pure substances and multi-component mixtures, and the applicable examples include critical temperature, critical pressure, critical volume, boiling point, freezing point, viscosity, thermal conductivity, and Gibbs free energy.

Albahril method [53]**:** The flammability properties are characterized by Albahril as the macroscopic properties of compounds that are related to the molecular structure. The following equation (Eq. (2-38)) is given to quantitatively characterize the flammability limits.

$$\Phi = a + b\left(\sum_i \Phi_i\right) + c\left(\sum_i \Phi_i\right)^2 + d\left(\sum_i \Phi_i\right)^3 + e\left(\sum_i \Phi_i\right)^4 \qquad (2\text{-}38)$$

where, Φ refers to LFL or UFL; Φ_i is the molecular structure group contributions ; a, b, c, d, and e, are constants.

Seaton method [54]**:** Derived from Le Chatelier's law, Seaton developed a mathematical model to estimate the flammability limits of vapors in air. The parameters in the proposed model were obtained by a group contribution procedure which is based on the second order structural groups of the kind defined by Benson and Buss [51]. The LFL and UFL can be estimated from proposed equation, Eq. (2-39).

$$FL = \frac{\sum_i ng_i f_i}{\sum_i ng_i \frac{f_i}{h_i}} \qquad (2\text{-}39)$$

where, FL represents LFL or UFL; ng_i is the number of occurrence of group i; the data for different structural contributions, f_i and h_i, for the LFL and UFL are given in Seaton method [54].

Shebeko method [55]**:** Shebeko proposed a method to estimate LFL by using atomic contributions. The LFL is calculated directly from the sum of the contributions as Eq. (2-40).

$$LFL = \frac{100}{\sum_i ng_i \cdot lfl_i} \tag{2-40}$$

where, ng_i is the number of occurrence of group i; lfl_i is the structural contribution of group i.

Nuzhda method [56]**:** Nuzhda used structural contributions to estimate the UFL of organic compounds with the correlation in Eq (2-41).

$$UFL = \left(15.4 + \sum_i ng_i \cdot A_i\right) exp\left(-0.15\left(n_c - 1\right)^{0.5}\right) \tag{2-41}$$

where, ng_i is the number of occurrence of group i; A_i is the structural contribution for group i.

High-Danner method [57]**:** High and Danner developed a structural contribution method for calculating UFL (Eq. (2-42)) for organic chemicals.

$$ln(UFL) = 3.817 - 0.2627 n_C + 0.0102 n_C^2 + \frac{\sum_i ng_i \cdot UFL_i}{\sum_i ng_i} \tag{2-42}$$

The sum in the denominator is the total number of groups used to represent the compound, and UFL_i is the contribution for i.

Kondo F-Number method [58-60]: Kondo introduced an index, the F-Number to address the flammability characteristics. The definition of F-number is as follows:

$$F = 1 - \left(\frac{L}{U}\right)^{0.5} \tag{2-43}$$

where L is the lower flammability limit and U the upper flammability limit.

The F-Number takes values ranging from zero to unity depending on the degree of flammability of substances. Specifically, substances would be super flammable when F number lies within 0.8-1.0; if the F number falls into the range of 0.6-0.8, substances are strongly flammable; when F is at the interval of 0.4-0.6, substances are normally flammable; those with F number of 0.2-0.4 are weakly flammable; and those with F-Number value of 0.0-0.2 are treated as vaguely flammable. The F-Number can be obtained using Eq. (2-44).

$$F = p_1 \times \begin{pmatrix} 1 + p_2 C_1 + p_3 R_{OE} + p_4 R_{CO} \\ + p_5 R_{COO} + p_6 R_{NH} + p_7 R_{RNG} \\ + p_8 R_{ARM} + p_9 R_{US} \end{pmatrix} \times \begin{pmatrix} 1 + p_{10} R_F + p_{11} R_{Cl} + p_{12} R_{Br} \\ + p_{13} R_{OH} + p_{14} R_{NO_2} + p_{15} R_{NH_2} \\ + p_{16} R_{CN} + p_{17} R_{COOH} \end{pmatrix} \tag{2-44}$$

where, C_1 takes the value of one or zero according to whether the molecule is a compound of mono-carbon skeleton or not; however, the methane derivatives that contain CO, COO, CN, or COOH group are treated exceptionally, and C_1 will take the value of zero for these compounds. R_{OE}, R_{CO}, R_{COO}, and R_{NH} denote numbers of ether, carbonyl, ester, and imine group, respectively, divided by the total number of skeletal carbons. R_{RNG} and R_{ARM} denote numbers of aliphatic and aromatic rings divided by the

total number of skeletal carbons. R_{US} denotes the total number of unsaturations in the carbon skeleton including aliphatic and aromatic rings divided by the total number of skeletal carbons. R_F, R_{Cl} , …, and R_{COOH} denote number of F, Cl, …, and COOH divided by the total number of hydrogen atoms in the corresponding pure hydrocarbon molecule.

The lower flammability limit and upper flammability limit can be calculated by Eq. (2-45) and Eq. (2-46).

$$LFL = (UL)^{0.5}(1-F) \tag{2-45}$$

$$UFL = \frac{(UL)^{0.5}}{1-F} \tag{2-46}$$

where, $(UL)^{0.5}$ is a function of the chemical formula of a general molecule given by $C_iH_jO_kF_lCl_mBr_nN_p$, which can be calculated using Eq. (2-47). M is the molecular weight, and C_{st} is the stoichiometric concentration.

$$\frac{(UL)^{0.5} - C_{st}}{C_{st}} = 0.00472(M - 32.00) \tag{2-47}$$

Gharagheizi method [61, 62]**:** Gharagheizi provided a quantitative structure-property relationship (QSPR) approach to estimate LFL and UFL of pure compounds. By using the AICHE recommended database of DIPPR 801, the molecular structures of all selected pure compounds were drawn into Hyperchem software, and then the molecular descriptors were calculated by dragon software. After calculating the

molecular descriptors, the genetic algorithm based multivariate linear regression (GA-MLR) was applied to find a linear equation that can predict the UFL with four parameters as Eq. (2-48) and five parameters for LFL as Eq. (2-49).

$$UFL = 10.35415 - 1.35486Jhetv - 42.28779PW_5 + 18.59571SIC_0 - 0.98203MATS4m + 0.68363MLOGP \quad (2\text{-}48)$$

$$LFL = 0.76022 - 3.5775PW_5 - 1.47971AAC + 8.57528SIC_0 - 0.0198MLOGP \quad (2\text{-}49)$$

where, Jhetv is the Balaban-type index from van der Waals weighted distance matrix; PW_5 is the path/walk Randic shape index; SIC_0 is the structural information content with zero-order neighborhood symmetry; MATS4m is the Moran autocorrelation-lag 4 weighted by atomic masses; MLOGP is the Moriguchi octanol-water partition coefficient (logP); and AAC is the mean information index on atomic composition.

2.6 Fuel mixture flammability limit

2.6.1 Le Chatelier's mixing rule

Le Chatelier arrived at his mixture rule for the LFL of gas mixture from his experiments with methane and other lower hydrocarbons [63]. The proposed empirical mixing rule is expresses as Eq. (2-50).

$$\frac{1}{LFL_{mix}} = \sum_{i=1}^{N} \frac{y_i}{LFL_i} \quad (2\text{-}50)$$

where, y_i is the mole fraction of the i^{th} component considering only the combustible species ($\sum y_i = 1$); LFL_i is the lower flammability limit of the i^{th} component in volume percent; LFL_{mix} is the lower flammability limit of the gas mixtures.

In addition, Kondo [64] has shown that Le Chatelier's Law can be extended to the UFL estimation for some blended fuels with acceptable accuracy. That is,

$$\frac{1}{UFL_{mix}} = \sum_{i=1}^{N} \frac{y_i}{UFL_i} \tag{2-51}$$

However, since Le Chatelier's method is intrinsic for blended gases containing only flammable compounds, it is not applicable as mixing flammables containing inert gases or with extra oxygen content. Modification of Le Chatelier's mixing rule was conducted by some researchers [27, 64-66]. For example, Kondo [64] developed an extended Le Chatelier's formula to explain the inert gas dilution effect on the flammability limits of flammable gases. Eq. (2-52) and Eq. (2-53) are specifically applicable to blend gases consisting of one flammable gas and one diluent gas.

$$\frac{C_1}{LFL_{fuel}} = \frac{C_1}{LFL_1} + pC_{in} \tag{2-52}$$

$$\frac{C_1 n_1}{100 - (UFL_{fuel} / C_1)} = \frac{C_1 n_1}{100 - UFL_1} + qC_{in} + rC_{in}^2 + sC_{in}^3 \tag{2-53}$$

where LFL_1 and UFL_1 are the lower flammability limit and the upper flammability limit of fuel in air; LFL_{fuel} and UFL_{fuel} are the lower flammability limit and the upper

flammability limit of fuel-inert gas mixtures; C_1 and C_{in} are the mole fraction of the fuel gas and inert gas in the fuel-inert blend ($C_{in} = 1 - C_1$); p, q, r, s are parameters to be determined experimentally.

2.6.2 Calculated flame temperature modeling of fuel mixture LFL

Previous flame temperature modeling on flammability limits treated reaction system at adiabatic conditions, but heat loss do affect experimental flammability limits, especially when the flammability apparatus quenching effect becomes indispensable, for example, in a narrow tube. Zhao [67] developed an accurate LFL estimation method for the LFL of fuel mixtures with the consideration of heat losses from reaction system to the surroundings.

CFT modeling is a four-step procedure [67]: (i) collect pure fuel LFL data through experimental tests; (i) estimating the pure fuel's average flame temperature; ii) solving for the average flame temperature of the burned gas for fuel mixtures; (iv) determining fuel mixture's LFL.

The LFL data for pure fuels were experimentally determined using a cylindrical flammability apparatus with inside diameter 10.22 cm and two ends closed. The final flame temperature for the pure fuel was estimated from the calculated flame temperature governing equation, Eq. (2-54).

$$f(T_f) = \left(\Delta H_c - \Delta nRT_0\right) + \sum_{prods} n_j \int_{T_0}^{T_f} C_{V_j}\, dT - (Q_c + Q_r) - W = 0 \qquad (2\text{-}54)$$

where, ΔH_c is the enthalpy of combustion; T_0 is initial temperature, and T_f is final flame; Δn is total mole number change in a certain chemical reaction; n_j is the molar numbers of the reaction product *j*; heat exchange between the reaction system and its surrounding mainly includes heat convection (Q_c) and heat radiation (Q_r), and heat conduction is usually negligible in the combustion chamber; W is the work done on the reaction system.

To estimate the adiabatic flame temperature for fuel mixture, Vidal [50] proposed a linear equation that correlates fuel mixture with its containing combustibles indicated as Eq. (2-55).

$$T_{f,mix} = x_1 \cdot T_{f,1} + x_2 \cdot T_{f,2} \qquad (2\text{-}55)$$

where, $T_{f,mix}$, $T_{f,1}$and T_{f2} are final flame temperatures for fuel mixture, fuel-1 and fuel-2 respectively on the binary fuel mixture basis

Finally, the CFT governing equation (Eq. (2-54)) was applied again to estimate fuel mixture LFL, which is the function of the fuel mixture flame temperature obtained from Eq. (2-55).

2.6.3 DIPPR SGC method for fuel mixture lower flammability limit

DIPPR SGC method [68] is an extended application of Shebeko method for fuel mixture LFL estimation. In this method, the fuel mole fraction on the combustible basis acts as the weighing factor of the group contributions. Specifically, fuel mixture LFL can be estimated using Eq. (2-56).

$$LFL = \frac{100}{\sum_i \left[X_i \sum_j ng_j \cdot lfl_j \right]} \tag{2-56}$$

where X_i is mole fraction of gas i in mixture (considering fuel only; air and diluents are ignored); ng_j is the number of groups of type j in compound i; lfl_i is group factor for group j.

CHAPTER III

FLAMMABILITY APPARATUS AND EXPERIMENTAL METHOD

3.1 Flammability apparatus overview

The flammability apparatus used in this research is a device used to measure the flammability limits of pure fuels and fuel mixtures. This apparatus was developed by Wong [69] at Texas A&M University. A schematic configuration of the flammability apparatus is showed in Figure 3.1. The key design feature consists of five parts: (i) gas feeding system; (ii) cylindrical reaction vessel; (iii) gas mixer; (iv) ignition system; and (v) data acquisition system. The applicability of this apparatus is limited to room temperature and 1atmospheric pressure.

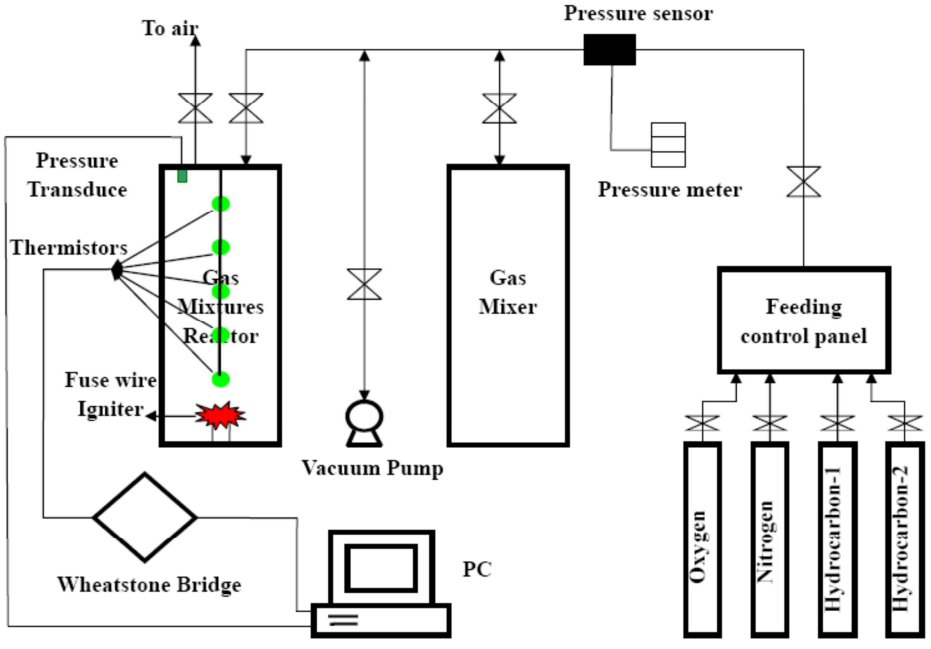

Fig. 3.1. Schematic representation of the experimental apparatus.

3.1.1 Cylindrical reaction vessel

The reaction vessel (Figure 3.2) is a two-end-closed cylinder with diameter 4 inch nominal (11.43 cm O.D., 10.22 cm I.D.) and length 100 cm. It hangs from a top plate permanently affixed to the vessel enclosure. At the central line of the reaction vessel, there are five fast responding temperature sensors with same interval distance. These temperature sensors are NTC thermistors from Thermometrics (series number: FP07DB104N; response time: 0.1 sec in still air; resistance: 100 KΩ at 25^{o} C), which was not for temperature measurement, but for frame front detection when fuel/air mixtures ignite and burn upwardly. The ignition source lies at the lower position, 5 cm away from the reaction vessel bottom.

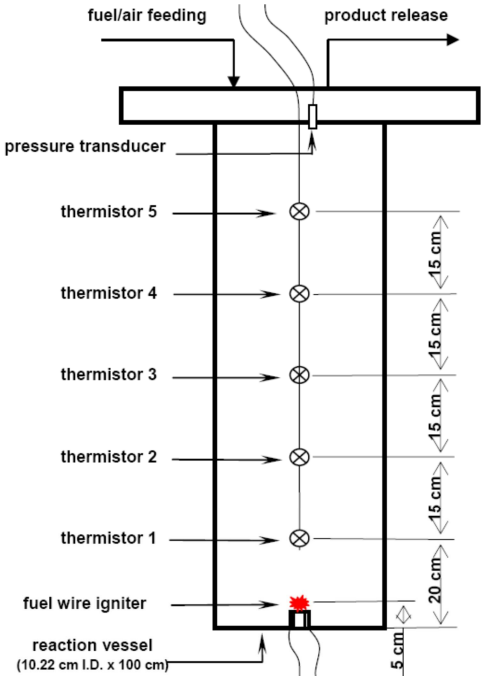

Fig. 3.2. Configuration of reaction vessel.

The greatest distance from the ignition source to the top thermistor is 75 cm. This design property is consistent with the flammability apparatus of U.S. Bureau of Mines, by which visual observation with at least 75 cm distance of flame propagation was used as the flammability limit detection criterion [13]. Thermistor 1 is located at the distance of 15 cm away from the ignition source, which can effectively lower the heat impact from the ignition source. The interval distance between the even-separated thermistors is 15 cm. There is a dynamic pressure transducer (Omega DPX 101, with a range of 0 to 250 psig pressure rise, 0 to 5 V nominal output signal, 1 μs rise time, 1% amplitude linearity and temperature effect of 0.03%/F), which is mounted on the top plate at the top of the reaction vessel and used to record the pressure variation when fuel/air mixtures ignite or explode. Previous work has shown that reaction vessels with similar dimension have sufficient width to minimize quenching effect of typical fuel flames [12]. Specifically, the diameter of the reactor applied in this research is larger than those employed in U.S. Bureau of Mines (5 cm in diameter) and European standard EN 1389 T (8 cm in diameter), which means a less quenching effect can be obtained using this flammability apparatus.

Because the reaction vessel is likely to experience pressure from the combustion, the vessel design took this into consideration. According to observations by U.S. Bureau of Mines, combustion can occur as a deflagration or a detonation. During deflagration the flame velocity is less than the speed of sound, and the combustion can produce pressure waves roughly 8 times that of the starting pressure. During detonation the flame velocity exceeds speed of sound, and the combustion can produce a pressure wave

roughly to 40 times the starting pressure. A conservative estimate that the maximum pressure wave is 50 times that of planned initial pressure, either due to error in vessel loading or an unusually powerful detonation, yields a theoretical maximum pressure of approximately 50 bars. For more safety margin, this reaction vessel was designed to fail at 103.4 bar or higher using modified guidelines from ASME design guide. The reaction vessel has been tested hydrostatically to 82.74 bars, sufficient for the needs of the apparatus. In addition, two independent safety measures are in place, a relief valve and an enclosure around the reaction vessel. The relief valve at the top of the reaction vessel (Swagelok®, R4 Proportional Relief Valve) relieves directly into the laboratory vent at 500 psig or higher, which mitigates the pressure damage without releasing flames or hot gases into the laboratory. The vessel enclosure provides two functions. The enclosure walls (1/8 in thick steel or double layers of 1/4 in thick Lexan®) offer protection from shrapnel in extreme cases where the vessel is unable to withstand pressure produced during combustion. It also supports the apparatus at a sufficient height such that disassembly of the reaction vessel can be accomplished with the lowering of the reactor body rather than lifting, thus reducing safety hazards of reactor body weight during maintenance and modification.

3. 1.2. Gas feeding system

The gas feeding system includes a manifold that connects to the gas cylinders (fuels, air, oxygen, nitrogen, and others), a vacuum pump (Welch Mfg. Duoseal Pump with ultimate vacuum 1.0×10^{-3} mmHg), the gas mixer, and the reaction vessel. The gas

mixtures used with the experimental apparatus are prepared by loading the individual components from gas cylinders in a proper consequence for minimum fire potential hazard. The gas feeding manifold is illustrated in Figure 3.3. The combined gas line from all pressurized cylinders leads to a cross junction, which includes a pressure transducer (Omega PX603, 0.4% accuracy with 0.04%/F thermal zero and span effect) connected with a pressure meter. Mixture composition was controlled through partial pressure gauging recommended by Bureau of Mines [70]. At external conditions of room temperature and ambient pressure, the fuel/air mixtures can be treated as ideal gas mixtures.

The gas loading manifold is usually blocked from the reaction vessel with a closed stainless steel plug valve (Swagelok®, or Cajon®) with a pressure rating of 3000 psig. In the case where the valve is left open by operator error, the components in the manifold may experience high pressure. The ¼ in tubing, the plug valves, and the metering valve in the manifold are all stainless steel with Swagelok® compression fittings and working pressure ratings of 2000 psig or higher. Since the pressure ratings of components in the manifold are greater than the expected maximum pressure, the hazard from higher than normal operating pressures in the manifold components is negligible.

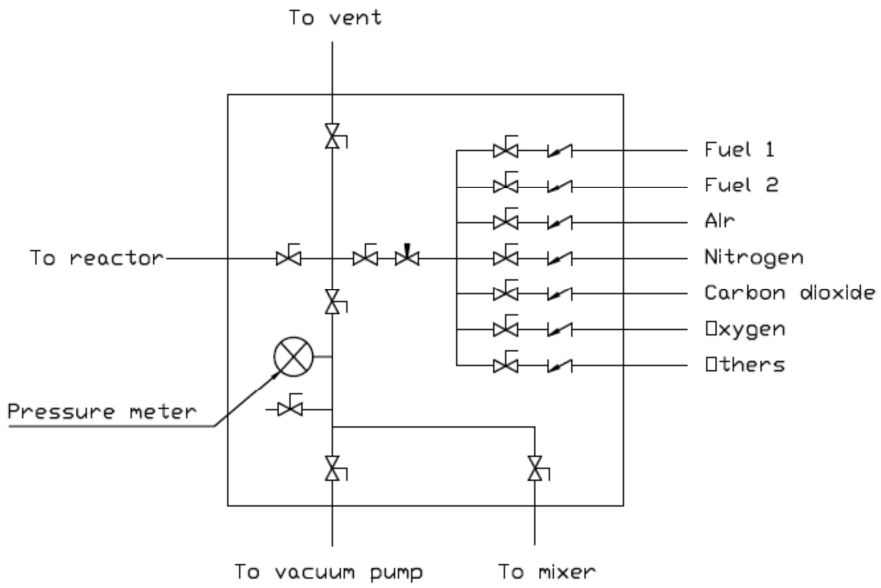

Fig. 3.3. Gas feeding manifold.

3.1.3 Gas mixer

Premixed fuel/air mixtures are employed in this research to measure the flammability limit. The feeding gas mixtures (Figure 3.4) are made to be homogeneous using a gas mixer which is a cylinder containing a cylindrical Teflon block. This block can slide along the length of the vessel, and the block diameter is slightly smaller than the gas mixer's internal diameter, which allows smooth movement of the block. Gas mixing is obtained by rotating the mixer. Gases moving between the block and the vessel wall create highly turbulent zones in front of and behind the moving block, and these zones facilitate fast mixing of the gases. The volume of gas mixer approximates the volume of the reaction vessel, which ensures precise gauging of feeding components

through partial pressures (not small volumes), easy handling, and cost effectiveness (not big volume).

The mixing vessel usually contains higher than atmospheric pressure gas mixtures (~23 psig) during loading and mixing. Naturally, it presents a very low hazard from combustion because the only internal wetted components are a Teflon® block and the grounded stainless steel vessel walls, neither of which can provide an ignition source. Moreover, the gas mixer was manufactured at the similar failure pressure with the reaction vessel, which is sufficient for the needs of the flammability apparatus.

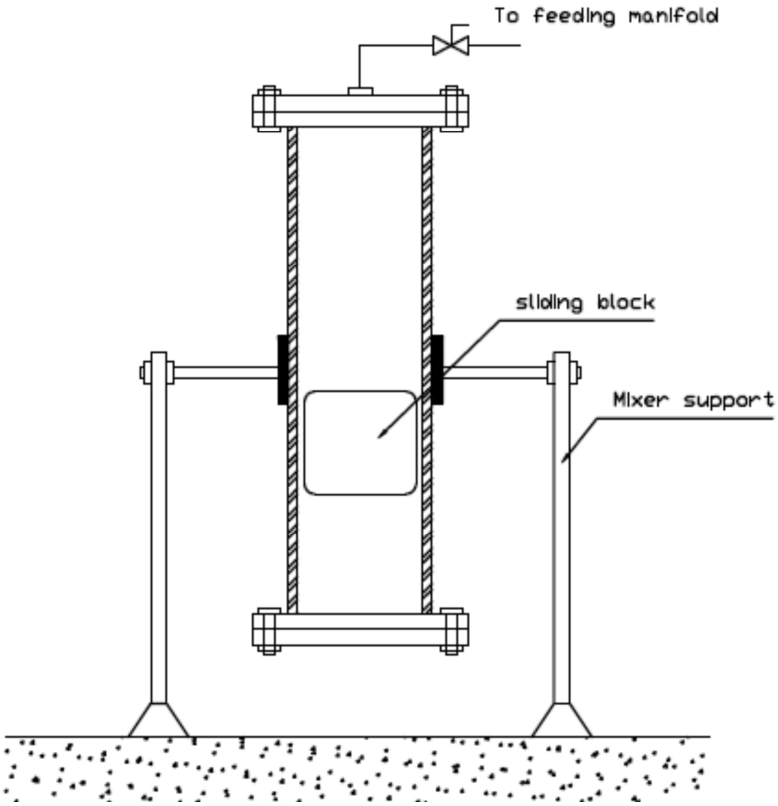

Fig. 3.4. External mixing vessel.

3.1.4 Gas mixture ignition system

Designing of the gas mixture ignition system used in this research followed the standard from ASTM E 918-83, which was demonstrated by Mashuga to be capable of inputting 10 J of energy with a repeatable power delivery [71]. The ignition source is a 10 mm piece of AWG 40 tinned copper wire, which is vaporized by a 500 VA isolation transformer (Hammond 171 E) at 115 V AC switched on with a zero-crossing solid state relay (Omega, model #SSRL240DC 100), and the current is delivered beginning at the zero point of each AC cycle. Figure 3.5 shows the igniter system circuitry.

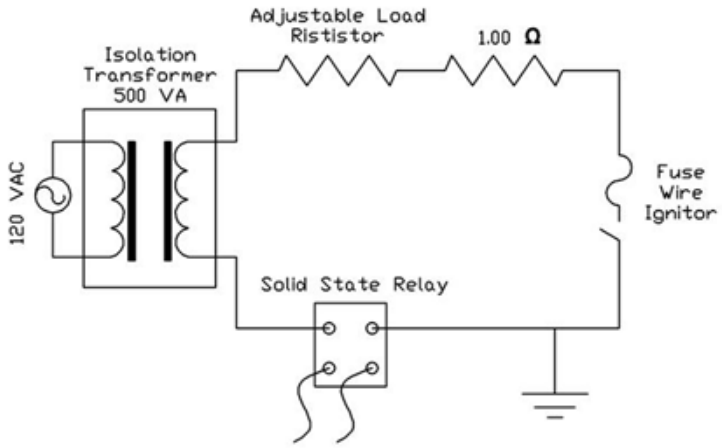

Fig.3.5. Igniter system circuitry.

The igniter that holds the fuse wire consists of a wire holder section and a vessel seal section. The wire holder section is a pair of square copper rods with a spring loaded wire grip section mounted on a cylindrical platform made of non-conducting polymer. The fuse wire is connected to the igniter circuit via the copper rods, which are soldered

to wiring that leads outside the reaction vessel via the vessel seal section. The wire holder section is connected to the seal section with a short ¼ in stainless steel tube, which also contains the circuit wiring. The seal section is a Cajon® VCO O-ring face seal connector gland and screw cap. The center of the gland is fitted with a stainless steel plug and welded. The circuitry wiring is routed through a ¼ in hole in the plug, which is filled with epoxy to provide a hermetic seal. The igniter port on the bottom of the ignition vessel consists of a tapped 1 in NPT hole with the VCO face seal male connector portion (with Viton® O-ring) installed. The pressure seal is accomplished by inserting the igniter into the port and tightening the screw cap. Figure 3.6 shows the igniter design.

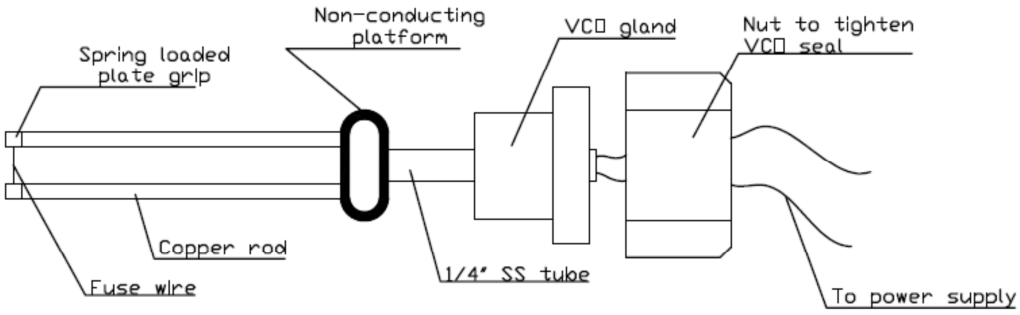

Fig. 3.6. Igniter.

3. 1.5 Data acquisition system

Temperature sensors: In this research, five NTC thermistors are used to detect combustion and record temperature change in the reaction vessel. Of five thermistors,

each is the resistance to be measured (R_T) in a Wheatstone bridge circuit consisting of three other resistors with constant resistance (R_1, R_2, R_3), as shown in Figure 3.7. The advantage of five parallel Wheatstone bridge circuits is that, unlike resistance, the voltage difference can be measured directly and converted to resistance values as long as the values of three constant resistors are known. In this case the bridges are initially balanced with each V_{out} equal to zero. When any one of the thermistors detects a flame, the related bridge deviates from the balance and a nonzero V_{out} value indicates the temperature change at the position of this thermistor. For the purpose of flame detection rather than flame temperature determination, calculation of the temperature is not necessary as passage of a flame will induce sharp increases in the voltage signal because the temperature trends of the gas mixture during and after combustion can be observed.

The thermistors are suspended at the center axis of the reaction vessel at certain lengths from the top by a frame consisting of two 1/8 in thick rods hanging from the top plate with short rods welded on at regular intervals for the signal wires to bundle around. The signal wires are AWG 26 enamel coated copper wires covered with Voltrex tubing insulation to prevent electrical shorts. They connect outside the reaction vessel by a pair of electrical feedthroughs constructed from 1/2 in diameter stainless steel sleeve around 1/4 in tubing sealed with epoxy (J-B Industro-Weld) and topped with silicone sealant to protect the wiring from damage. The signal wires are connected through shielded cables to the Wheatstone bridge circuit to prevent interference from external electromagnetic sources (power lines, and other electrical devices in the lab).

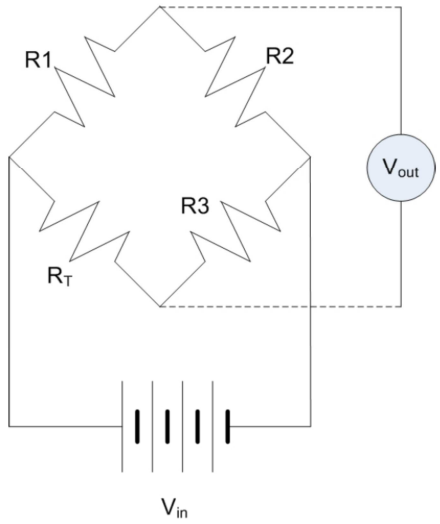

Fig. 3.7. Wheatstone bridge circuit used for flame detection.

Pressure sensor: The pressure within the reaction vessel is monitored with a dynamic pressure transducer (Omega DPX 101) mounted on the top plate. The piezoelectric quartz transducer has a range of 0 to 250 psig pressure rise, with 0 to 5 V nominal output signal, 1 us rise time, 1 % amplitude linearity, and temperature effect of 0.03 %/°F. The pressure transducer is mounted on the 1/8 in NPT port on the top plate of the reaction vessel, sufficiently distant from the ignition source so that heat effects on the measured pressures are negligible. Maximum pressure is obtained by integrating the portion of the dynamic pressure *vs*. time curve that is above the baseline, and applying a conversion factor of 51.02 psi per V·sec (from manufacturer specification).

Data Acquisition using LabVIEW program: The hardware used for data acquisition include a desktop computer (Dell® Optiplex 210L, with Windows XP®) equipped with a video capture device (Belkin® USB Videobus II), and a Keithley® data

acquisition card (Keithley® KPCI-3102, 8 differential inputs with total of 225k signals per second @ 0.05 % accuracy) with screw terminal attachment (Keithley®, STP-68). The data acquisition card measures differential voltages, allowing it to measure both the thermistors and the pressure transducer. The data acquisition program for the measurement process is coded using LabVIEW® (National Instruments, version 7.1). Figures 3.8 and 3.9 are the LabVIEW data acquisition program of block diagram window and front panel, respectively.

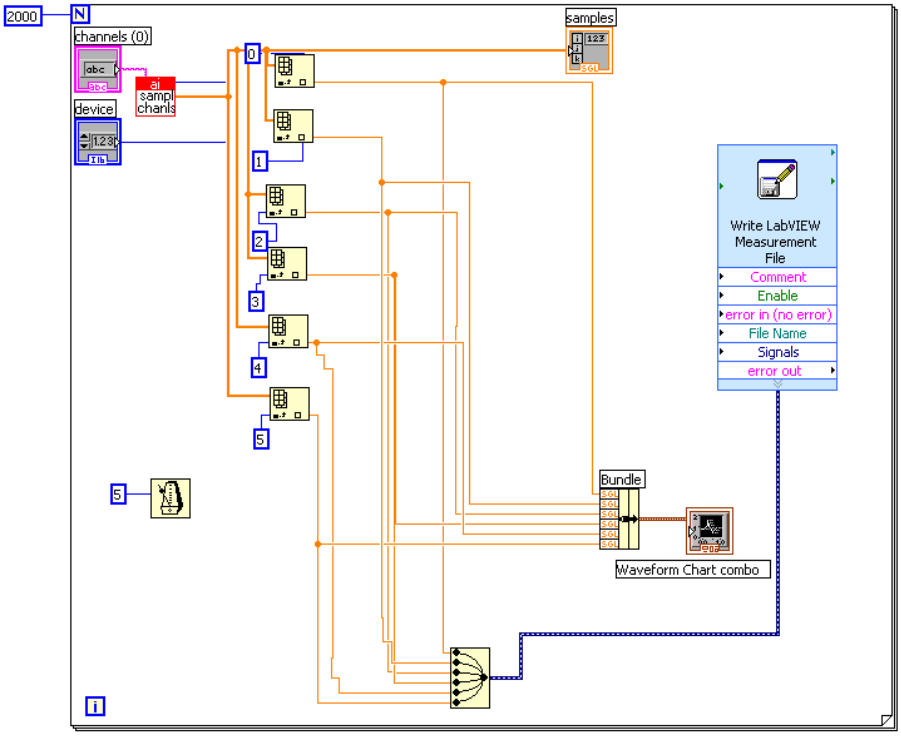

Fig. 3.8. LabVIEW data acquisition program (block diagram window).

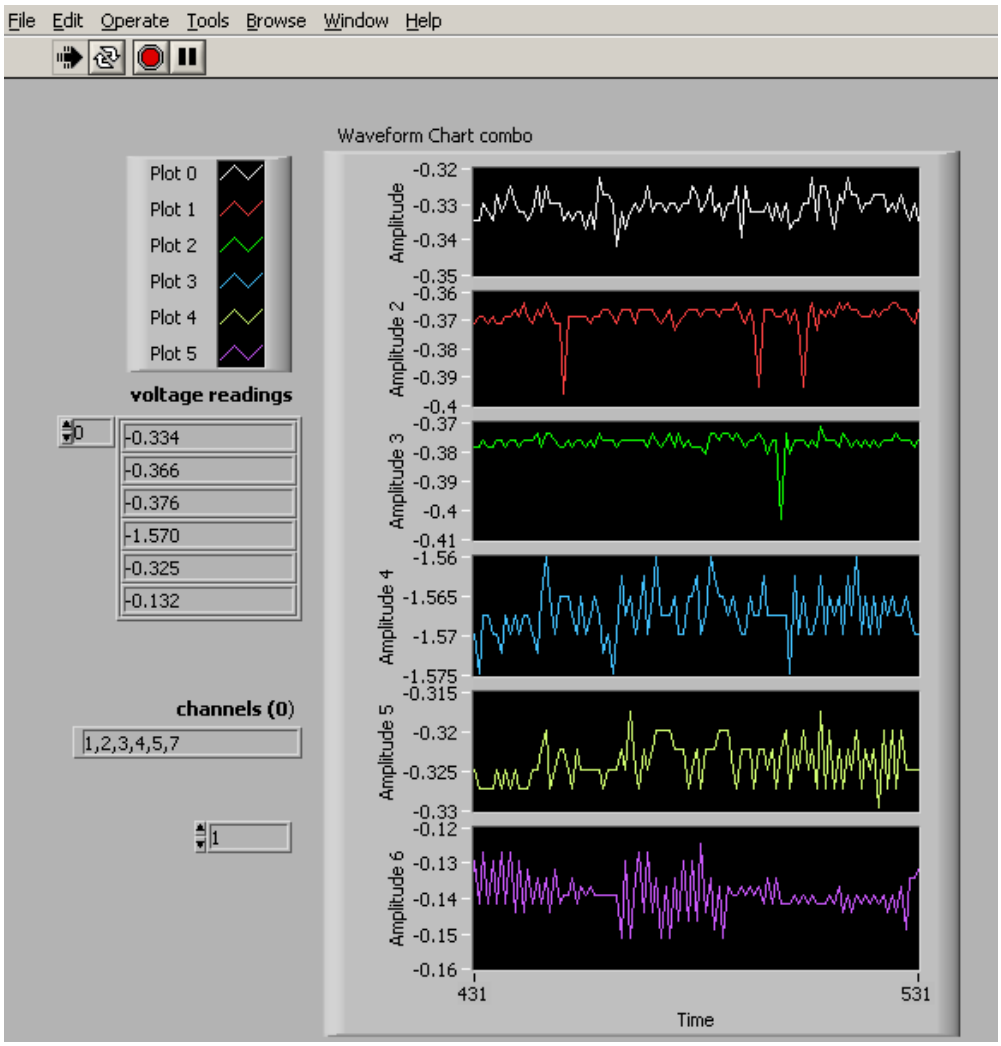

Fig. 3.9. LabVIEW data acquisition program (front panel).

3. 2 Experiment procedures

Flammability measurement is a systematic operation, which includes a series of actions as follow:

(i) Evacuation of the gas vessel and tubing lines including gas mixer, reaction vessel, and feeding manifold;

(ii) Gas gauging and loading;

(iii) Mixing of gas mixture;

(iv) Premixed gas mixture transfer;

(v) Ignition of premixed gas mixture;

(vi) Flammability data acquisition;

(vii) Purging of gas mixer, reaction vessel, feeding manifold and tubing lines.

Because the original objective for this research is to find the critical fuel concentrations, LFLs and UFLs, at different inert gas contents, all the operations should follow the proper sequences for accurate gas feeding, especially at the stage of controlling plug valves (Figure 3.10). Following is the step-by-step operation procedure for one entire experiment. The components of gas mixture tested for flammability limits include fuel 1, fuel 2, air, and additional nitrogen.

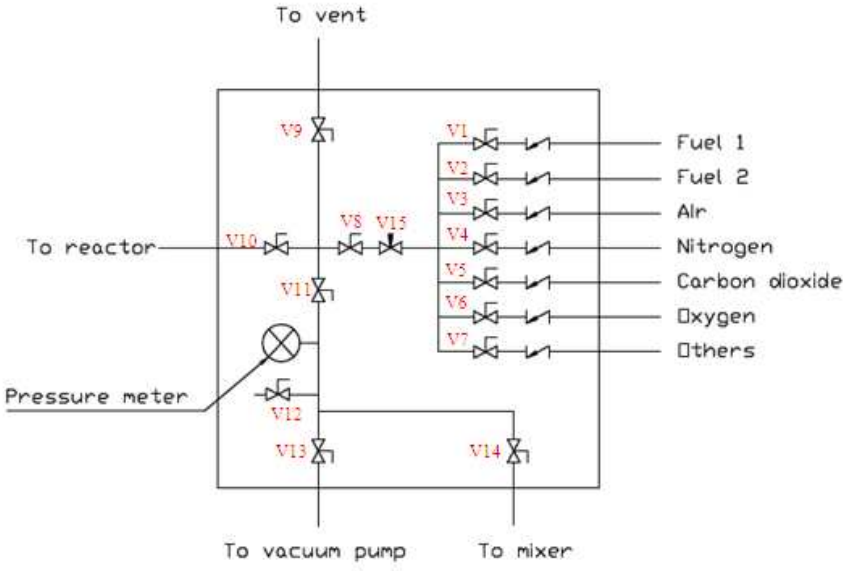

Fig. 3.10. Gas feeding manifold and marked controlling plug valves.

Step 1: Preparation for gas feeding. Needle valve V15 is adjusted to high flow rate. Vacuum pump is activated to evacuate the tubing lines connected to the gas components (V1, V2, V3, V4, V8, V11, and V13 open; all other plug valves closed) until the pressure is constant for over one minute (pressure change no greater than 0.01 psi). Then close V1, V2, V3, and V4, and open gas cylinder valves. Subsequently, the vacuum pump continues working to evacuate gas feeding manifold and gas mixer (V8, V11, V13 and V14 open; all other plug valves closed), and then gas mixer pressure is recorded on an Excel spreadsheet for gas mixture volume composition calculation.

Step 2: Loading gases one by one. Nitrogen is loaded first (V4, V8, V11, and V14 open; all other plug valves closed), followed by Fuel 1 (V1, V8, V11, and V14 open; all other plug valves closed), Fuel 2 (V2, V8, V11, and V14 open; all other plug valves closed), and air (V3, V8, V11, and V14 open; all other plug valves closed). The gas loading manifold is evacuated between every component loading. The needle valve V15 is adjusted to control the gas loading flow rate to avoid overloading. The loading amounts are controlled by the predetermined pressure values gauged by a pressure meter. The final pressure is recorded on the Excel spreadsheet to convert into the gas component volume concentrations.

Step 3: Mixing the feeding gas mixture. The external mixer is utilized after the gas loading is complete. Care should be taken to ensure the plug valve on the top of the mixing vessel is closed, and the manifold is opened to the ventilation (V9, V11, and V14 open; all other plug valves closed). After disconnection with the manifold, start the rotation motor with slowly increasing voltage to the pre-set value (30 rounds per min).

The motor is deactivated after 4 minutes, and the mixing vessel is reconnected to the manifold.

Step 4: Loading the premixed gas mixture into the reaction vessel. After the feeding gas components are mixed, the gas mixer is deactivated and stays quiescent for several minutes. During this waiting period of time, the reaction vessel and the feeding manifold are vacuumed. The premixed gas mixture is transferred to the reaction vessel by opening V10, V11 and V14, and closing all other plug valves. Once the reaction vessel has filled to one atmosphere pressure (14.7 psi), it is isolated from the manifold by closing V10. The gas mixtures are allowed to sit in the reaction vessel for five minutes to reach thermal equilibrium and become quiescent.

Step 5: Gas mixture ignition and data acquisition. Before this operation starts, the LabVIEV program is activated to begin recording. Approximately 5 sec after the data acquisition starts, the gas mixture is ignited by a fuse wire igniter, and the program LabVIEW continues running to record the flame temperature until the premixed gas mixture is consumed by traveling to the top of the reaction vessel. The ignition and subsequent combustion can be detected by thermistor and pressure transducer readings for a period of time ~17 s. The readings are voltage values with 2,000 data points for each sensor (5 thermistors and 1 pressure transducer).

Step 6: Purging reaction vessel, gas mixer, gas feeding manifold, and other tubing lines using nitrogen or other inert gases.

Step 7: Repeating the same experimental operations as indicated above.

3.3 Combustion types in the reaction vessel

Combustion behavior in reaction vessel was classified into five categories over a range of concentrations that span from below the lower flammability limits to above the upper flammability limits for gas mixture [72].

(i) Non-propagation;

(ii) Flash combustion;

(iii) Discontinuous flame propagation;

(iv) Temperate continuous flame propagation;

(v) Violent continuous flame propagation.

The sampling experiments were conducted with methane/air and ethylene/air mixtures. The data from thermal and pressure sensors were acquired and interpreted to identify the combustion types.

3.3.1 Non-propagation combustion

Non-propagation combustion is characterized by the property of lacking flame propagation after ignition, which can be due to a variety of factors, such as very low fuel or oxidizer concentrations, low ignition energy input or low ignition energy density [69, 72]. Normally, non-propagation behavior in the flammability apparatus has no or negligible temperature and pressure fluctuations.

3. 3.2 Flash combustion

Flash combustion is flame with vertical flame propagation, but little or no horizontal propagation, which terminates within a short distance of the ignition source to produce minor temperature and pressure increases [69, 72]. The reasonable explanation is that a combusting gas mixture will travel upward because of buoyancy force, and due to heat loss its temperature will decrease continuously until it drops to ambient temperature of gas mixture.

3.3.3 Discontinuous flame propagation

Discontinuous flame propagation is a flame that propagates vertically and horizontally but terminates before reaching the top of the reaction vessel [69, 72], which differs substantially from the profiles of flash combustion. The maximum pressure is significantly greater than the pressure rise caused by flash combustion, because a greater portion of the gas in the reaction vessel participates in combustion than that in the flash combustion behavior.

3.3.4 Temperate continuous flame propagation

Temperate continuous flame propagation occurs when the flame is able to propagate vertically and horizontally and does not terminate until it reaches the top of the reaction vessel [69, 72]. In this case, all the thermistors detect the flame front in succession and then slowly decrease as the gas around the thermistors cools, so they

exhibit similar temperature profiles. Comparing with flash combustion and discontinuous flame propagation, a greater pressure rise is obtained, which illustrates more gas is combusted in the experiment. Of five combustion types, temperate continuous flame propagation is the result we seek after with tests of different fuel concentrations, because the fuel concentrations marked in this combustion type are used to determine the lower and upper flammability limits of gas mixtures.

3.3.5 Violent continuous flame propagation

Violent continuous flame propagation describes that a gas mixture in reaction vessel combusts violently, the flame propagates upward and dynamic pressure varies much more rapidly than the temperate continuous flame propagation [72]. The experimental result indicates some fuels, e.g., ethylene, can exhibit violent combustion when the fuel concentration approaches to stoichiometric one.

3.4 Flammability criterion and calibration

This work uses an innovative thermal criterion for flammability determination [69, 72]. In the closed reaction vessel, five NTC thermistors at multiple locations are employed to track flame propagation, which indicates the sensitive thermistors can locate the flame traveling distance from the ignition source in real time. U.S. Bureau of Mines used a certain flame propagation distance, which is equal to half of reaction tube length with150 cm total, as the detection criterion by visual observation. This working

mechanism is similar to the thermal criterion using thermistors to detect flame propagation instead of naked eyes. Meanwhile, the new thermal criterion is connected to a relative pressure rise criterion that is well standardized by ASTM E 2079. A dynamic pressure transducer lying on the top of reaction vessel can record the dynamic pressure change in the reaction vessel to confirm the occurrence of fire or an explosion in the reaction vessel. Not exact relative pressure rise was recorded because the main basis for the thermal criterion is flame propagation distance.

Based on the information of five different combustion types, fuel concentrations could be easily characterized by temperature profiles. When continuously increasing fuel concentrations, we observed that flame traveled farther up till to the top of reaction vessel, where the thermistor 5 locates. Figure 3.11 is an example illustrating flame propagation distance variation with different concentrations of methane in air.

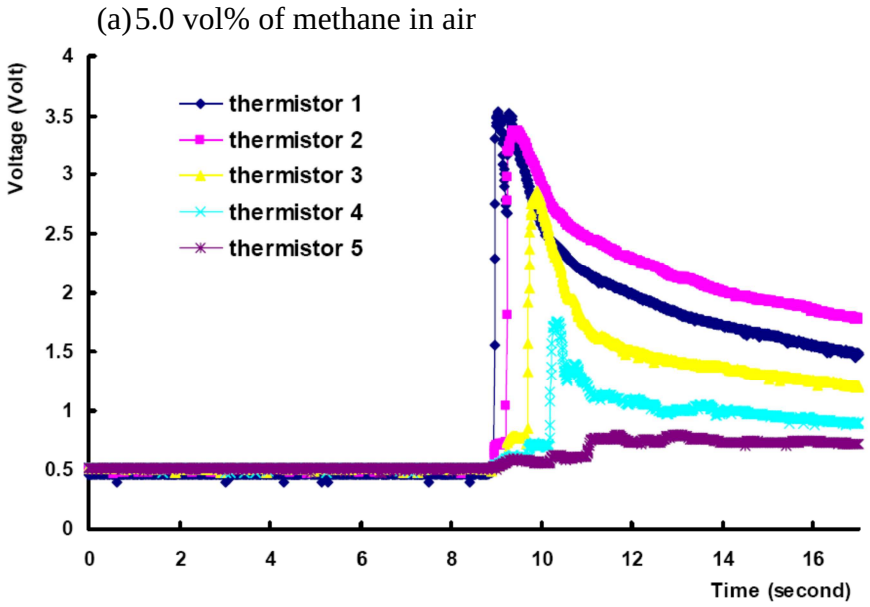

Fig. 3.11. Flame propagation temperature profiles with different methane concentrations in air: (a) 5.0 vol%; (b) 5.1 vol%; (c) 5.2 vol%; and (d) 5.25 vol%.

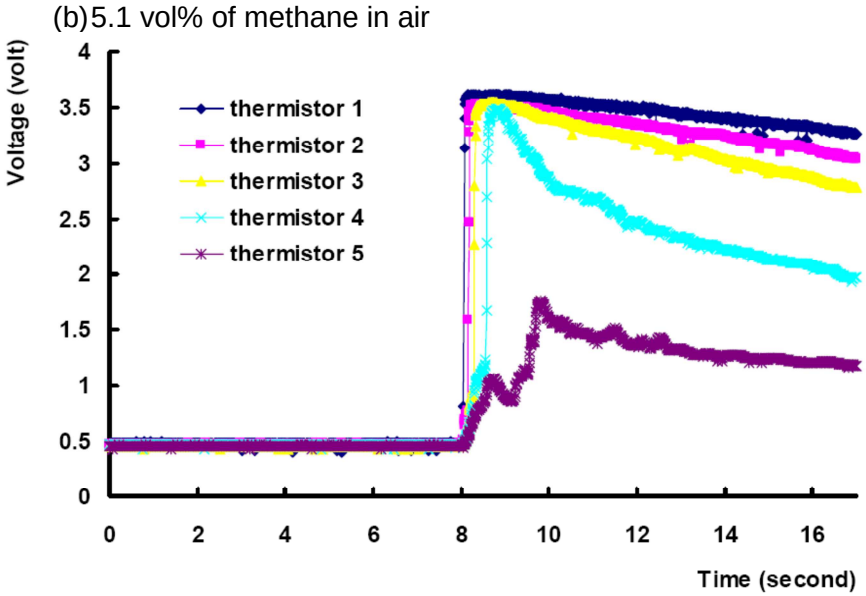

Fig. 3.11. Continued.

(c) 5.2 vol% of methane in air

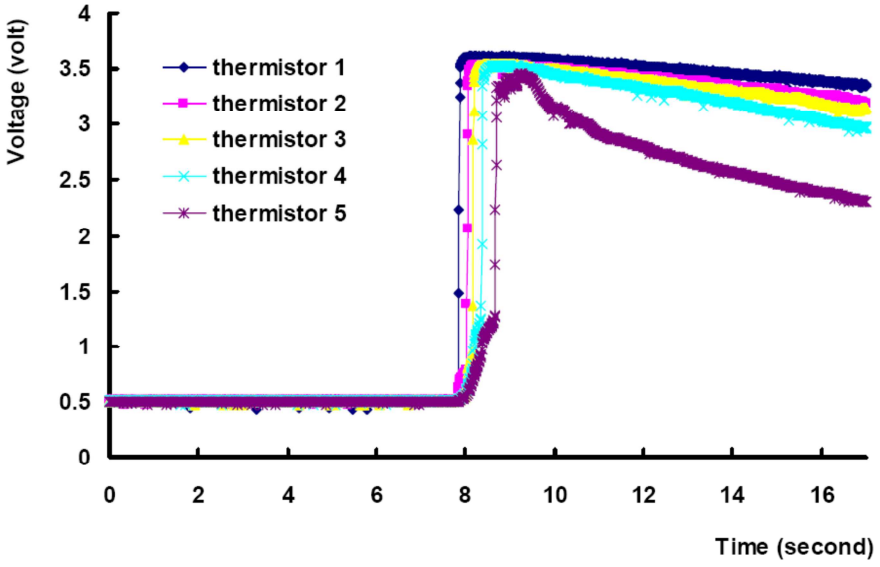

Fig. 3.11. Continued.

(d) 5.25 vol% of methane in air

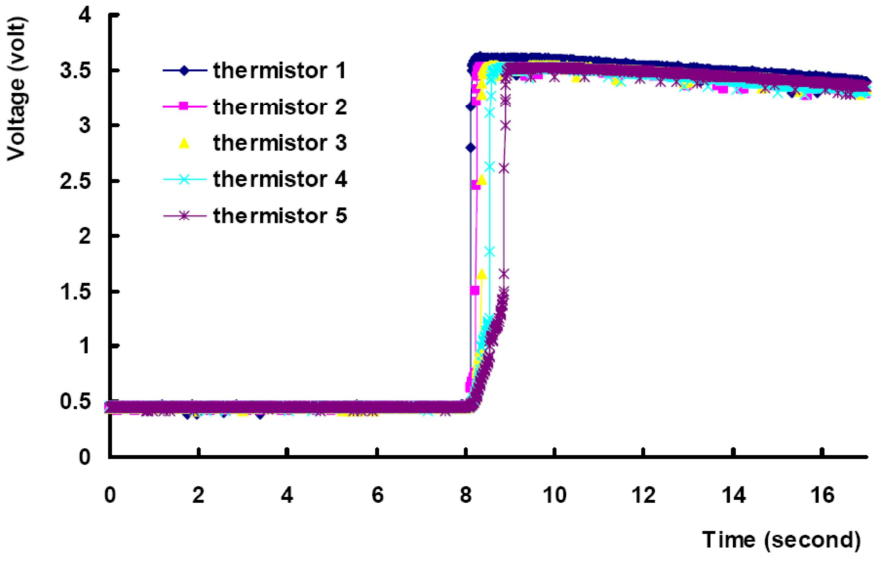

Fig. 3.11. Continued.

Table 3.1 shows the probability of continuous flame propagation at different volume concentrations of ethylene in air. At every concentration point, experimental measurement was repeated 10 times, and the probability of continuous flame propagation was calculated by the ratio of continuous flame propagation times to the total experimental times. The probability of continuous flame propagation against ethylene volume concentration was plotted in Figure 3.12. The LFL of ethylene in air was obtained by picking methane concentration point with 50% probability of continuous flame propagation.

Table 3.1 Probabilities of continuous flame propagation at different concentrations of ethylene in air.

Ethylene Conc. (molar %)*	Measurement times	Continuous Flame Propagation times	Probability of Continuous Propagation
2.78	10	0	0%
2.79	10	2	20%
2.80	10	4	40%
2.81	10	6	60%
2.82	10	7	70%
2.83	10	7	70%
2.84	10	10	100%

* @ room temperature (25 ^{o}C) and 1 atmospheric pressure

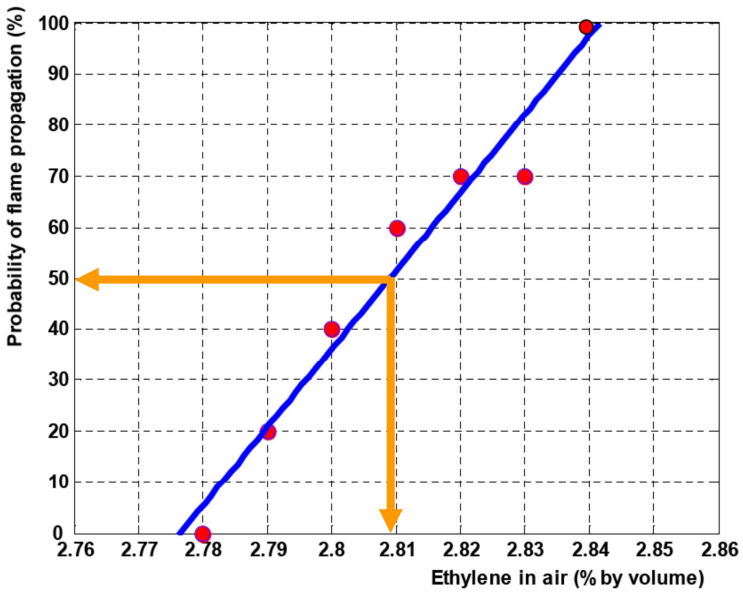

Fig. 3.12. Determination of ethylene LFL in air using thermal criterion.

Experimental LFLs of pure ethylene in this research were compared with some literature data with different experimental apparatus and detection criteria. The comparisons are shown in Table 3.2. Obviously, the experimental results from this research differ from previous measurements because the experimental flammability limits are extremely sensitive to the flammability apparatus and detection criteria.

Table 3.2 Low flammability limits of ethylene in air ((25 ºC and 1 atm).

Ethylene LFL in air (vol %)	**Apparatus types**
3.05	Vertical glass cylinder
2.62	20 L sphere, 7% pressure rise
2.4	EN 1839 (T)
2.6	EN 1839 (B)
2.81±0.09	This research

CHAPTER IV

FUEL MIXTURE FLAMMABILITY IN AIR WITHOUT INERT GAS ADDITION

The flammability limits (LFL and UFL) of binary hydrocarbon mixtures in air without addition of inert gases were measured in my previous work [72]. The experimentally determined flammability limits for binary hydrocarbons were compared with the predictions from Le Chatelier's law. In conclusions, the predictions of fuel mixture lower flammability limits using Le Chatelier's law can fit experimental data well within the experimental uncertainties. For upper flammability limits of fuel mixtures that contain two saturated hydrocarbons, the experimental observations can be roughly fit by the estimations from Le Chatelier's law; however, when fuel mixtures contain at least one unsaturated hydrocarbon component, Le Chatelier's law loses its power to predict the upper flammability limits of fuel mixtures.

Modification of Le Chatelier's law was conducted for fuel mixtures which contains unsaturated hydrocarbon. The way to conduct the modification was done by powering the percentage concentrations of fuels in the original Le Chatelier's law from maximum R-square values (close to 1). This empirical modification significantly increases the prediction accuracy for industrial purposes. As examples, Equations 4.1 - 4.4 represent the best fitting curves of the modified Le Chatelier's law for the

hydrocarbon combinations of methane and ethylene, methane and acetylene, ethylene and propylene, and ethylene and acetylene [72].

$$\frac{1}{UFL_{methane/ethylene}} = \frac{x^{1.3}}{UFL_{methane}} + \frac{(1-x)^{0.6}}{UFL_{ethylene}} \tag{4-1}$$

$$\frac{1}{UFL_{methane/acetylene}} = \frac{x^{2.1}}{UFL_{methane}} + \frac{(1-x)^{0.3}}{UFL_{acetylene}} \tag{4-2}$$

$$\frac{1}{UFL_{ethylene/propylene}} = \frac{x^{0.3}}{UFL_{ethylene}} + \frac{(1-x)^{1.3}}{UFL_{propylene}} \tag{4-3}$$

$$\frac{1}{UFL_{ethylene/acetylene}} = \frac{x}{UFL_{ethylene}} + \frac{(1-x)^{1.3}}{UFL_{acetylene}} \tag{4-4}$$

A more detailed information can be referred from the author's previous work: "F. Zhao, W.J. Rogers, M.S. Mannan, Experimental measurement and numerical analysis of binary hydrocarbon mixture flammability limits. Process Safety and Environmental Protection, 87 (2009) 94-104."

CHAPTER V

FUEL MIXTURE FLAMMABILITY IN AIR WITH INERT GAS ADDITION

5.1 Overview

As a result of high safety requirements imposed on process plants, the larger flexibility to facilitate variety in feedstock, the design of new processes making use of intensified conditions and in general for hazard analysis, accurate prediction of explosion limits of mixtures of flammable substances is highly desirable. The evaluation of flammability limits is not absolute, but rather depends on experimental conditions. There are no definite parameters to quantitatively characterize the flammability limits. In practice, the limits of flammability of a particular system of air-fuel are affected by a variety of factors including temperature, pressure, oxygen concentration, inert gas addition, size and shape of equipment.

Due to the non-ozone-depleting, non-toxic and non-pyrolytic properties, some inert gas agents, mostly including nitrogen, carbon dioxide, and argon, are classified as clean fire-extinguishing agents of interest for fire suppression. To control fire and explosion, inert additives are sometimes added to mixtures in order to narrow their flammable ranges or to render the mixture entirely non-flammable. Besnard's [11] report provided some excellent examples of the influence of inert gases on the flammability limits, where different inert gas inactivating capacities to reduce the flammable ranges of

fuel-air mixtures are systematically investigated. For most hydrocarbon gases, nitrogen in the amount of 40-50 vol % must be added to a fuel/air mixture to make it non-flammable [4].

In this section, the experimentally determined lower flammability limits, upper flammability limits, and minimum inerting concentrations (MICs) were collected at ambient conditions for binary hydrocarbon mixtures with additional nitrogen at different concentrations. The experimentally conducted hydrocarbons include methane, ethylene, ethane, propylene, propane and n-butane. The binary hydrocarbon mixtures include methane and propane, ethane and propane, methane and ethylene, and n-ethylene and propylene. From experimental observation, apparently, when progressive amounts of an inert gas are added to a fuel-air mixture, LFL and UFL come closer and merge into a unique value, the MIC. All of the additives are able to make a mixture non-flammable if the added is in sufficient quantities. Particularly, fuel mixture LFLs almost keep constant with addition of extra nitrogen, while UFLs decline dramatically.

Furthermore, numerical data analysis was conducted in this section to quantify nitrogen dilution effect on hydrocarbon mixture flammability limits. Here, a specific parameter, the inert gas dilution coefficient, was introduced from each pure hydrocarbon flammability limit data, and the inert gas dilution effect of fuel mixture was numerically regressed based on hydrocarbon mixture experimental results. The flammability limits of hydrocarbon mixtures with addition of nitrogen were quantitatively characterized by combining the inert gas dilution coefficient and Le Chatelier's law (or modified Le Chetelier's law).

5.2 Experimental results

The flammability limits (LFLs and UFLs) with varied amounts of additional inert gas, nitrogen, were measured for pure hydrocarbons and some of their binary mixtures in air at room temperature and ambient atmospheric pressure. As an example, Figure 5.1 shows methane flammability limit with dilution of nitrogen in the triangular and rectangular coordinate systems. Approximately, methane lower flammability limit remains constant with addition of nitrogen; the upper flammability limit, however, decreases dramatically. These two values become closer with continuous addition of nitrogen, and finally merge at the MIC point, beyond which fire or explosion is impossible. The region enclosed by the LFL and UFL curves is called the flammable zone. Outside of this region, fuel mixture is non-flammable. Specifically, a small zone close to the point, MIC, is set aside and defined as the flammability nose, where the flammability properties become deviant.

Figure 5.2 shows a comparison of experimental methane flammability limits from this research and US. Bureau of Mines (BMs) [4]. Although the same flame propagation criteria were applied for flammability detection in this research and BMs, the exhibited differences may come from other sources, very possibly the different geometries and configurations of reaction vessels from each other. Taking into account the experimental uncertainty and the non-fundamental property of flammability, the obtained experimental data here are reasonable, and also feasible for industrial application.

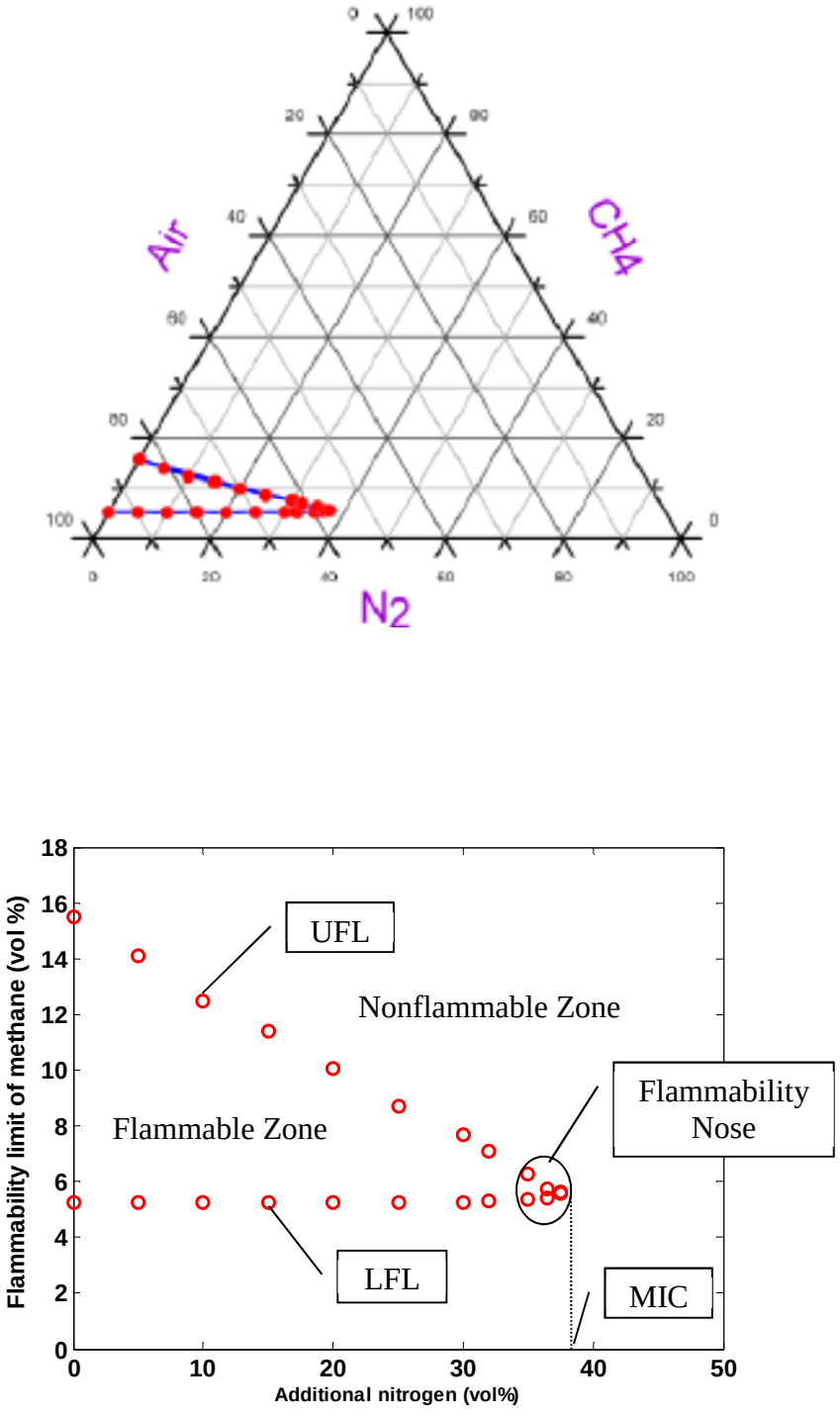

Fig. 5.1. Methane flammability properties with dilution of nitrogen (25 °C and 1 atm) in the triangular (top) and rectangular coordinate (bottom) systems.

Because most of the hydrocarbons and their mixtures have narrow flammable zones, all the tested flammability limit data were plotted in the rectangular coordinate system for easily reading, where x-axis represents the volume percentage (vol%) of additional nitrogen, y-axis is the flammability limit. Air volume percentage (vol%) can be easily calculated using Eq. (5-1).

$$Air\ vol\% = 100\% - Fuel\ vol\% - Nitrogen\ vol\% \tag{5-1}$$

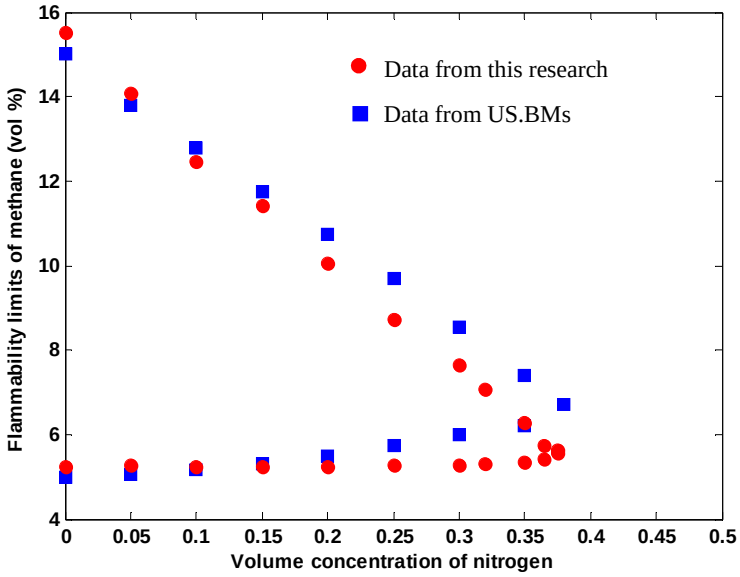

Fig. 5.2. Comparison of methane flammability limit with nitrogen dilution between this research and a previous one from U.S. BMs.

Figures 5.3 – 5.7 show the flammability envelopes of pure hydrocarbons, ethane, propane, n-butane, ethylene, and propylene, respectively, in rectangular coordinate systems.

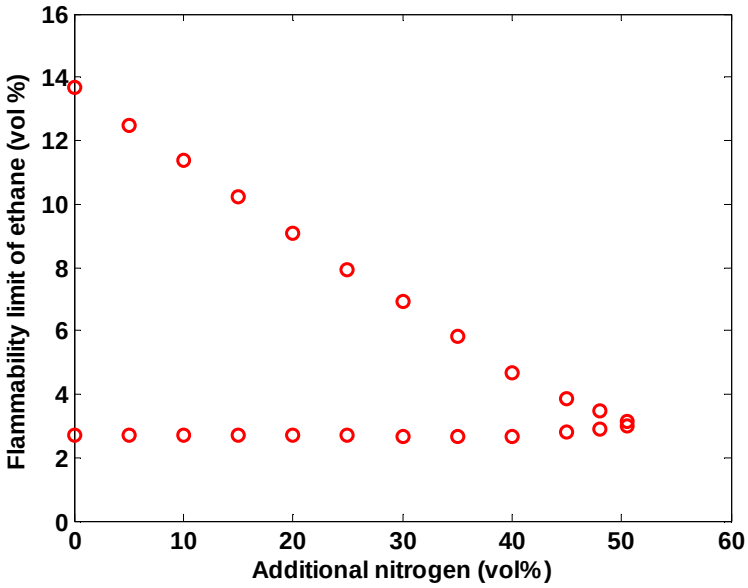

Fig. 5.3. Ethane flammability properties with dilution of nitrogen (25 °C and 1 atm).

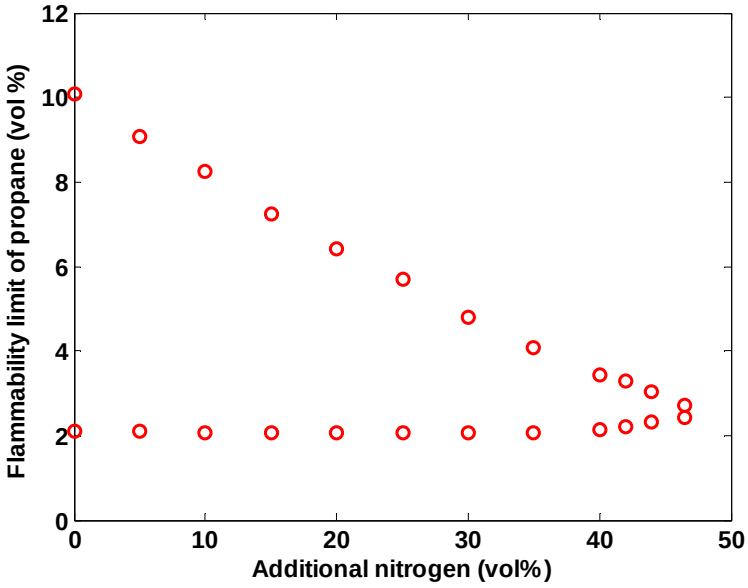

Fig. 5.4. Propane flammability properties with dilution of nitrogen (25 °C and 1 atm).

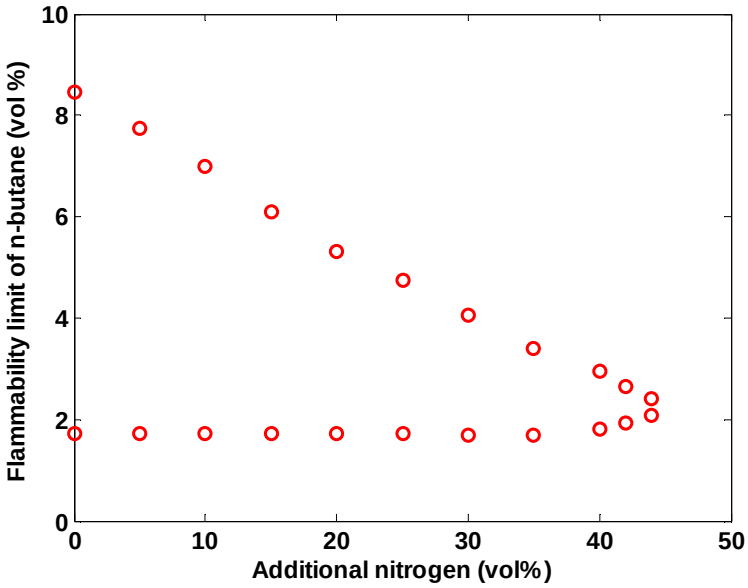

Fig. 5.5. N-butane flammability properties with dilution of nitrogen (25 °C and 1 atm).

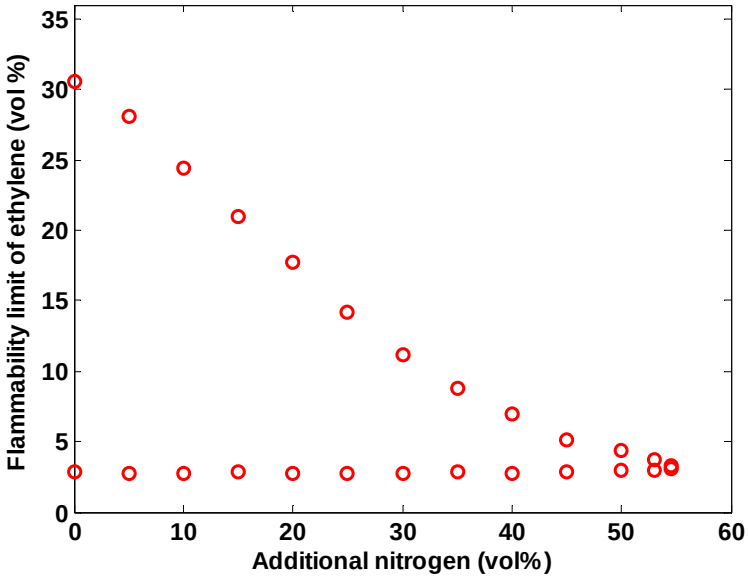

Fig. 5.6. Ethylene flammability properties with dilution of nitrogen (25 °C and 1 atm).

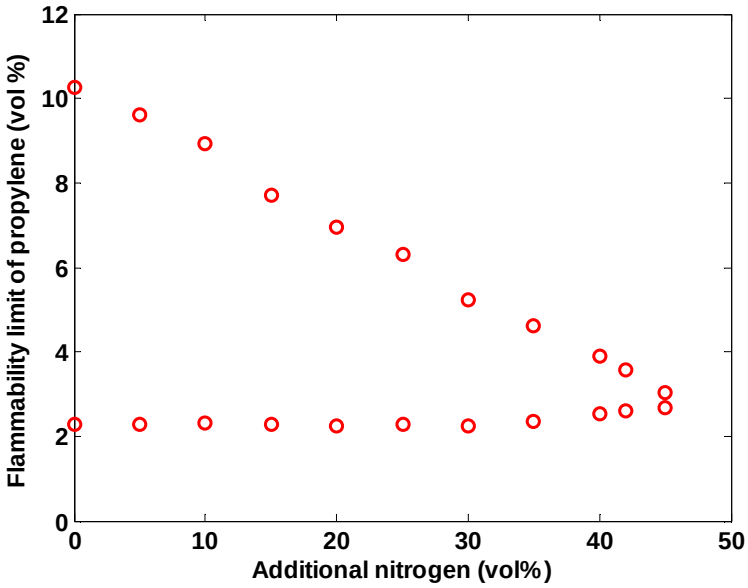

Fig. 5.7. Propylene flammability properties with dilution of nitrogen (25 °C and 1 atm).

Figures 5.8 – 5.11 show the flammability envelopes of binary hydrocarbon mixtures of methane and propane, ethane and propane, methane and ethylene, and ethylene and propylene at different molar ratios (20 %/80%, 40%/60%, 60%/40%, and 80%/20%).

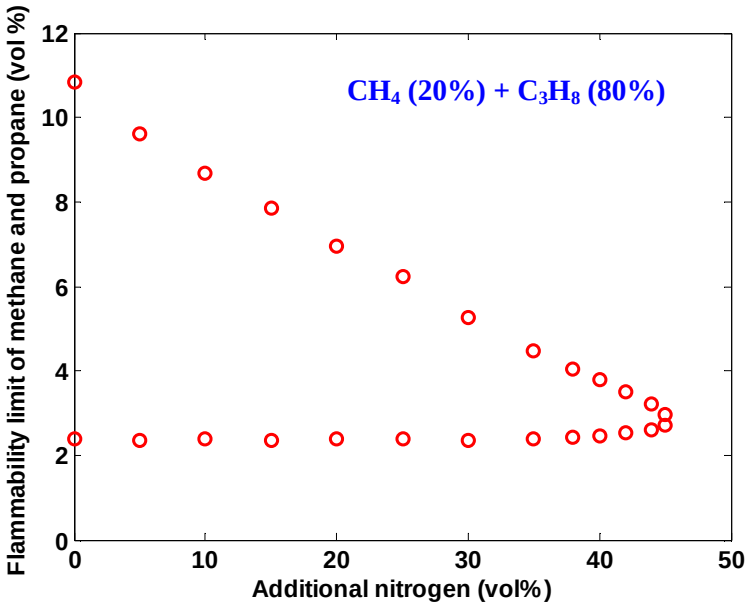

Fig. 5.8. Flammability properties of methane and propane at different molar radios (20 %/80%, 40%/60%, 60%/40%, and 80%/20%) with dilution of nitrogen (25 °C and 1 atm).

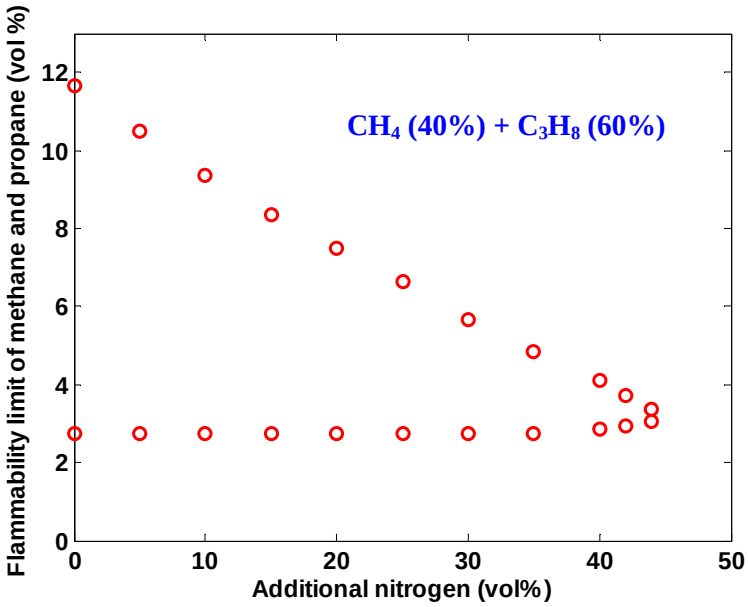

Fig. 5.8. Continued.

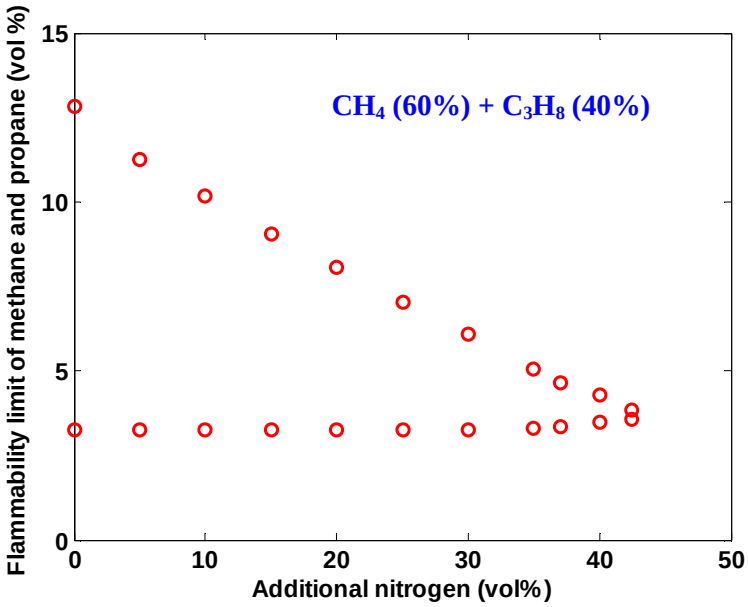

Fig. 5.8. Continued.

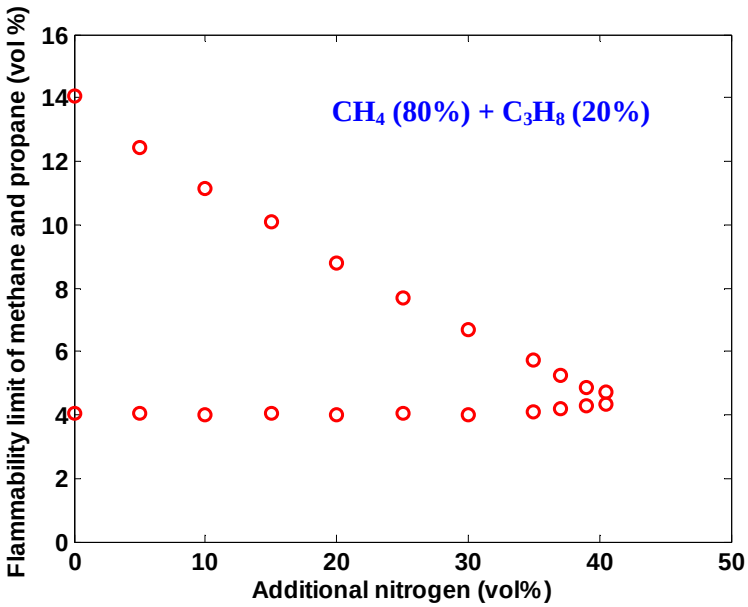

Fig. 5.8. Continued.

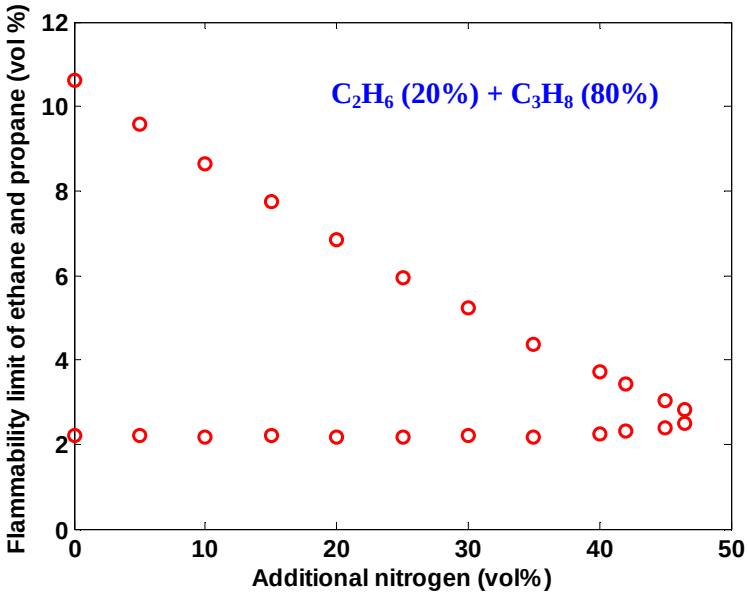

Fig. 5.9. Flammability properties of ethane and propane at different molar radios (20 %/80%, 40%/60%, 60%/40%, and 80%/20%) with dilution of nitrogen (25 °C and 1 atm).

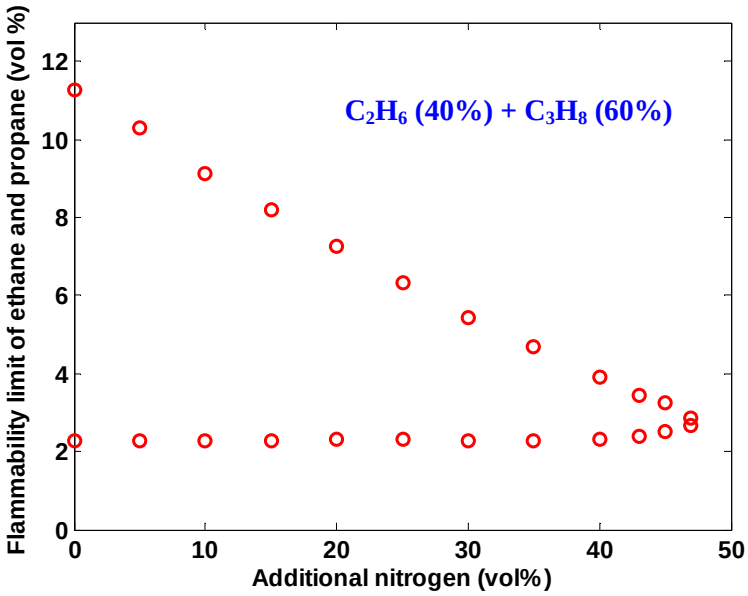

Fig. 5.9. Continued.

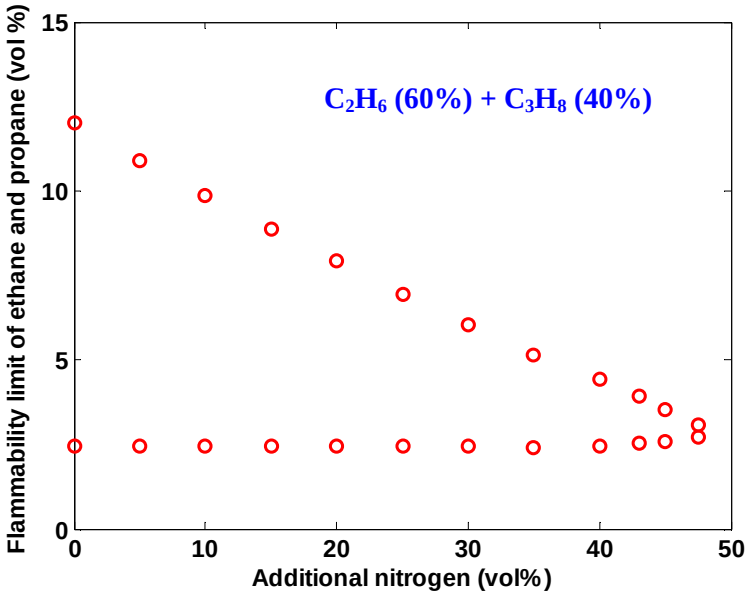

Fig. 5.9. Continued.

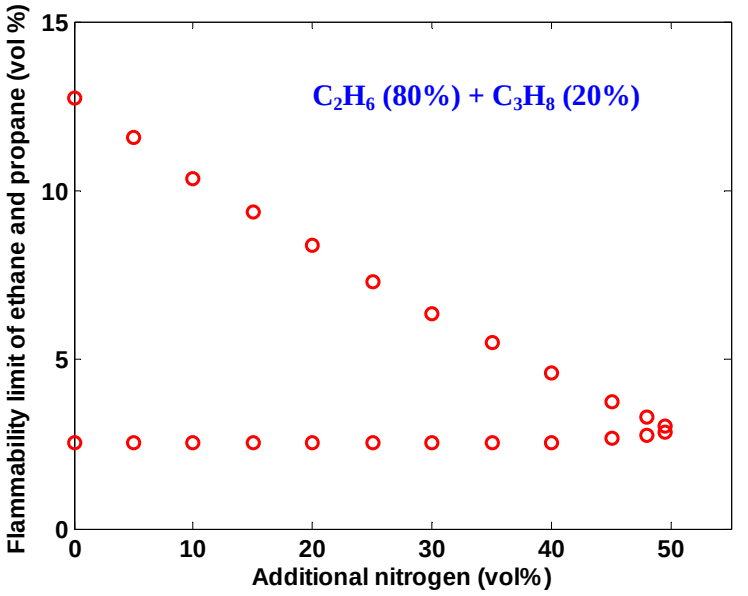

Fig. 5.9. Continued.

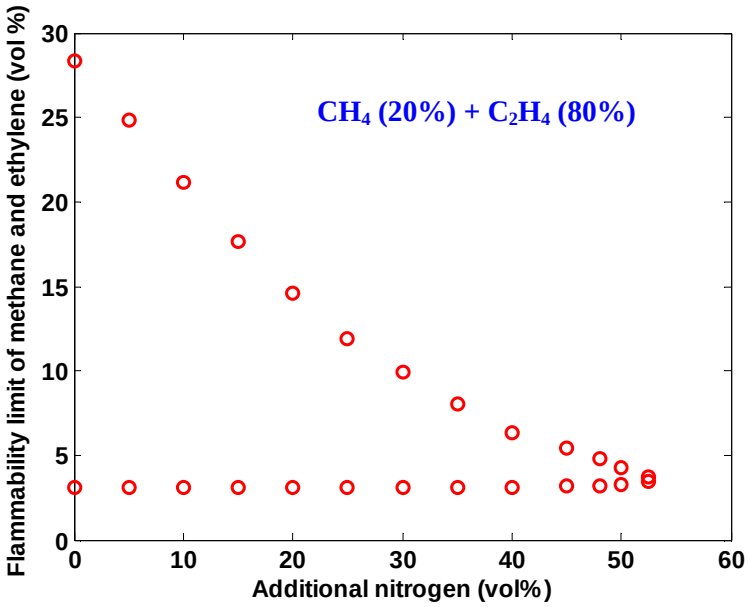

Fig. 5.10. Flammability properties of methane and ethylene at different molar radios (20 %/80%, 40%/60%, 60%/40%, and 80%/20%) with dilution of nitrogen (25 °C and 1 atm).

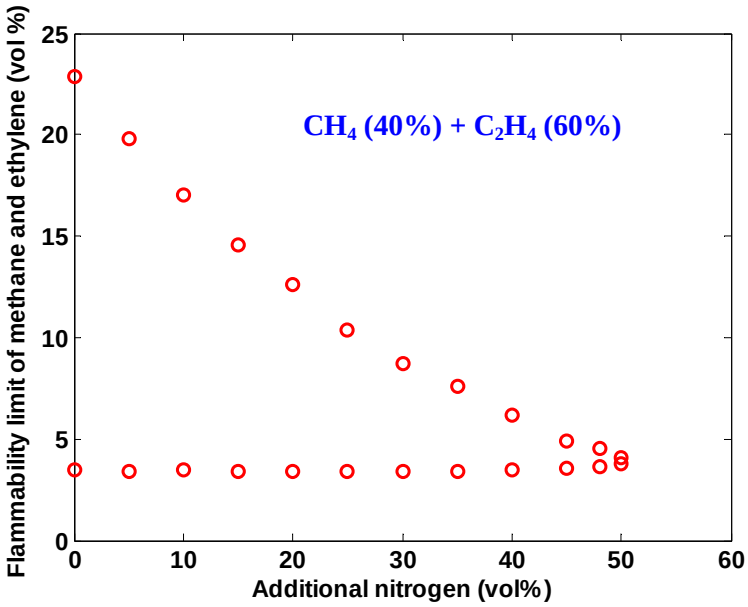

Fig. 5.10. Continued.

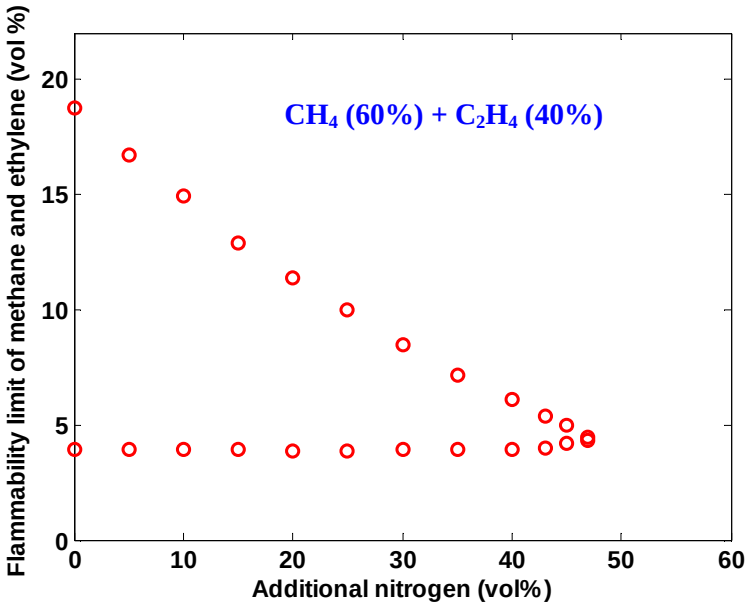

Fig. 5.10. Continued.

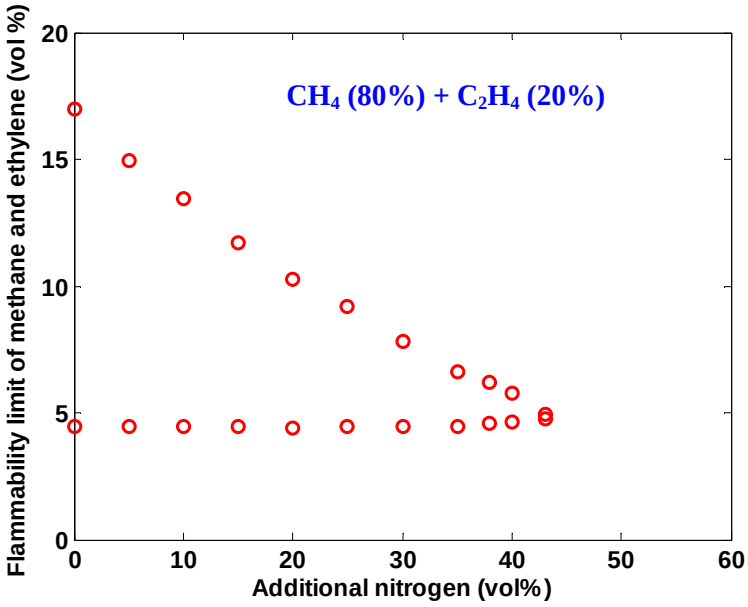

Fig. 5.10. Continued.

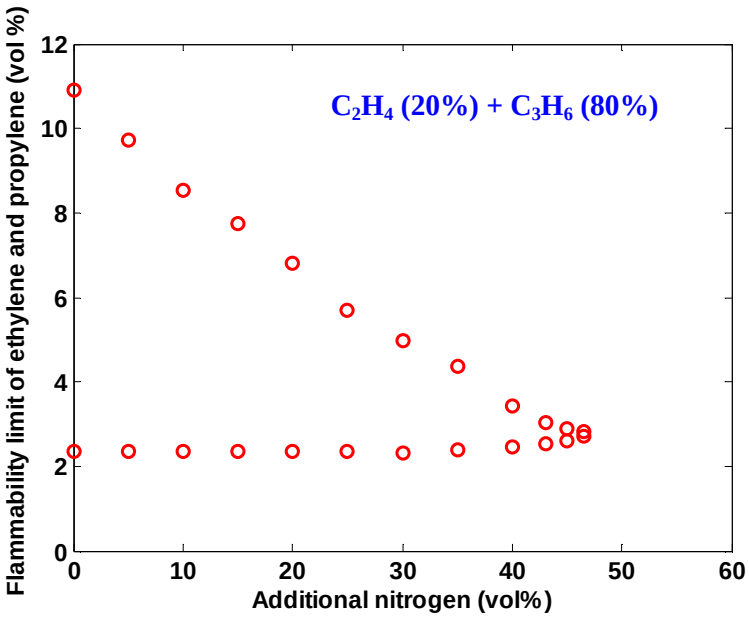

Fig. 5.11. Flammability properties of ethylene and propylene at different molar radios (20 %/80%, 40%/60%, 60%/40%, and 80%/20%) with dilution of nitrogen (25 °C and 1 atm).

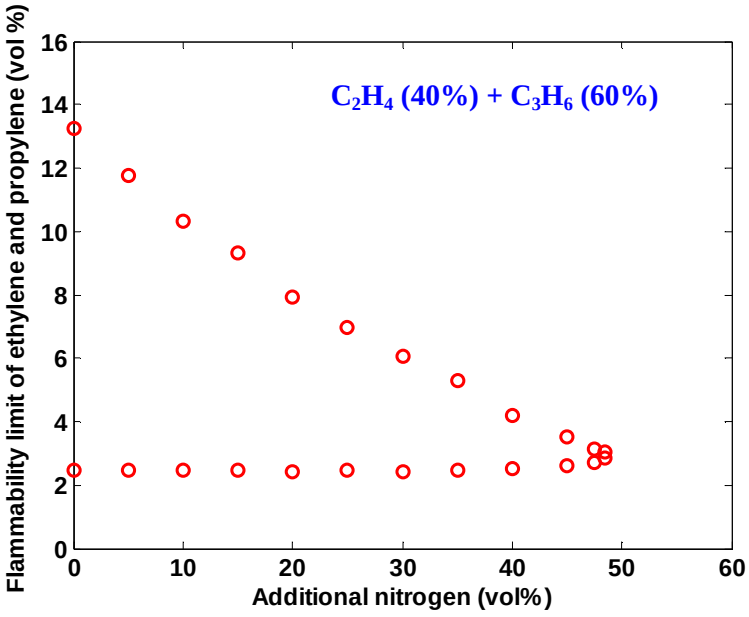

Fig. 5.11. Continued.

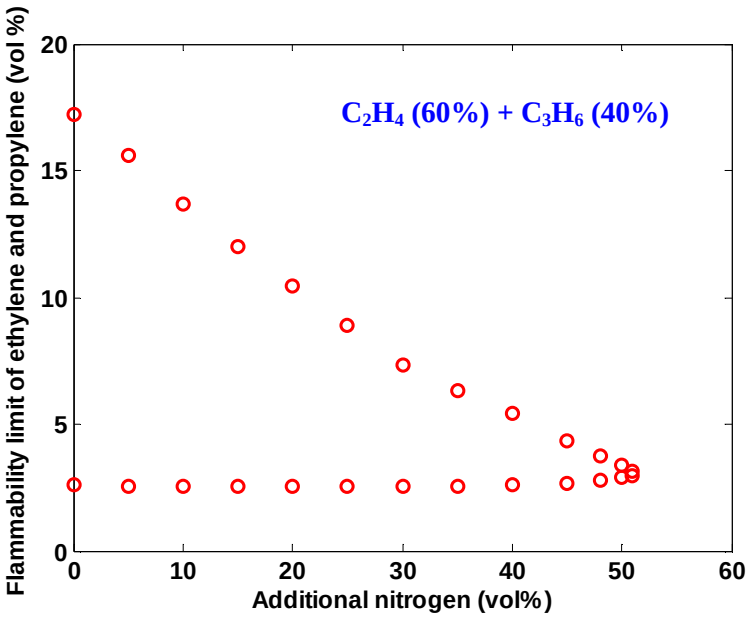

Fig. 5.11. Continued.

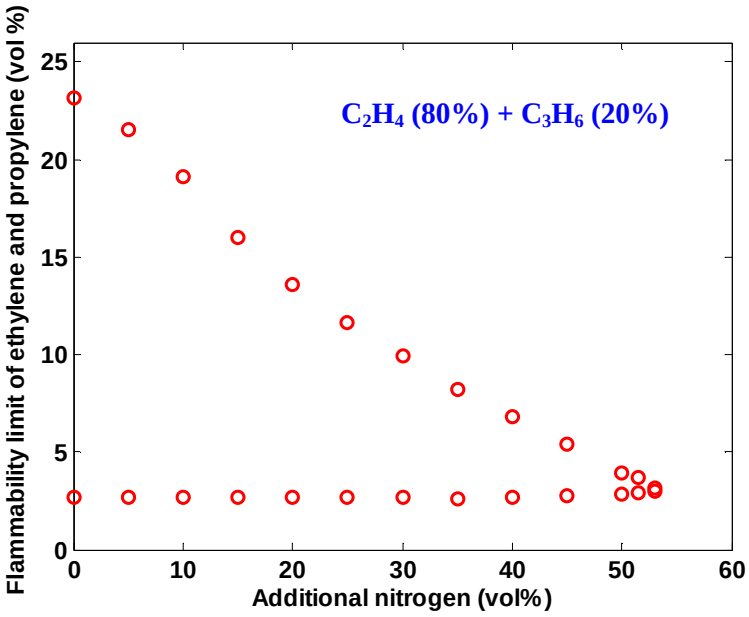

Fig. 5.11. Continued.

5.3 Numerical data analysis

Le Chetalier's law is extensively used because of its simplicity and effectiveness to estimate the flammability limits of fuel mixtures; its application, however, focuses on fuel mixture in air without additional inert component introduced [64]. In the chemical process industries, fire suppression or storage tank blanketing using inert gas, for example, nitrogen, is strongly recommended; therefore, fuel mixture flammability properties diluted with nitrogen is becoming an extremely significant safety issue today. In this section, numerical data analysis was conducted to extend Le Chatelier's law application, which included some proposed empirical equations, e.g., LFL and UFL quantitative characterization with addition of inert gas nitrogen, and MIC at different fuel mixture compositions.

5.3.1 Hydrocarbon mixture LFL

Modification of Le Chatelier's law on binary hydrocarbon mixture LFL with dilution of inert gas was conducted by introducing the concept of the inert gas dilution coefficient, $\gamma^{L,inert}$, for every pure fuel. $\gamma^{L,inert}$ is defined as the ratio of lower flammability limit change (ΔLFL) to the related change of the inert gas volume concentration (ΔX) (Eq. (5-2)).

$$\gamma^{L,inert} = \frac{\Delta LFL}{\Delta X} \tag{5-2}$$

As illustrated in the experimental results, the LFLs of all selected pure hydrocarbons change slightly with addition of nitrogen, and approximately they can be linearly related within the experimental uncertainty. For simplicity, we took the slope of the regressed linear curve as the inert gas dilution coefficient, and intercept as the fuel lower flammability limit in air without additional nitrogen. Figures 5.12 – 5.17 show the regressed linear curve from experimental LFLs of pure hydrocarbons (methane, ethane, propane, n-butane, ethylene, and propylene, respectively) with dilution of nitrogen. The obtained nitrogen dilution coefficients for all the selected pure hydrocarbons are listed in Table 5.1.

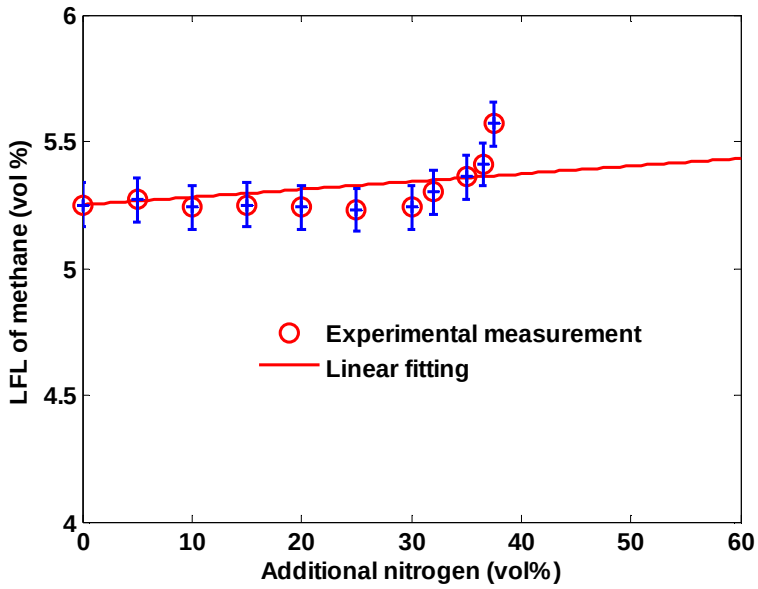

Fig. 5.12. Experimental methane LFL diluted with N_2 and the regressed linear curve.

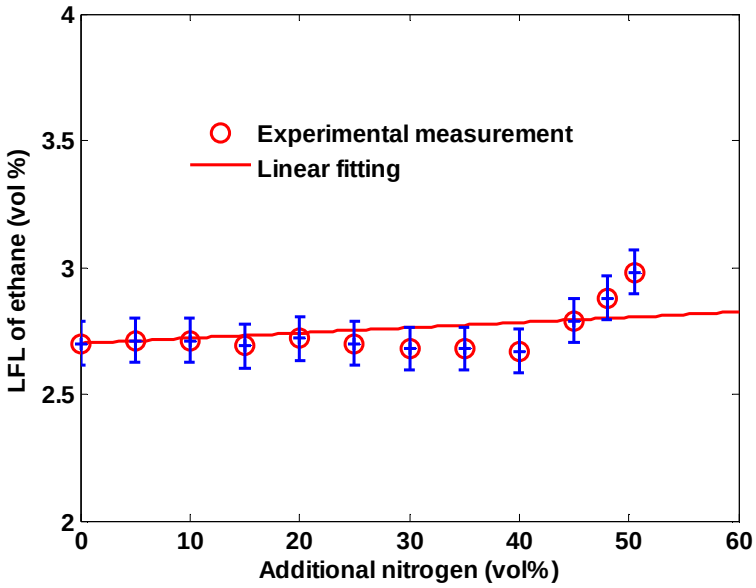

Fig. 5.13. Experimental ethane LFL diluted with N_2 and the regressed linear curve.

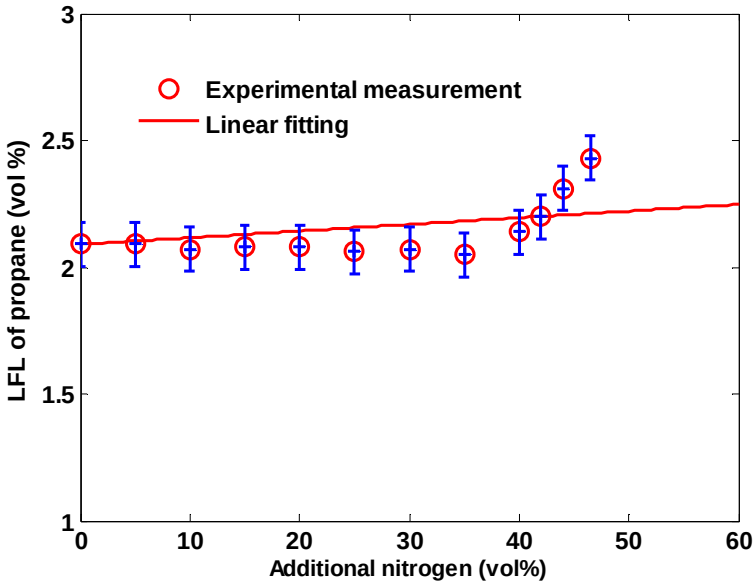

Fig. 5.14. Experimental propane LFL diluted with N_2 and the regressed linear curve.

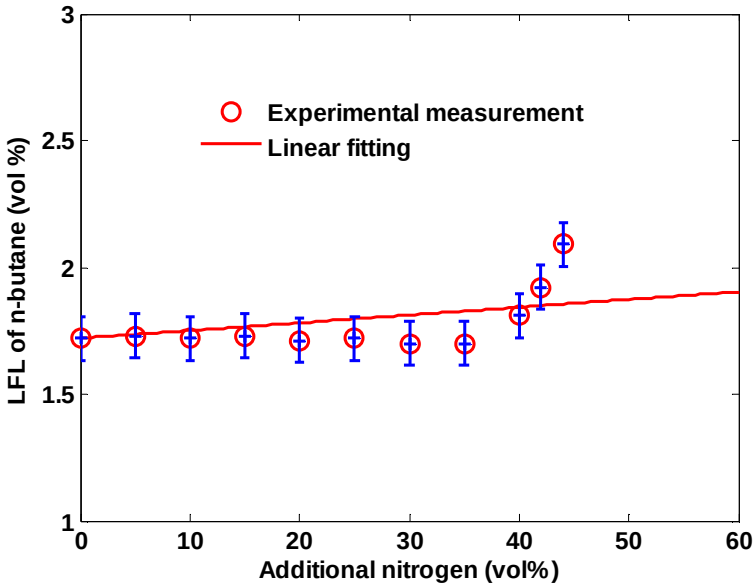

Fig. 5.15. Experimental n-butane LFL diluted with N_2 and the regressed linear curve.

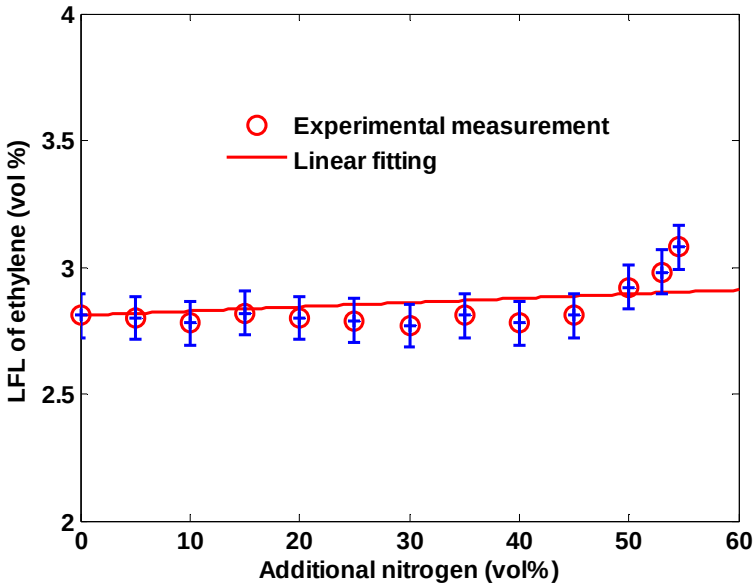

Fig. 5.16. Experimental ethylene LFL diluted with N_2 and the regressed linear curve.

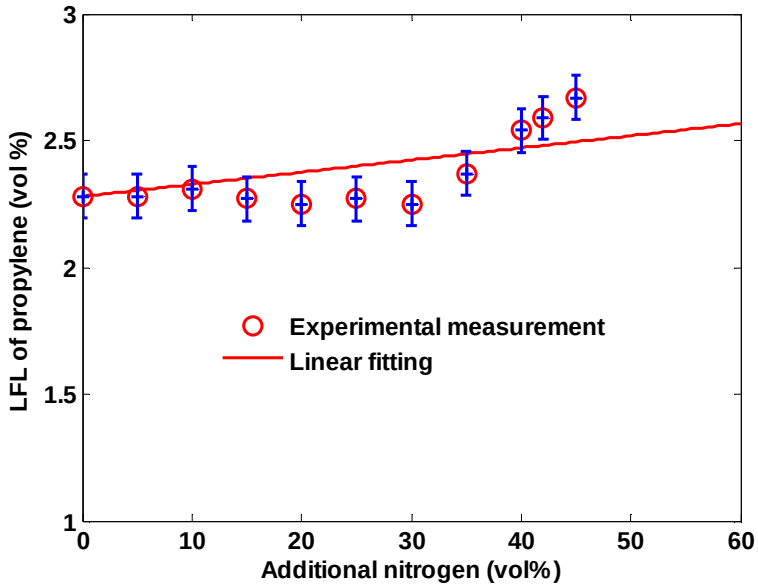

Fig. 5.17. Experimental propylene LFL diluted with N_2 and the regressed linear curve.

Table 5.1. N_2 dilution coefficients on LFLs of pure hydrocarbons.

Chemicals	γ^{L,N_2}
Methane	0.0031
Ethane	0.0021
Propane	0.0026
n-butane	0.0031
Ethylene	0.0017
Propylene	0.0048

The LFL of a binary hydrocarbon mixture with additional nitrogen dilution was quantitatively correlated to pure fuel flammability properties as the modified Le Chatelier's law. Typically, the fuel mixture LFL values are linearly related to the additional nitrogen volume concentrations. The intercept of the linear curve is the fuel

mixture LFL in air without nitrogen added. The slope is the nitrogen dilution coefficient on fuel mixture (Eq. (5-3)), which can be optimized to a simple equation with the similar expression as the Le Chatelier's law. Figures 5.18 – 5.21 show the experimental data, the modified Le Chatelier's law, and the linear fitting results for the binary hydrocarbon mixtures of methane and propane, ethane and propane, methane and ethylene, and ethylene and propylene at different molar ratios (20 %/80%, 40%/60%, 60%/40%, and 80%/20%).

$$LFL_m^{N_2} = LFL_m + \gamma_m^{L,N_2} X_{N_2} \tag{5-3}$$

where,

$$\frac{1}{LFL_m} = \frac{x_1}{LFL_1} + \frac{x_2}{LFL_2} \qquad \frac{1}{\gamma_m^{L,N_2}} = \frac{x_1}{\gamma_1^{L,N_2}} + \frac{x_2}{\gamma_2^{L,N_2}}$$

$LFL_m^{N_2}$, LFL_m are LFLs of fuel mixture with and without additional nitrogen. LFL_1 and LFL_2 are LFLs of pure fuel-1 and fuel-2 without nitrogen added. γ_1^{L,N_2}, γ_2^{L,N_2}, and γ_m^{L,N_2} are nitrogen dilution coefficients on the LFLs of fuel-1, fuel-2, and their mixture, respectively. x_1, x_2 are the molar fractions of fuel-1 and fuel-2 on combustible basis ($x_1+x_2=1$).

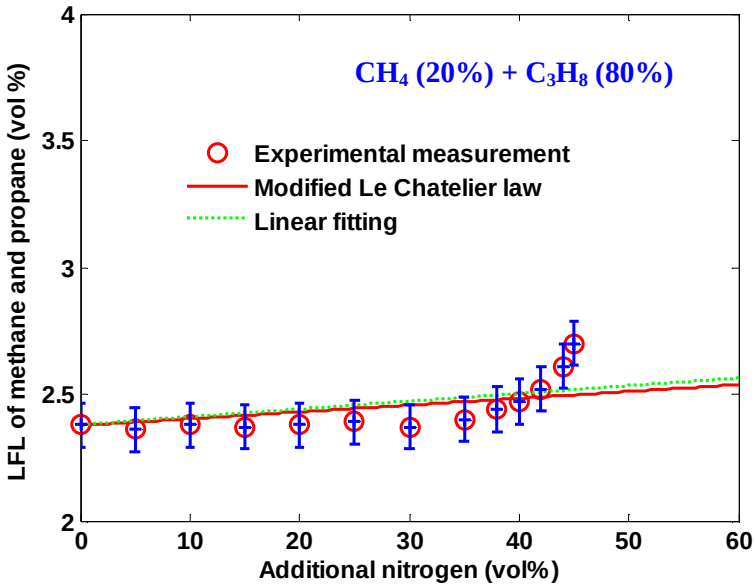

Fig. 5.18. LFL of methane and propane mixture and the modified Le Chatelier's law.

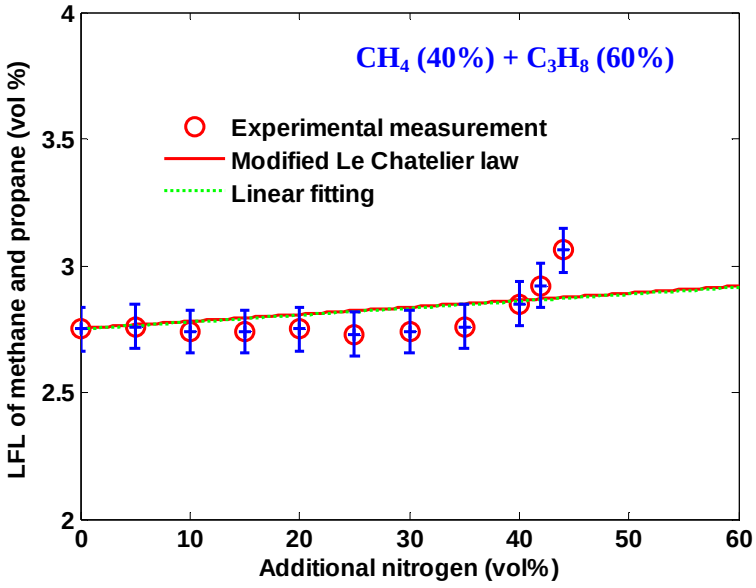

Fig. 5.18. Continued.

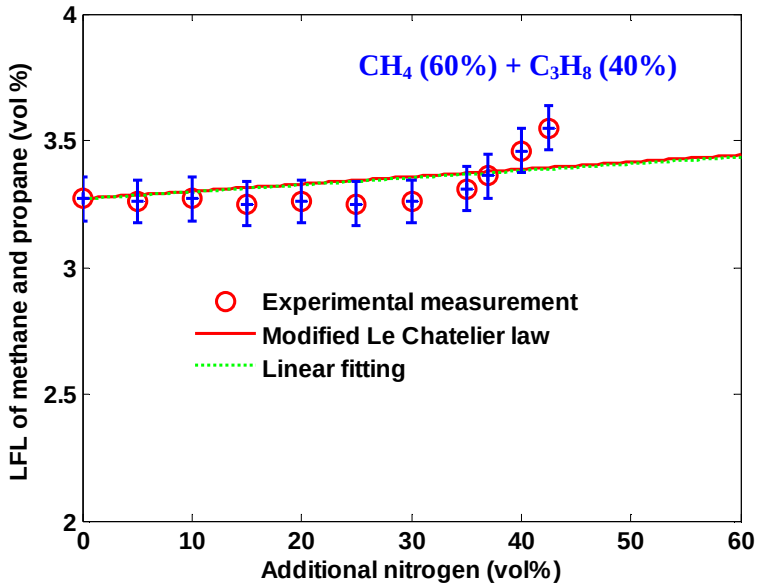

Fig. 5.18. Continued.

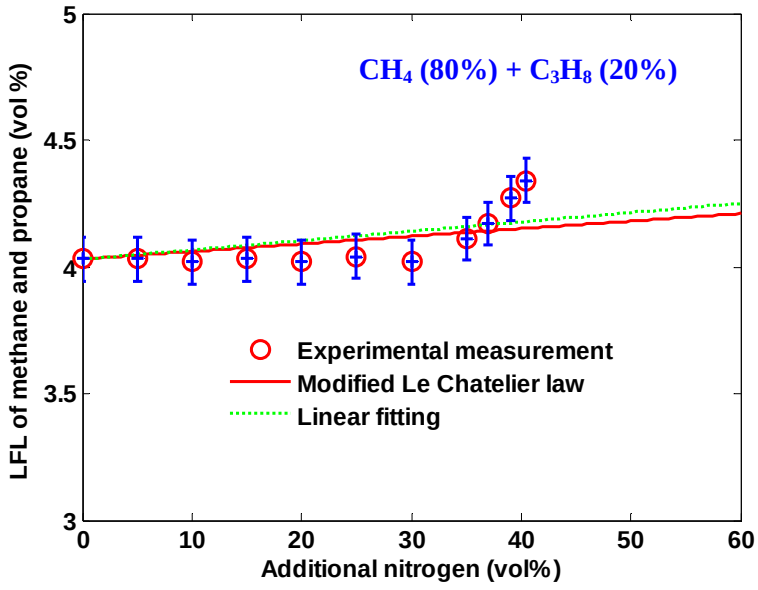

Fig. 5.18. Continued.

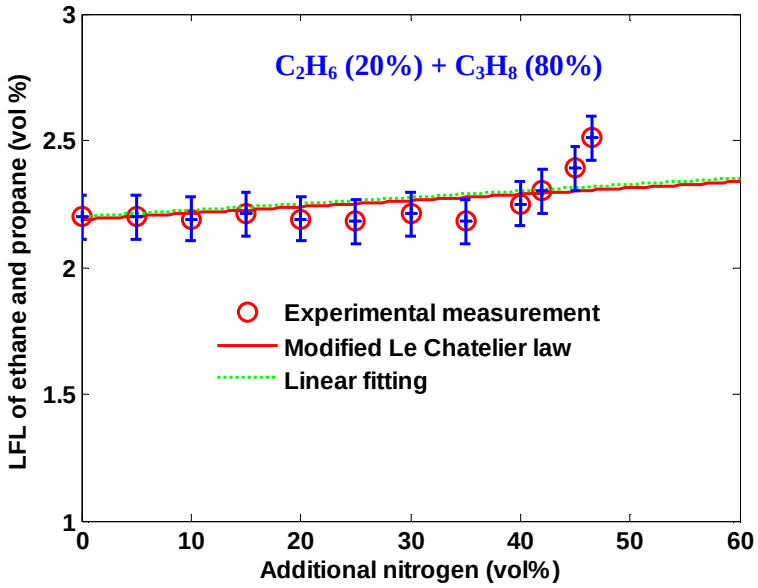

Fig. 5.19. LFL of ethane and propane mixture and the modified Le Chatelier's law.

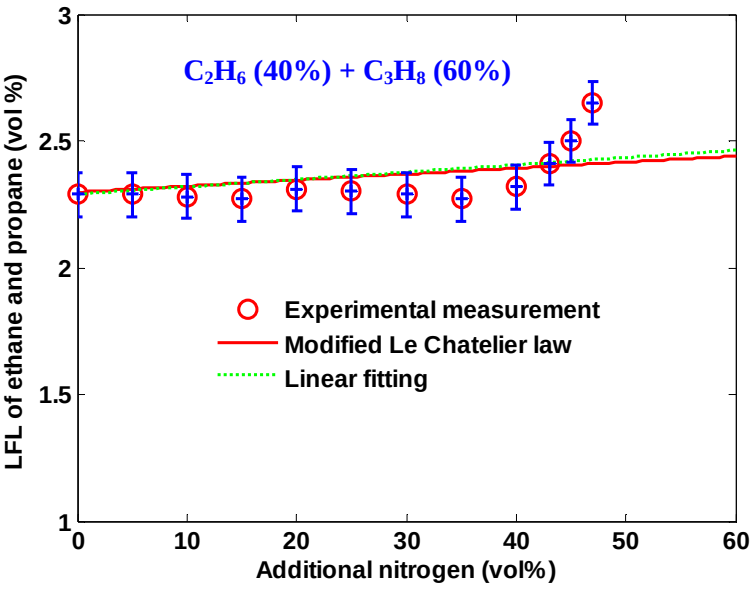

Fig. 5.19. Continued.

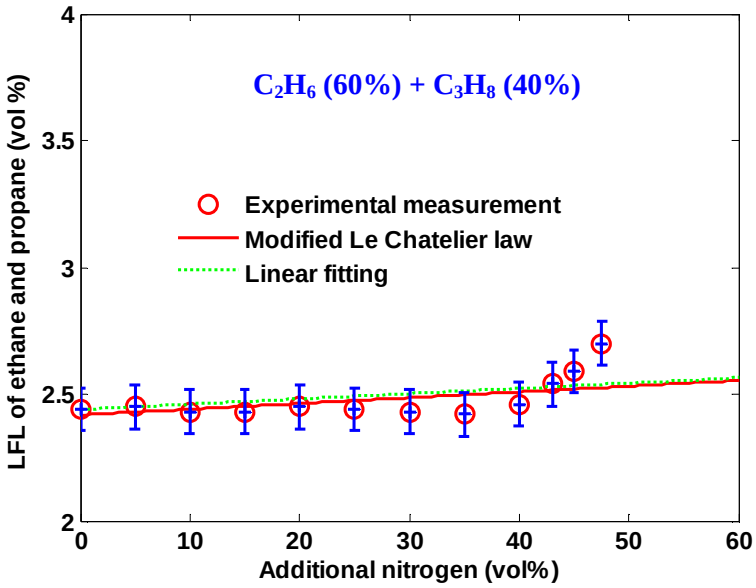

Fig. 5.19. Continued.

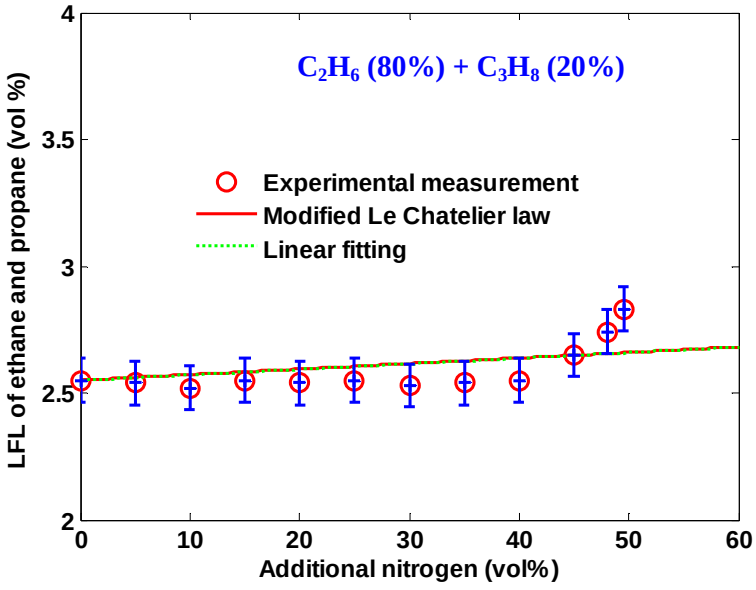

Fig. 5.19. Continued.

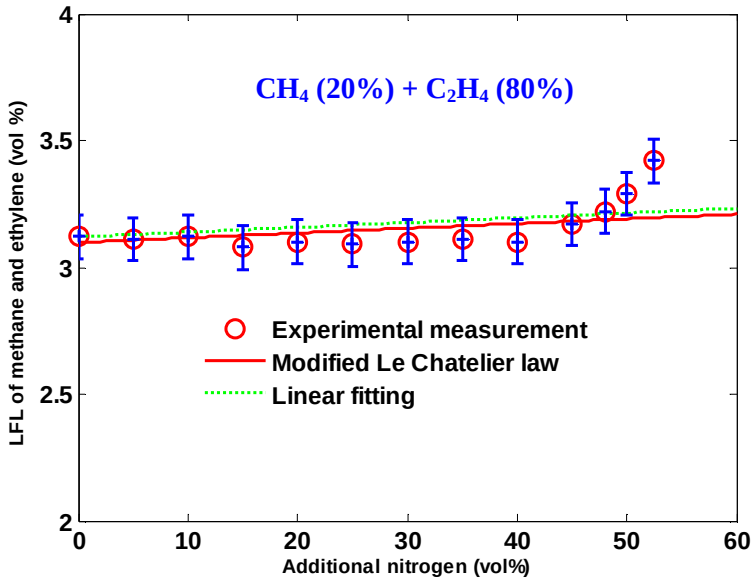

Fig. 5.20. LFL of methane and ethylene mixture and the modified Le Chatelier's law.

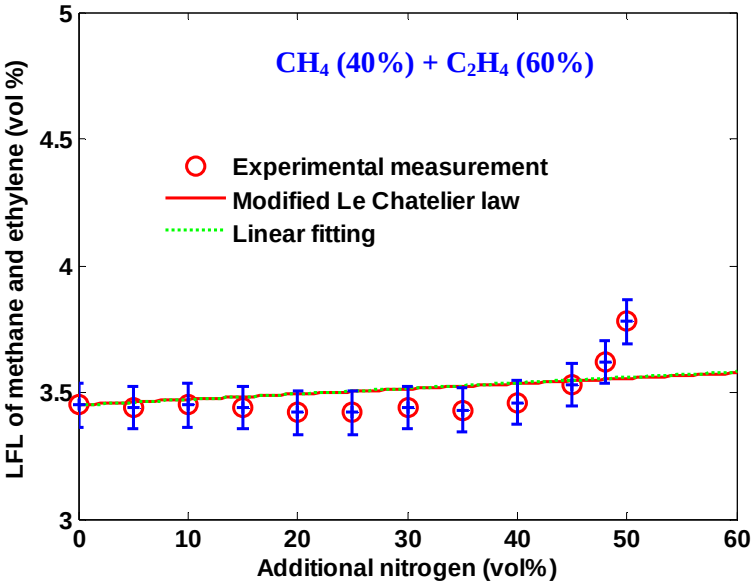

Fig. 5.20. Continued.

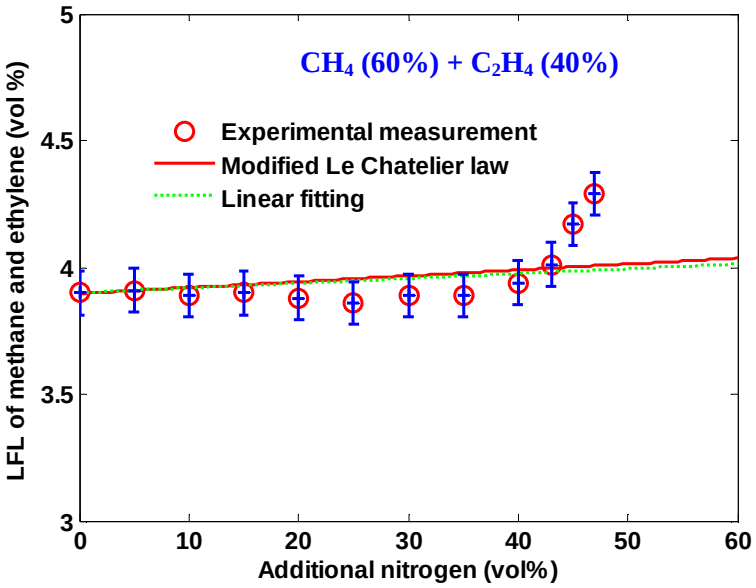

Fig. 5.20. Continued.

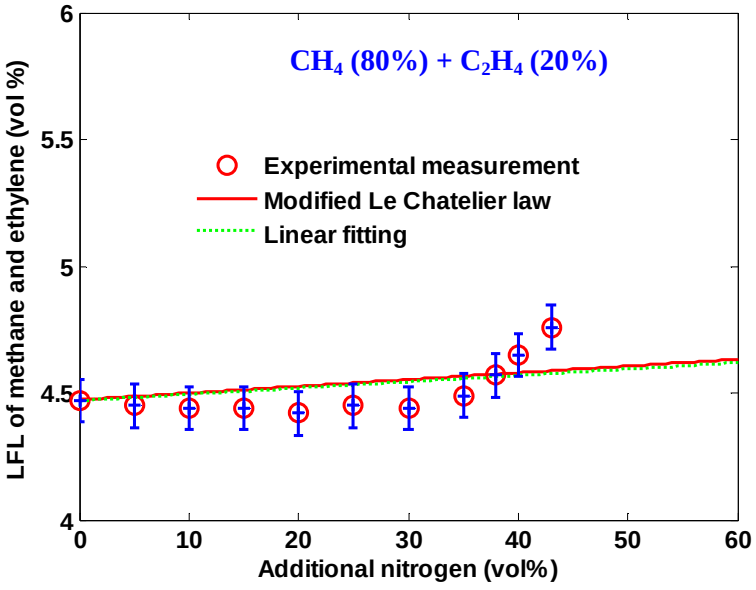

Fig. 5.20. Continued.

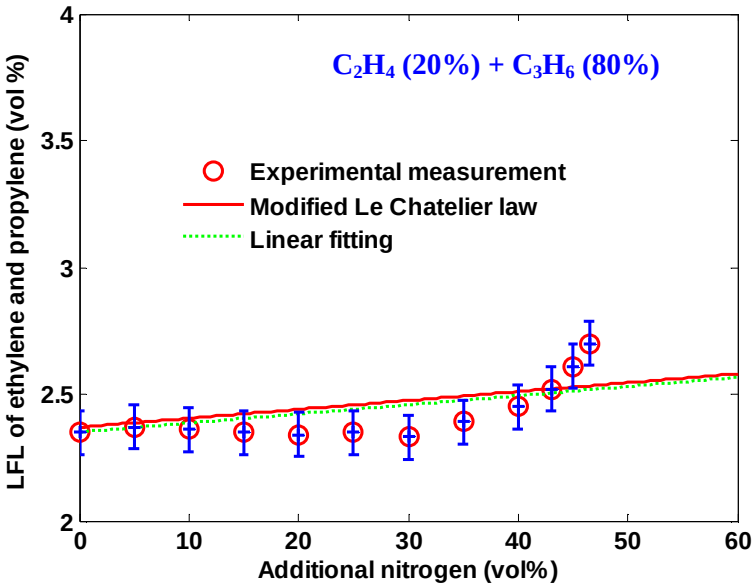

Fig. 5.21. LFL of ethylene and propylene mixture and the modified Le Chatelier's law.

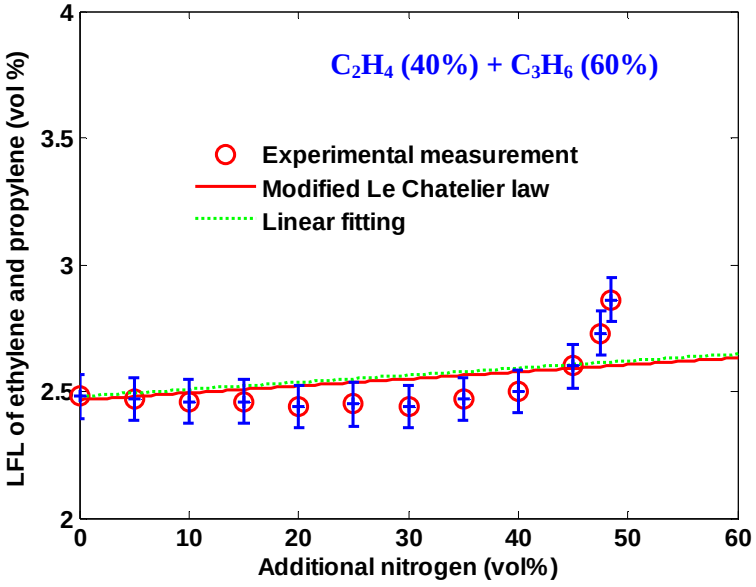

Fig. 5.21. Continued.

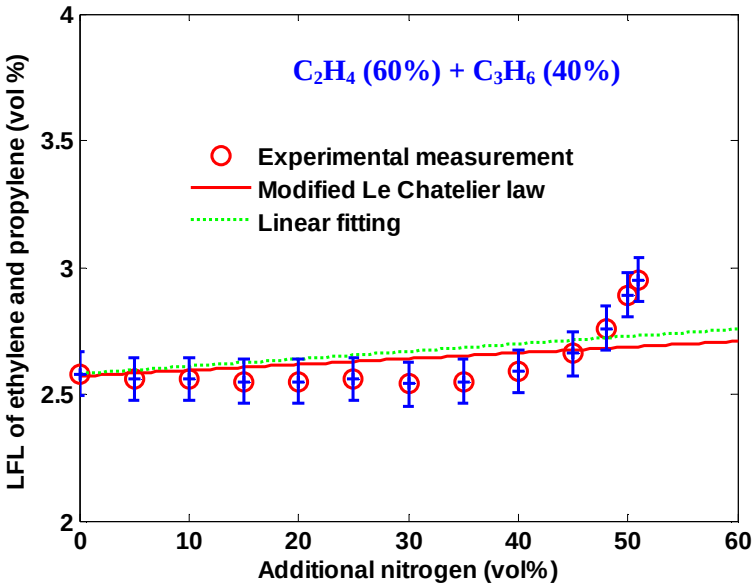

Fig. 5.21. Continued.

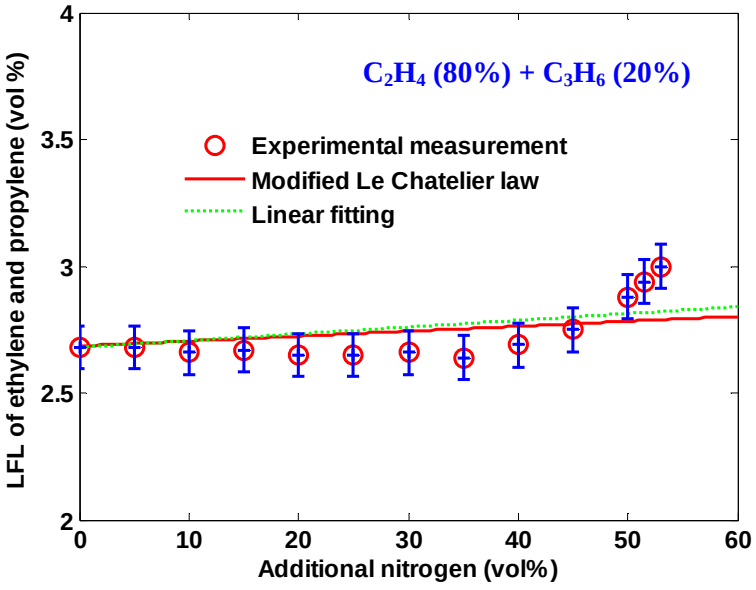

Fig. 5.21. Continued.

5.3.2 Hydrocarbon mixture UFL

Similar to the operation of numerical data analysis on the LFL of binary hydrocarbon mixtures, we introduced the inert gas dilution coefficient on pure hydrocarbon UFL, which was defined as the ratio of upper flammability limit change (ΔUFL) to the change of the related inert gas volume concentration (ΔX) (Eq. (5-4)).

$$\gamma^{U,inert} = \frac{\Delta UFL}{\Delta X} \tag{5-4}$$

Based on the experimental observation, the nitrogen dilution coefficient on the UFL of most selected hydrocarbons (methane, ethane, propane, n-butane, and propylene) can be simplified as the slope of the linearly regressed curve (UFL vs. additional nitrogen volume concentration). Figures 5.22- 5.26 illustrate the regressed lines for pure methane, ethane, propane, n-butane, and propylene, and the intercept of each linear fitting line is the UFL in air without additional nitrogen. Table 5.2 shows the obtained nitrogen dilution coefficients on pure hydrocarbon UFLs.

Table 5.2. N_2 dilution coefficients on UFLs of pure hydrocarbons.

Chemicals	γ^{U,N_2}
Methane	-0.266
Ethane	-0.219
Propane	-0.167
n-butane	-0.142
Propylene	-0.161

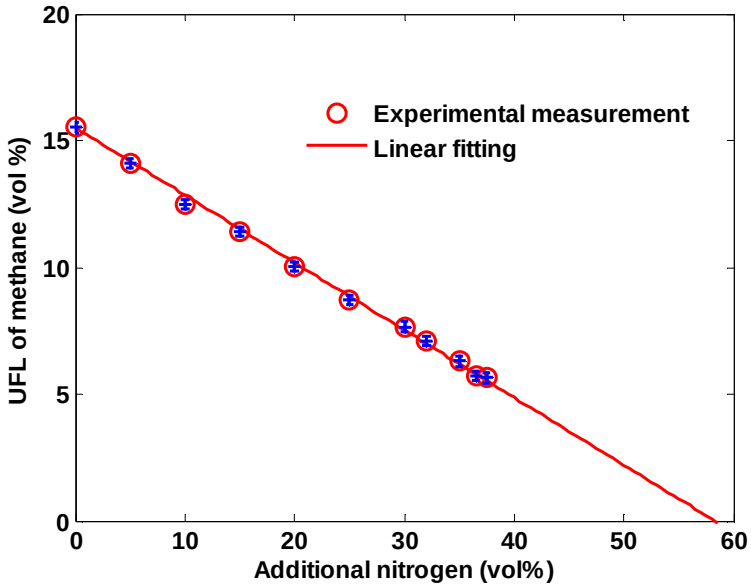

Fig. 5.22. Experimental methane UFL diluted with N_2 and the regressed linear curve.

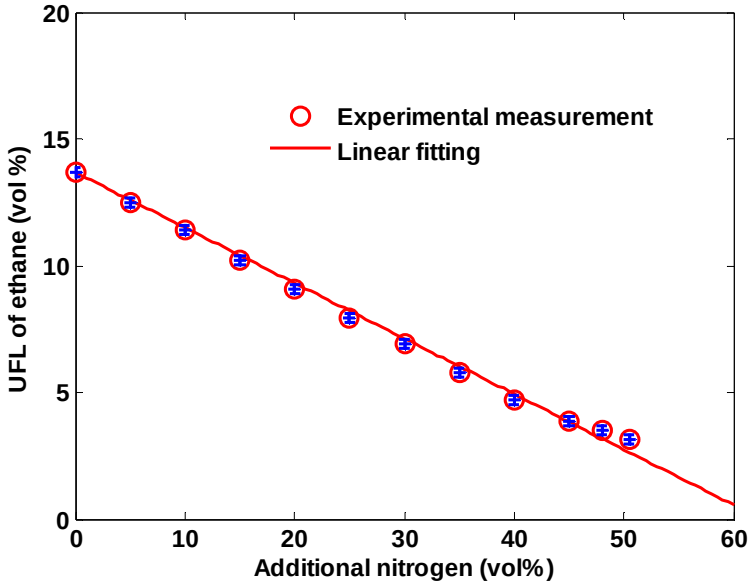

Fig. 5.23. Experimental ethane UFL diluted with N_2 and the regressed linear curve.

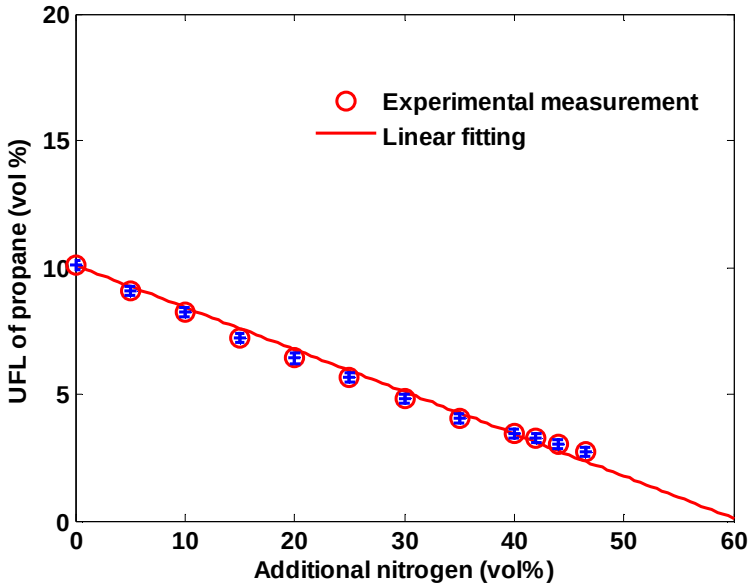

Fig. 5.24. Experimental propane UFL diluted with N_2 and the regressed linear curve.

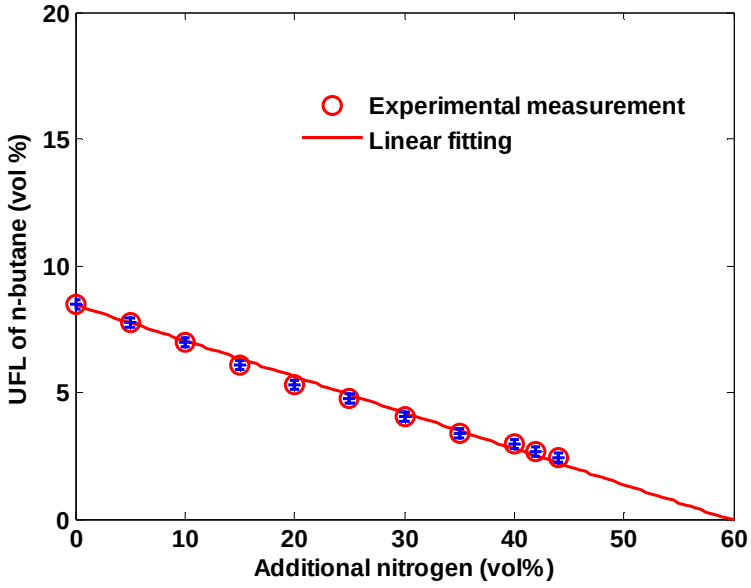

Fig. 5.25. Experimental n-butane UFL diluted with N_2 and the regressed linear curve.

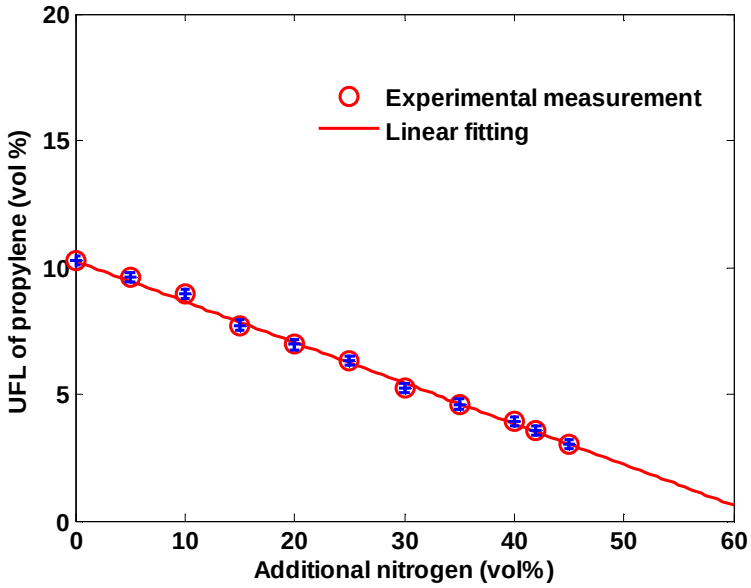

Fig. 5.26. Experimental propylene UFL diluted with N_2 and the regressed linear curve.

From the experimental ethylene UFL data, we defined the inert specified square root dilution coefficient (Eq. (5-5)) by linearly relating the change of square root UFL, $\Delta\sqrt{UFL}$, with additional nitrogen volume concentrations variation, ΔX.

$$\gamma^{\sqrt{U},inert} = \frac{\Delta\sqrt{UFL}}{\Delta X} \tag{5-5}$$

Figures 5.27 - 5.28 show the linear regression curves of ethylene UFL with additional nitrogen concentration (vol%) and the $\sqrt{UFL}$ with additional nitrogen concentration (vol%).

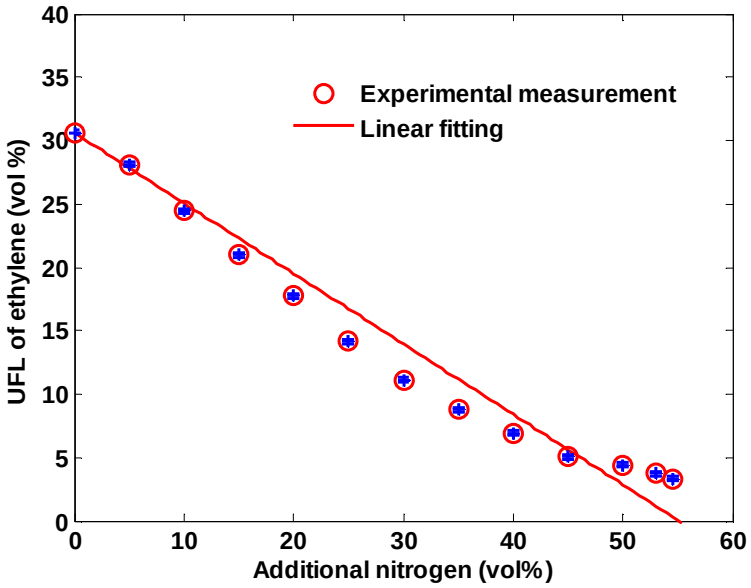

Fig. 5.27. Experimental ethylene UFL diluted with N_2 and the regressed linear curve.

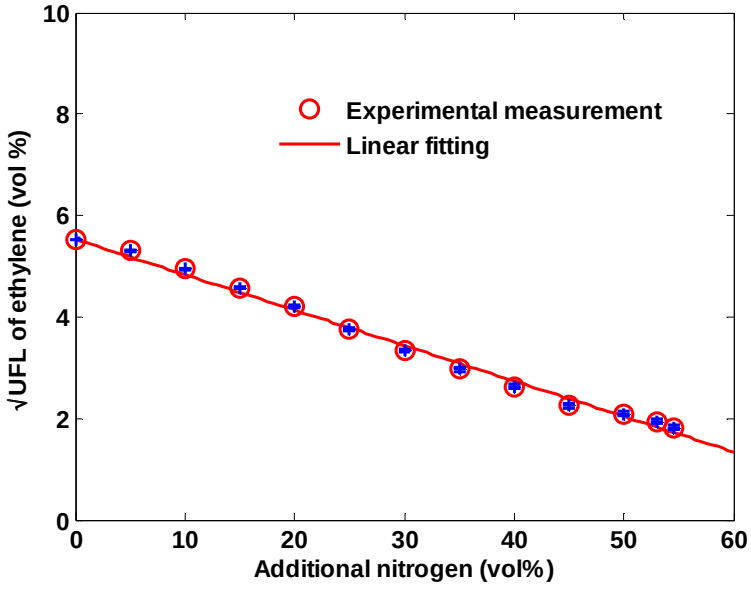

Fig. 5.28. Experimental ethylene $\sqrt{UFL}$ diluted with N2 and the regressed linear curve.

Modification of Le Chatelier's law on the hydrocarbon mixture UFL with nitrogen dilution was conducted separately, in term of the condition whether the hydrocarbon ethylene exists or not in the fuel mixtures. Similar to the hydrocarbon mixture LFL, the UFL of binary hydrocarbon mixtures containing no ethylene can be approximated by a linear relation with additional nitrogen concentration (vol%) as Eq. (5-6),

$$UFL_m^{N_2} = UFL_m + \gamma_m^{U,N_2} X_{N_2} \tag{5-6}$$

where,

$$\frac{1}{UFL_m} = \frac{{x_1}^{\alpha_1}}{UFL_1} + \frac{{x_2}^{\alpha_2}}{UFL_2} \qquad \frac{1}{\gamma_m^{U,N_2}} = \frac{{x_1}^{\kappa_1}}{\gamma_1^{U,N_2}} + \frac{{x_2}^{\kappa_2}}{\gamma_2^{U,N_2}}$$

$UFL_m^{N_2}, UFL_m$ are the UFLs of fuel mixtures with and without additional nitrogen. UFL_1 and UFL_2 are UFLs of pure fuel-1 and fuel-2 without nitrogen added. $\alpha_1$and α_2 are the molar fraction adjusting factors. The relationship of UFL_m with UFL_1 and UFL_2 is related to the Le Chatelier's law. Specifically for hydrocarbon mixture containing only saturated hydrocarbons, this relationship is the original Le Chatelier's law (α_1=1 and α_2=1), and when fuel mixtures have at least one component of unsaturated hydrocarbon, it is the modified Le Chatelier's law ($\alpha_1 \neq 1$ and $\alpha_2 \neq 1$). $\gamma_1^{U,N_2}, \gamma_2^{U,N_2}, \gamma_m^{U,N_2}$ are the nitrogen dilution coefficients on UFL of fuel-1, fuel-2, and their constituting mixture. Eq. (5-6) indicates their optimized correlation, where, similarly, $\kappa_1$and $\kappa_1$are the molar fraction adjusting factors, which are specified numerically based on the experimental data. For all the selected binary hydrocarbon mixtures, all the $\kappa_1$and κ_2 can be simplified to 1.

Figures 5.29 – 5.30 show the experimental data and predictions from the modified Le Chatelier's law for binary hydrocarbon mixtures of methane and propane, and ethane and propane.

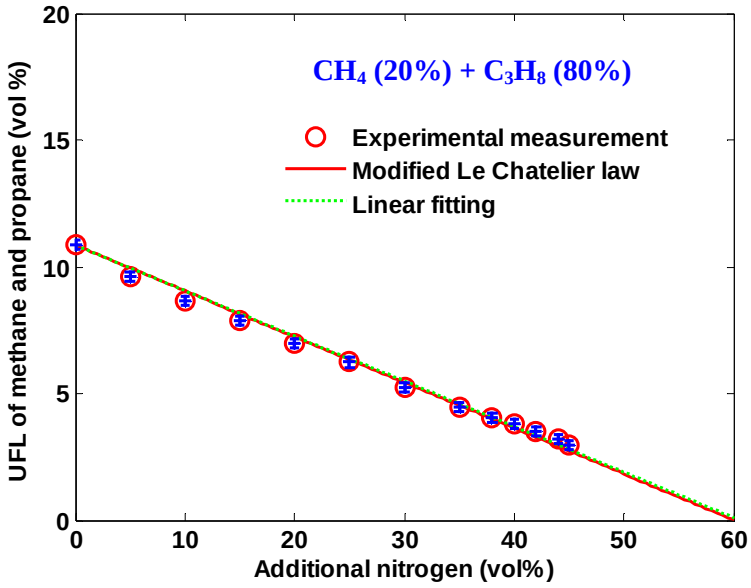

Fig. 5.29. UFL of methane and propane mixture and the modified Le Chatelier's law.

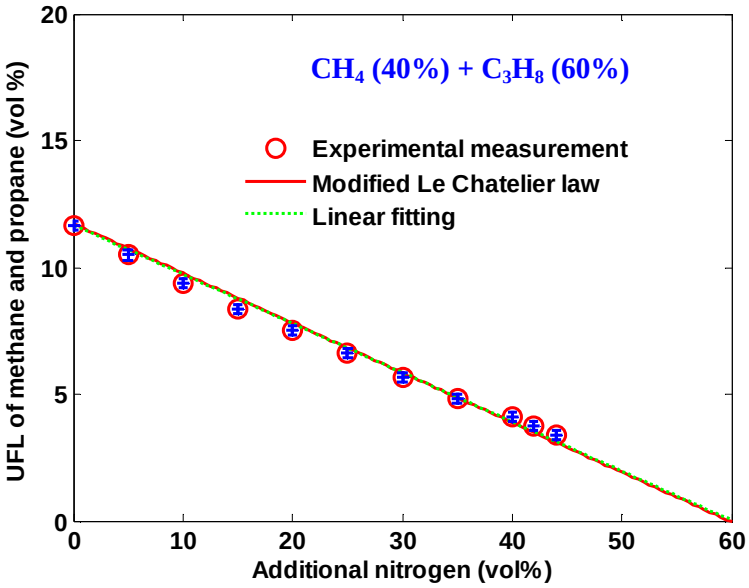

Fig. 5.29. Continued.

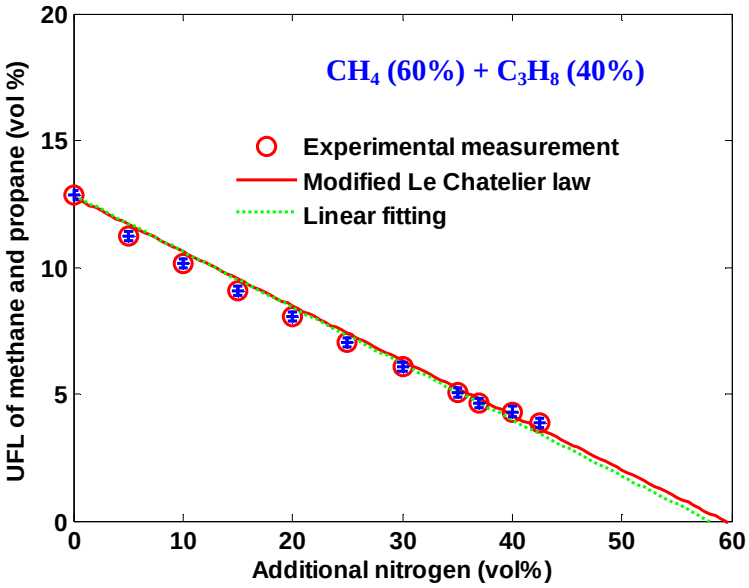

Fig. 5.29. Continued.

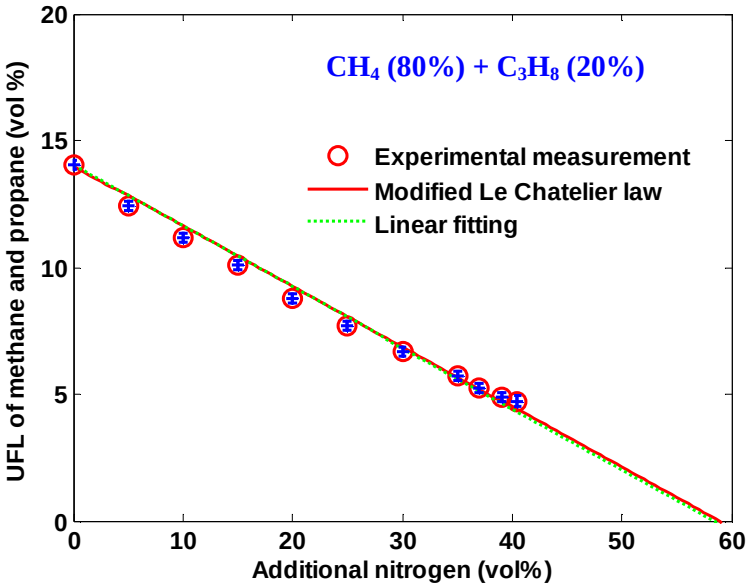

Fig. 5.29. Continued.

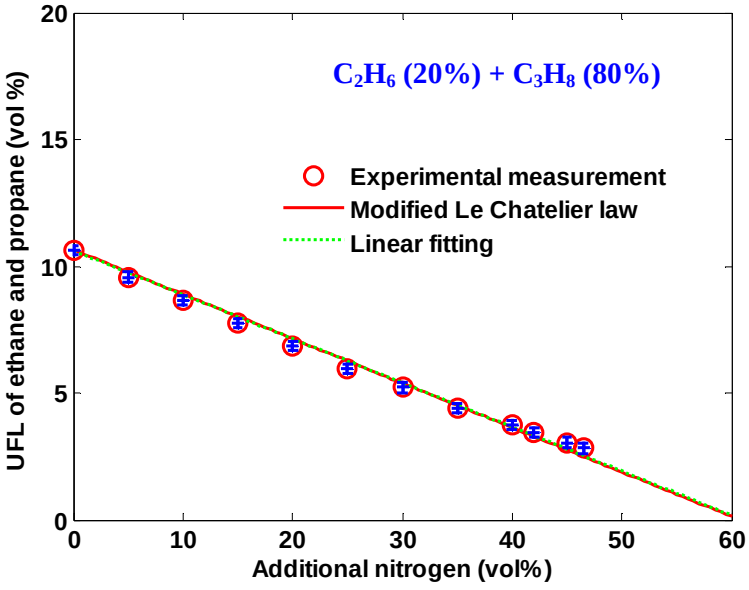

Fig. 5.30. UFL of ethane and propane mixture and the modified Le Chatelier's law.

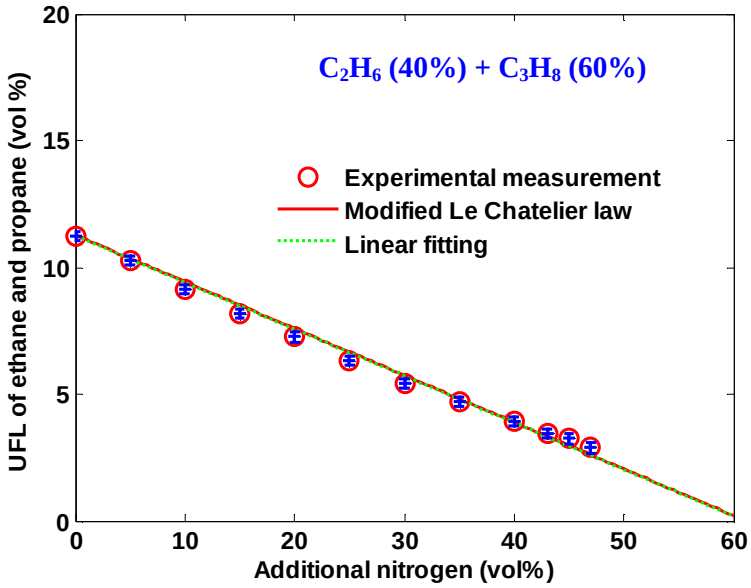

Fig. 5.30. Continued.

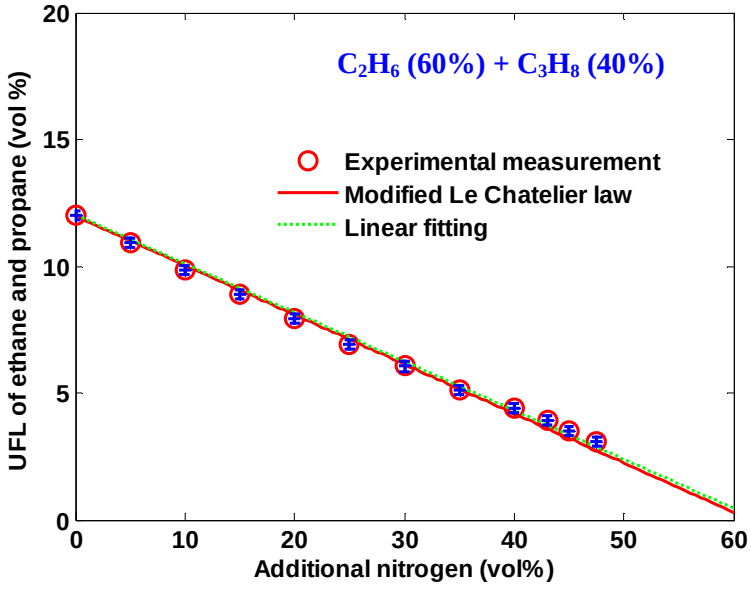

Fig. 5.30. Continued.

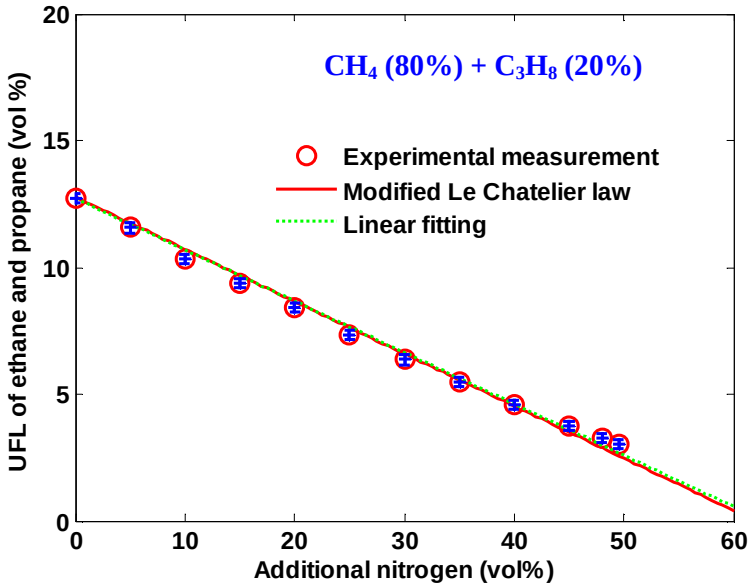

Fig. 5.30. Continued.

For the hydrocarbon mixtures containing ethylene, modification of Le Chatelier's law was represented as Eq. (5-7).

$$\sqrt{UFL_m^{N_2}} = \sqrt{UFL_m} + \gamma_m^{\sqrt{U},N_2} X_{N_2} \tag{5-7}$$

where,

$$\frac{1}{UFL_m} = \frac{x_1^{\alpha_1}}{UFL_1} + \frac{x_2^{\alpha_2}}{UFL_2} \qquad \frac{1}{\gamma_m^{\sqrt{U},N_2}} = \frac{x_1^{\lambda_1}}{\gamma_1^{\sqrt{U},N_2}} + \frac{x_2^{\lambda_2}}{\gamma_2^{\sqrt{U},N_2}}$$

$\gamma_1^{\sqrt{U},N_2}$, $\gamma_2^{\sqrt{U},N_2}$, $\gamma_m^{\sqrt{U},N_2}$ are the nitrogen specified square root dilution coefficients on $\sqrt{UFL}$ of fuel-1, fuel-2, and their mixture, respectively, and they can be correlated as Eq. (5-7). λ_1, and λ_2 are the molar fraction adjusting factors close to 1for the

hydrocarbon mixtures. For simplicity, they are set to be 1. Table 5.3 includes the specified square root nitrogen dilution coefficient for all the pure hydrocarbons.

Table 5.3. Specified square root nitrogen dilution coefficients on UFLs of pure hydrocarbons.

Chemicals	$\gamma^{\sqrt{U},N_2}$
Methane	-0.041
Ethane	-0.038
Propane	-0.033
n-butane	-0.030
Ethylene	-0.070
Propylene	-0.031

Figures 5.31 – 5.32 show the experimental data and predictions from the modified Le Chatelier's law for binary hydrocarbon mixtures of methane and ethylene, and ethylene and propylene.

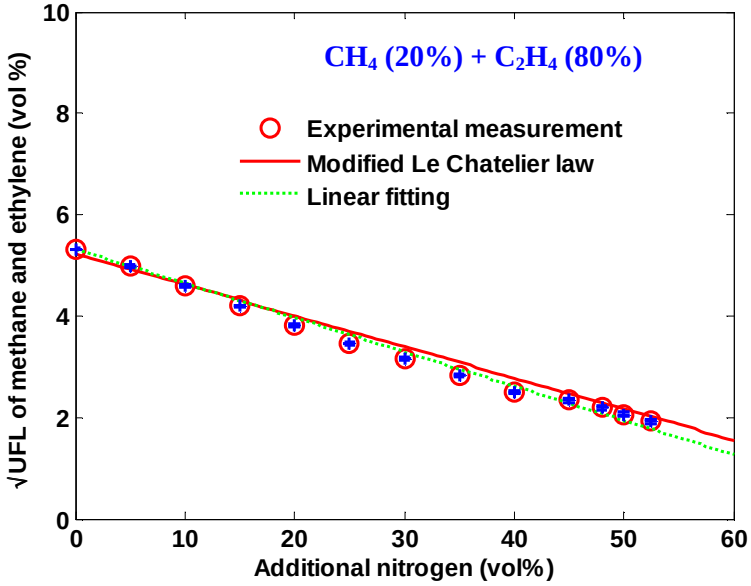

Fig. 5.31. $\sqrt{UFL}$ of methane and ethylene mixture and the modified Le Chatelier's law.

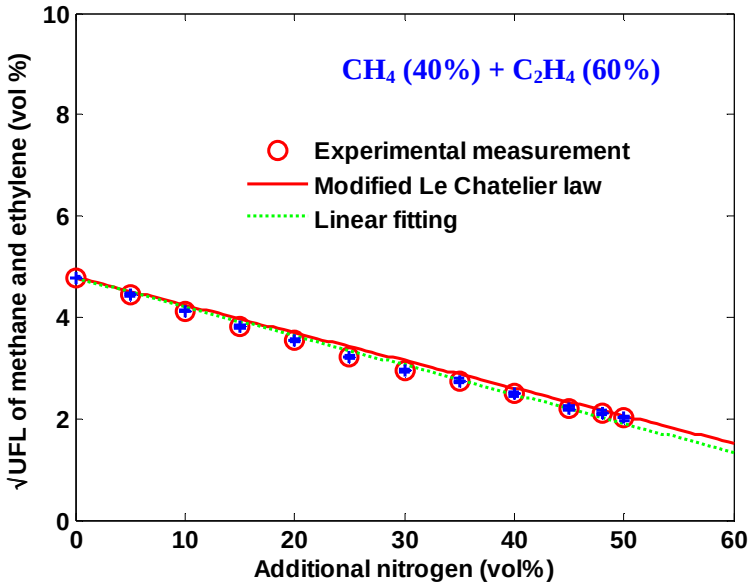

Fig. 5.31. Continued.

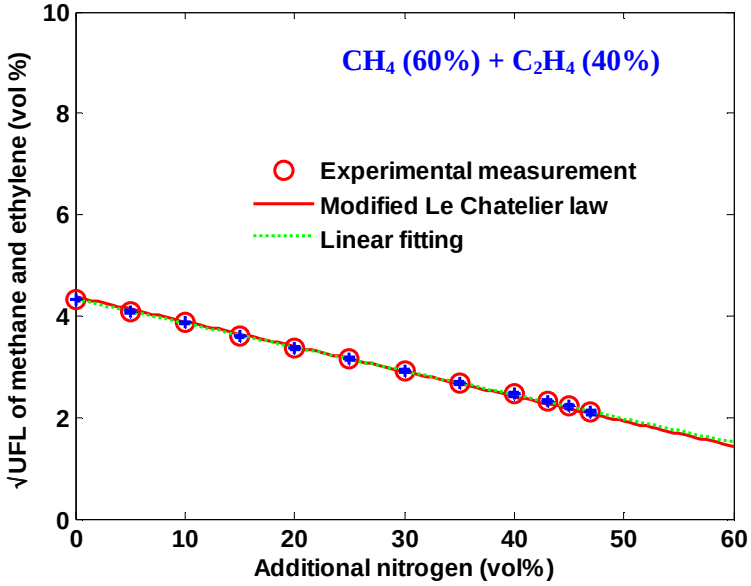

Fig. 5.31. Continued.

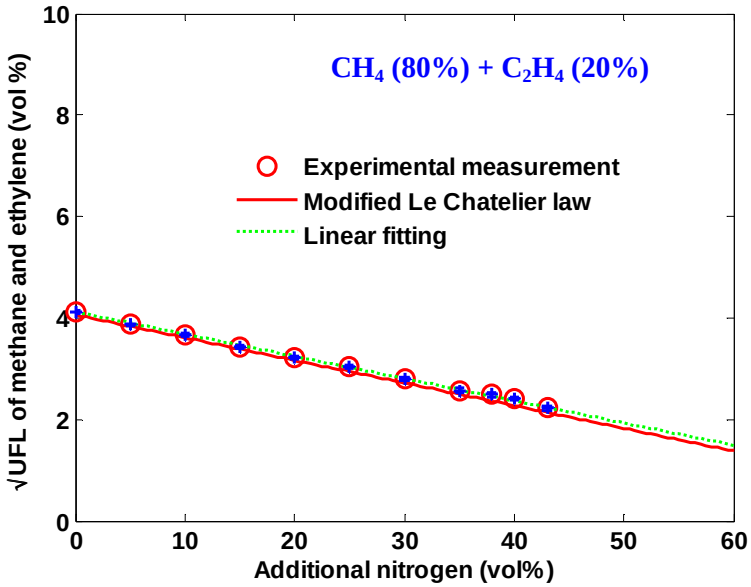

Fig. 5.31. Continued.

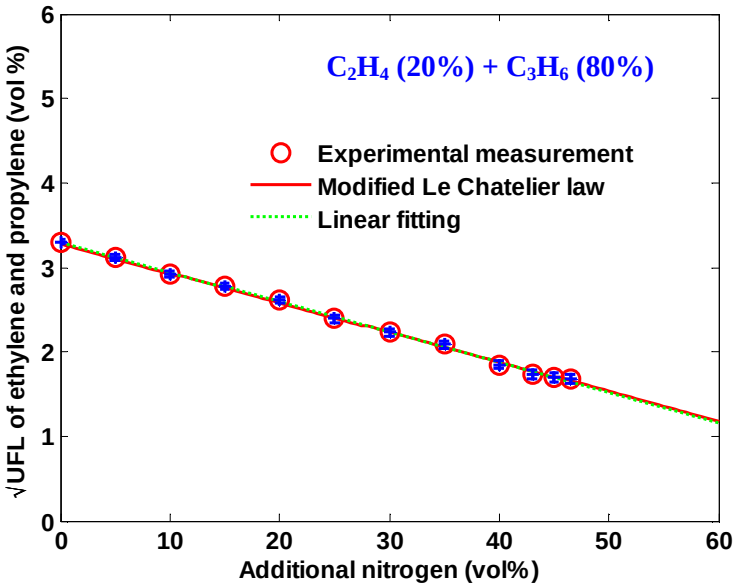

Fig. 5.32. $\sqrt{UFL}$ of ethylene and propylene mixture and the modified Le Chatelier's law.

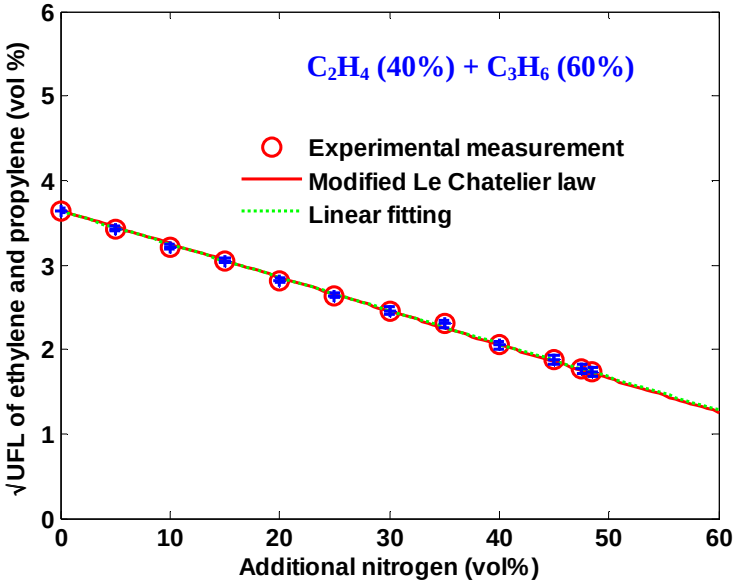

Fig. 5.32. Continued.

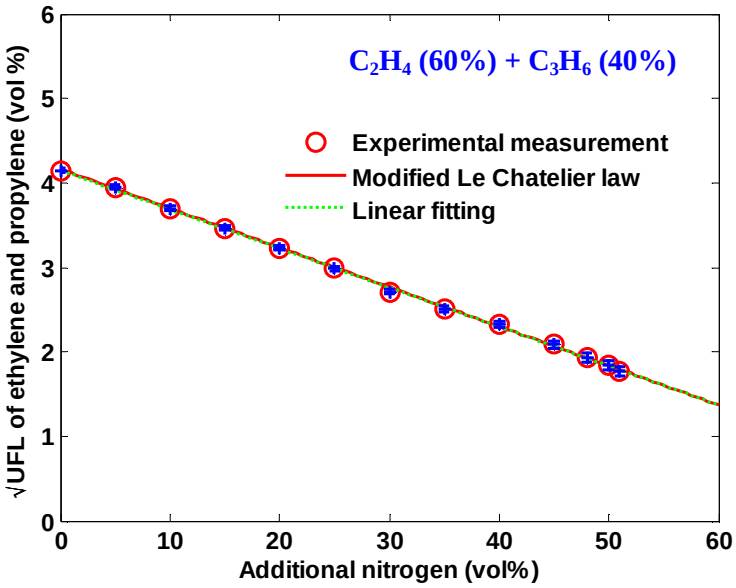

Fig. 5.32. Continued.

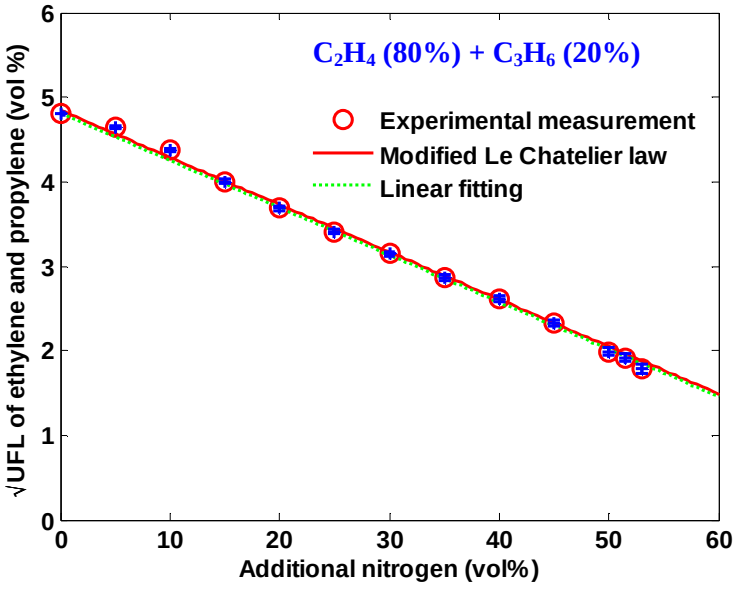

Fig. 5.32. Continued.

5. 4 Fuel mixture MIC

As indicated from experiment results, the flammability limit range become narrow with increase of additional nitrogen concentration, and finally the flammability limits converge to a point, the minimum inerting concentration (MIC), where UFL and LFL become equal. Therefore, MIC can be estimated through Eq. (5-4) and Eq. (5-7) for a certain fuel mixture containing no ethylene, and MIC is expressed as Eq. (5-8). Table 5.4 and 5.5 show the comparisons of experimental MICs and calculated MICs using this equation for the binary hydrocarbon mixtures of methane and propane, and ethane and propane.

$$MIC_{N_2} = \frac{UFL_m - LFL_m}{\gamma_m^{L,N_2} - \gamma_m^{U,N_2}} \tag{5-8}$$

Table 5.4. MICs of methane and propane mixtures from experimental measurement and calculation using Eq. (5-8).

Binary hydrocarbon mixtures		**MIC (exp.)** (vol %)	**MIC (cal.)** (vol %)	**|Dev|**	**|Dev%|**
CH_4 (%)	C_3H_8 (%)				
0	100	46.5	47.2	0.7	1.51
20	80	45.0	46.3	1.3	2.89
40	60	44.0	45.1	1.1	2.50
60	40	42.5	43.6	1.1	2.59
80	20	40.5	41.4	0.9	2.22
100	0	37.5	38.1	0.6	1.60

Table 5.5. MICs of ethane and propane mixtures from experimental measurement and calculation using Eq. (5-8).

Binary hydrocarbon mixtures		**MIC (exp.)** (vol %)	**MIC (cal.)** (vol %)	**|Dev|**	**|Dev%|**
C_2H_6 (%)	C_3H_8 (%)				
0	100	46.5	47.2	0.7	1.51
20	80	46.5	47.6	1.1	2.37
40	60	47.0	48.0	1.0	2.13
60	40	47.5	48.5	1.0	2.11
80	20	49.5	49.1	0.4	0.81
100	0	50.5	49.7	0.8	1.58

For fuel mixtures with the constituent of ethylene, we did linear regression of $\sqrt{LFL}$ with additional nitrogen concentration (vol%), which is similar to $\sqrt{UFL}$ with additional nitrogen addition. At the point of MIC, $\sqrt{UFL}$ and $\sqrt{LFL}$ are equal, so the MIC can be estimated using Eq. (5-9).

$$MIC_{N_2} = \frac{\sqrt{UFL_m} - \sqrt{LFL_m}}{\gamma_m^{\sqrt{L},N_2} - \gamma_m^{\sqrt{U},N_2}} \tag{5-9}$$

where, the nitrogen specified dilution coefficients on the LFLs of all selected hydrocarbons are simplified to 0 because the slopes of linearly regressed curves of $\sqrt{LFL}$ with additional nitrogen are very small, and accordingly $\gamma_m^{\sqrt{L},N_2}$ is ignorable compared to $\gamma_m^{\sqrt{U},N_2}$. Then Eq. (5-9) can be simplified as Eq. (10). Tables 5.6 and 5.7

show the comparison of experimental MICs and calculated MICs using Eq. (5-10) for the binary hydrocarbon mixtures of methane and ethylene, and ethylene and propylene.

$$MIC_{N_2} = \frac{\sqrt{LFL_m} - \sqrt{UFL_m}}{\gamma_m^{\sqrt{U},N_2}} \tag{5-10}$$

Table 5.6. MICs of methane and ethylene mixtures from experimental measurement and calculation using Eq. (5-10).

Binary hydrocarbon mixtures		**MIC (exp.)** (vol %)	**MIC (cal.)** (vol %)	**|Dev|**	**|Dev%|**
CH_4 (%)	C_2H_4 (%)				
0	100	54.5	55.1	0.6	1.10
20	80	52.5	56.6	4.1	7.81
40	60	50.0	53.7	3.7	7.40
60	40	47.0	49.0	2.0	4.26
80	20	43.0	43.5	0.5	1.16
100	0	37.5	40.2	2.7	7.20

Table 5.7. MICs of ethylene and propylene mixtures from experimental measurement and calculation using Eq. (5-10).

Binary hydrocarbon mixtures		**MIC (exp.)** (vol %)	**MIC (cal.)** (vol %)	**|Dev|**	**|Dev%|**
C_2H_6 (%)	C_3H_6 (%)				
0	100	45.0	54.5	9.5	21.11
20	80	46.5	49.8	3.3	7.10
40	60	48.5	52.1	3.6	7.42
60	40	51.0	55.0	4.0	7.84
80	20	53.0	57.3	4.3	8.11
100	0	54.5	55.1	0.6	1.10

Except pure propylene, the MICs of all other pure hydrocarbons and the selected binary hydrocarbon can represent experimental data well, especially the hydrocarbon mixtures without ethylene (|Dev%| < 3%). The large derivation for pure propylene comes from improper application of MIC prediction equation. As indicated from experimental observation, the UFL of pure propylene is well linearly correlated to the addition nitrogen concentration, while the selected equation here is a linear relation of $\sqrt{UFL}$ with additional nitrogen concentration. A simple calculation using Eq. (5.8) can easily get the pure propylene MIC 48.1 vol% with relative deviation 6.82%.

5.5 Conclusion

Nitrogen dilution effects on binary hydrocarbon mixture were tested in this section at ambient conditions, including LFL, UFL and MIC. The experimental results indicate that LFLs of binary hydrocarbon mixtures remain almost constant with addition of nitrogen, while UFLs decrease dramatically. The converging point of LFL and UFL is defined as MIC, and it changes with compositions of the constituting components in the fuel mixture. Approximately, all the binary hydrocarbon mixture LFLs are linearly related to the additional nitrogen concentrations, which is similar to the fuel mixtures UFL without ethylene.

A quantified expression of LFL with the added nitrogen volume concentration can be linearly characterized for all the selected hydrocarbons (methane, ethane, propane, n-butane, ethylene, propylene) and their combined binary mixtures. Modification of Le

Chatelier's law was conducted through the definition of inert gas dilution coefficient. The nitrogen dilution coefficient on LFL is defined as the slope of the linear fitting line from the selected pure hydrocarbons. A fuel mixture LFL can be estimated from pure fuel properties. The nitrogen dilution coefficient for the fuel mixture can be optimized as the summation of the reciprocal of the pure fuel's dilution coefficient with a volume composition weighting factor. The quantitative relationship of fuel mixture UFL with the added nitrogen is approximated to be linear except mixtures containing ethylene, and the similar operation was conducted to determine the nitrogen dilution effect on the UFL of pure hydrocarbons and binary hydrocarbon mixtures without ethylene. For fuel mixtures having ethylene, a relation of the square root of UFL with the additional introduced nitrogen is linearly illustrated. The MIC occurs at the converging point of the LFL and UFL with dilution of inert gases. An equal relation between them can be applied to calculate the MIC as a function of the fuel mixture LFL, UFL and the dilution coefficient.

CHAPTER VI

CAFT MODELING ON BINARY HYDROCARBON FLAMMABILITY WITH INERT GAS DILUTION

6.1 Overview

Calculated adiabatic flame temperature (CAFT) is the temperature that is obtained when combustion takes place at adiabatic conditions without heat losses. It indicates the temperature ceiling of the process [74] and is directly related to the flammability limits.

Currently, the calculated adiabatic flame temperature (CAFT) modeling is one of the most popularly used methods to estimate the flammability limits of pure fuels, especially LFLs with a high accuracy. In general, many organic substances approximately possess the same adiabatic flame temperatures at their LFLs. Some researchers agreed that this temperature is around 1550K [49] or 1200K [71], while others believe that this temperature is in the range of 1000–1500K [6]. For accurate flammability properties, Vidal [50] insisted that the adiabatic flame temperatures for different fuels at LFLs should be characterized separately. Compared to the condition at UFL concentration, the CAFT values are much more scattered and generally lower than those at LFLs [8].

In this section, an extended application of CAFT modeling on fuel mixture was proposed. Meanwhile, due to the difference of combustion mechanism for fuel mixtures

at the oxygen-lean and oxygen-rich conditions, CAFT modeling on fuel mixture LFL and UFL was discussed separately below.

6.2 CAFT modeling on binary hydrocarbon mixture LFLs

At the LFL concentration, the amount of oxygen present is sufficient for perfect combustion of hydrocarbons and their mixtures, so the main reaction products include water and carbon dioxide only. Since nitrogen does not take part in the reaction mechanism, and the dissociation products can be negligible at LFL concentration [21], the added nitrogen can be treated as a heat sink and the reaction mechanism remains unchanged with existence of nitrogen. Additionally, some previous research concluded that the adiabatic flame temperature is essentially constant for mixtures diluted with nitrogen [49, 75-77], which suggest the existence of a constant threshold flame temperature at LFL with a varied nitrogen concentration. Based on the first thermodynamic law, at the adiabatic condition, all the released energy from combustion heats the reaction products (H_2O, CO_2, remaining air, and added N_2), which can be expressed in Eq. (6-1) as the governing equation of CAFT modeling.

$$\Delta H_c + \sum_{prods} n_i \int_{T_0}^{T_f} C_{p_i} dT = 0 \tag{6-1}$$

where, ΔH_c is the enthalpy of combustion. T_0, T_f are the initial temperature and the final adiabatic flame temperature, respectively. n_i is the molar number of the reaction product

i. C_p is heat capacity at constant pressure. CAFT modeling on fuel mixture LFL with inert gas dilution is a three-step procedure:

1) Estimation of pure hydrocarbon CAFT;
2) Estimation of binary hydrocarbon mixture CAFT;
3) LFL prediction for binary hydrocarbon mixtures at varied amounts of nitrogen addition.

6.2.1 CAFT of pure hydrocarbon with additional nitrogen

The adiabatic flame temperature can be calculated separately for each pure hydrocarbon by using the CAFT modeling governing equation, Eq. (6-1), where the final CAFT is the function of the observed experimental LFL. In details, some facts or assumptions are listed below for combustion happening at LFL conditions:

1) Fuel is consumed completely and oxygen is in excess. The products include CO_2, water steam, and the left air and the additional nitrogen;
2) The inert gas nitrogen only works as a heat sink, adding the inert gas to the fuel does not change the reaction mechanism;
3) The adiabatic flame temperature is constant for a certain pure hydrocarbon regardless of addition of inert gases.

As to a general pure hydrocarbon, C_aH_b, with additional nitrogen added, it reacts completely with oxygen. The reaction products is calculated using the reaction equation (Eq. (6-2)), and the detailed reaction product data are presented in Table 6.1.

$$C_a H_b + (a + \frac{b}{4}) O_2 \rightarrow a CO_2 + \frac{b}{2} H_2 O \tag{6-2}$$

Table 6.1. Pure fuel (C_aH_b) combustion productions at LFL with additional nitrogen.

Compounds	**Amount before reaction** (mole)	**Amount after reaction** (mole)
C_aH_b	LFL	0
N_2 (additional)	X	X
Air	<1–X–LFL>	
O_2	0.21(1–X–LFL)	0.21(1–X–LFL)–(a+b/4)LFL
N_2	0.79(1–X–LFL)	0.79(1–X–LFL)
CO_2	0	aLFL
H_2O	0	(b/2)LFL

Not, putting the reaction productions (listed in Table 6.1) into the CAFT governing equation, Eq. (6-1), we can easily obtain the expanded expression of the governing equation as Eq. (6-3).

$$\Delta h_c LFL = n_{N_2} \int_{T_0}^{T_f} C_{p,N_2} dT + n_{O_2} \int_{T_0}^{T_f} C_{p,O_2} dT + n_{CO_2} \int_{T_0}^{T_f} C_{p,CO_2} dT + n_{H_2O} \int_{T_0}^{T_f} C_{p,H_2O} dT \tag{6-3}$$

where, Δh_c is the molar enthalpy of combustion, which is listed in Table 6.2 for all the selected hydrocarbons. Heat capacities of the reaction products include in Table 6.3.

Table 6.2. Combustion enthalpies of pure hydrocarbons.

Fuel	**ΔH_c** (kJ/mol-fuel)
CH_4	802.3
C_2H_4	1323.0
C_2H_6	1427.8
C_3H_6	1926.4
C_3H_8	2044.0
n- C_4H_{10}	2658.5

Table 6.3. Heat capacities of reaction products.

Products	**$C_P = a + b \cdot T + c \cdot T^2 + d \cdot T^3$ (J/mol•K)**			
	a	$b*10^2$	$c*10^5$	$d*10^9$
CO_2	22.243	5.977	-3.499	7.464
H_2O (g)	32.218	0.192	1.055	-3.593
N_2	28.883	-0.157	0.808	-2.871
O_2	25.460	1.519	-0.715	1.311
Air	28.088	0.197	0.480	-1.965

Solving for LFL from Eq. (6-3), we can eventually obtain pure hydrocarbon's LFL as a function of additional nitrogen concentration (Eq. (6-4)).

$$LFL^{N_2} = LFL + \gamma^{N_2} X_{N_2} \tag{6-4}$$

where, LFL^{N_2} is the LFL of pure hydrocarbon with varied concentration of additional nitrogen. X_{N_2} is the concentration of the additional nitrogen. Intercept LFL is the lower

flammability limit of pure hydrocarbon in air without nitrogen added (Eq. (6-5). Slope γ^{N_2} reflects nitrogen dilution effect on LFL of pure hydrocarbon (Eq. (6-6)).

$$LFL = \frac{0.79\int_{T_0}^{T_f} C_{p,N_2} dT + 0.21\int_{T_0}^{T_f} C_{p,O_2} dT}{\Delta h_c + \left[0.79\int_{T_0}^{T_f} C_{p,N_2} dT + (0.21 + a + \frac{b}{4})\int_{T_0}^{T_f} C_{p,O_2} dT - a\int_{T_0}^{T_f} C_{p,CO_2} dT - \frac{b}{2}\int_{T_0}^{T_f} C_{p,H_2O} dT \right]} \quad (6\text{-}5)$$

$$\gamma^{N_2} = \frac{0.21(\int_{T_0}^{T_f} C_{p,N_2} dT - \int_{T_0}^{T_f} C_{p,O_2} dT)}{\Delta h_c + \left[0.79\int_{T_0}^{T_f} C_{p,N_2} dT + (0.21 + a + \frac{b}{4})\int_{T_0}^{T_f} C_{p,O_2} dT - a\int_{T_0}^{T_f} C_{p,CO_2} dT - \frac{b}{2}\int_{T_0}^{T_f} C_{p,H_2O} dT \right]} \quad (6\text{-}6)$$

Now, inputting the experimental LFL of each pure hydrocarbon without additional nitrogen and solving for the adiabatic flame temperature T_f (=CAFT) using Eq. (6-5), we can obtain CAFTs of all the selected hydrocarbons (Table 6.4).

Table 6.4. Adiabatic flame temperatures of pure hydrocarbons at LFL.

Fuel	**LFL** (vol%)	$\mathbf{T_f}$ (K)
CH_4	5.25	1533
C_2H_4	2.81	1409
C_2H_6	2.70	1429
C_3H_6	2.28	1568
C_3H_8	2.09	1526
n- C_4H_{10}	1.72	1595

Nitrogen dilution effect on the LFL of each pure hydrocarbon can be quantitatively characterized by solving for γ^{N_2} using Eq. (6-6), where T_f is listed in Table 6.4, C_p in Table 6.3, and Δh_c in Table 6.2. All the selected hydrocarbon LFLs with additional nitrogen are plotted in Figures 6.1 – 6.6.

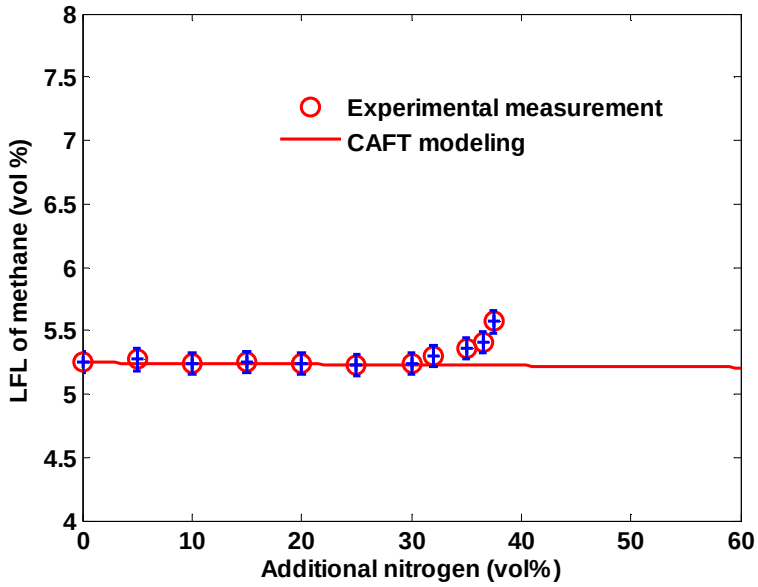

Fig. 6.1. Methane LFL with additional nitrogen using CAFT modeling.

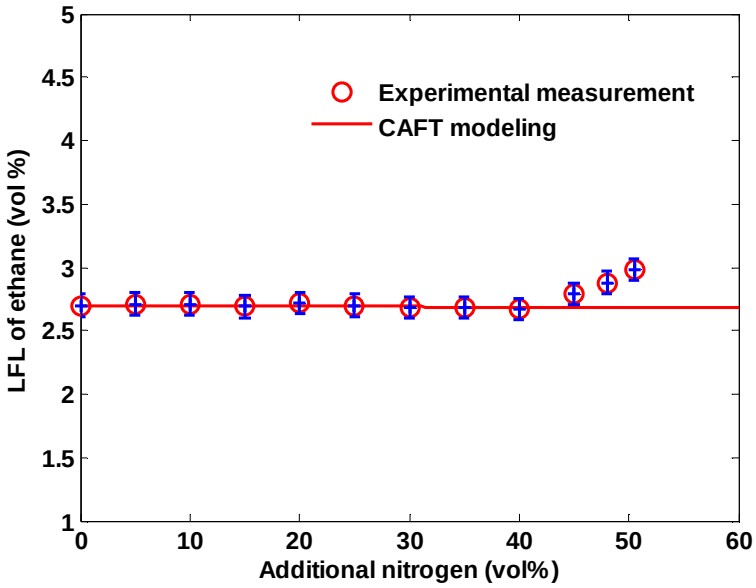

Fig. 6.2. Ethane LFL with additional nitrogen using CAFT modeling.

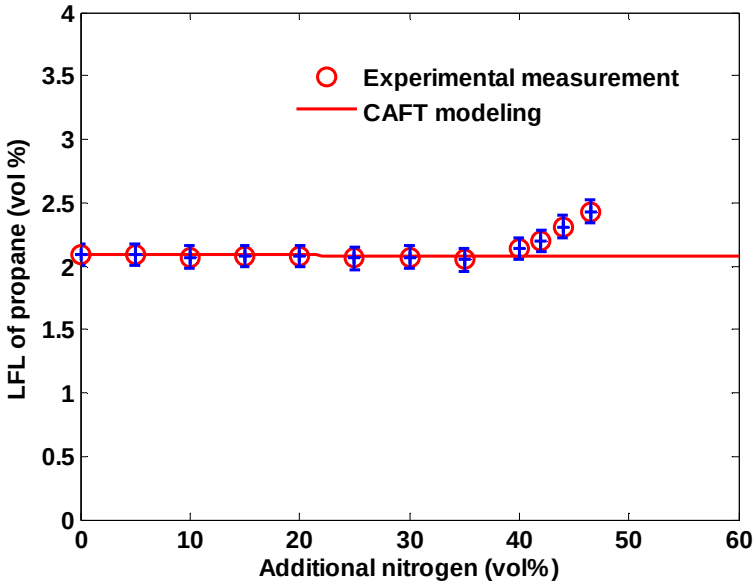

Fig. 6.3. Propane LFL with additional nitrogen using CAFT modeling.

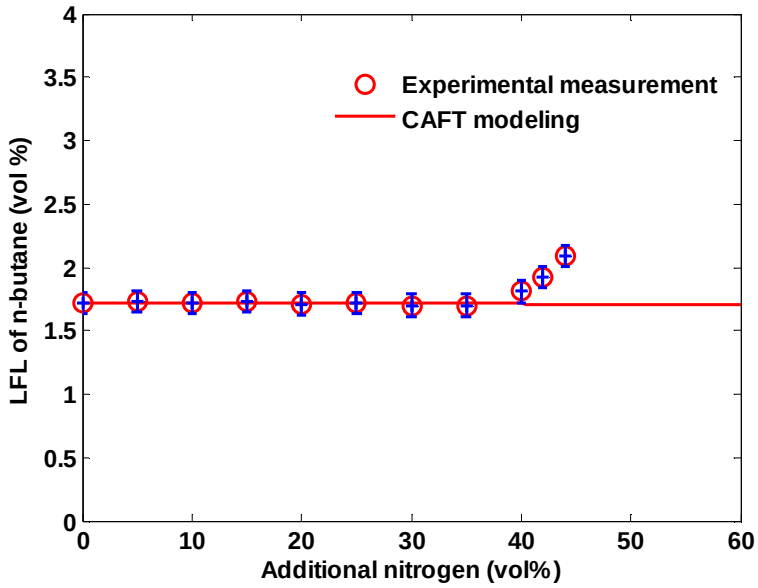

Fig. 6.4. N-butane LFL with additional nitrogen using CAFT modeling.

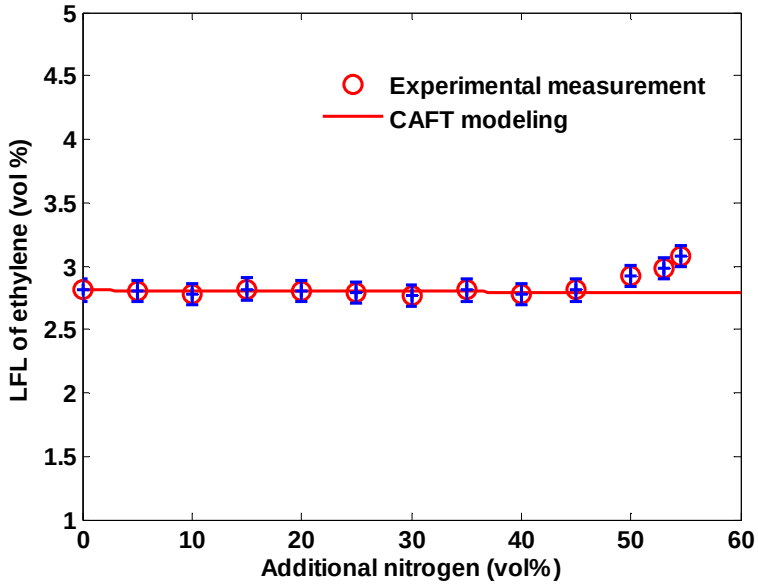

Fig. 6.5. Ethylene LFL with additional nitrogen using CAFT modeling.

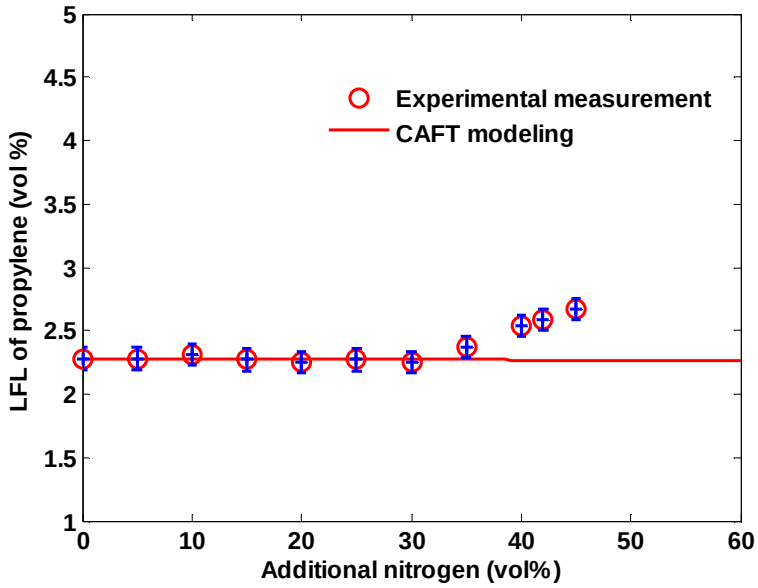

Fig. 6.6. Propylene LFL with additional nitrogen using CAFT modeling.

Except the flammability nose zone that is closed to the MIC, all the CAFT modeling LFLs can fit experimental data very well. The possible reason for the exception is the change of combustion mechanism. When additional nitrogen concentration increases, the oxygen environment becomes leaner, which results in some incomplete combustion products, and finally the non-constant CAFT. A complex combustion situation cannot be described by using the CAFT modeling on LFL illustrated above.

Another finding from CAFT modeling is the nitrogen dilution effect on hydrocarbon's LFL, which is mainly dependent on the heat capacities of nitrogen and oxygen (Eq. (6-3)). At the range of initial room temperature through final adiabatic

flame temperature, nitrogen heat capacity is almost equal to that of oxygen. Therefore, the LFLs of all the selected hydrocarbons nearly stay constant, which is consistent with experimental observations except the flammability nose zones.

Carbon dioxide dilution effects on methane and propylene are analyzed below with the same assumptions as those for nitrogen. The reaction products are listed in Table 6.5, and the final equation expression is Eq. (6-7), and the results are illustrated in Figure 6.7 and Figure 6.8.

$$LFL^{N_2} = LFL + \gamma^{CO_2} X_{CO_2} \tag{6-7}$$

where,

$$LFL = \frac{0.79\int_{T_0}^{T_f} C_{p,N_2} dT + 0.21\int_{T_0}^{T_f} C_{p,O_2} dT}{\Delta h_c + \left[0.79\int_{T_0}^{T_f} C_{p,N_2} dT + (0.21 + a + \frac{b}{4})\int_{T_0}^{T_f} C_{p,O_2} dT - a\int_{T_0}^{T_f} C_{p,CO_2} dT - \frac{b}{2}\int_{T_0}^{T_f} C_{p,H_2O} dT \right]} \tag{6-8}$$

$$\gamma^{CO_2} = \frac{\int_{T_0}^{T_f} C_{p,CO_2} dT - (0.79\int_{T_0}^{T_f} C_{p,N_2} dT + 0.21\int_{T_0}^{T_f} C_{p,O_2} dT)}{\Delta h_c + \left[0.79\int_{T_0}^{T_f} C_{p,N_2} dT + (0.21 + a + \frac{b}{4})\int_{T_0}^{T_f} C_{p,O_2} dT - a\int_{T_0}^{T_f} C_{p,CO_2} dT - \frac{b}{2}\int_{T_0}^{T_f} C_{p,H_2O} dT \right]} \tag{6-9}$$

Eq. (6-8) represents the LFL of pure hydrocarbon without additional carbon dioxide added, which is exactly same to Eq. (6-5). Eq. (6-9) is the carbon dioxide dilution effect on LFL of pure hydrocarbon.

Table 6.5. Pure fuel (C_aH_b) combustion productions at LFL with additional carbon dioxide.

Compounds	**Amount before reaction** (mole)	**Amount after reaction** (mole)
C_aH_b	LFL	0
Air	<1–X–LFL>	
O_2	0.21(1–X–LFL)	0.21(1–X–LFL)–(a+b/4)LFL
N_2	0.79(1–X–LFL)	0.79(1–X–LFL)
CO_2	X	X+aLFL
H_2O	0	(b/2)LFL

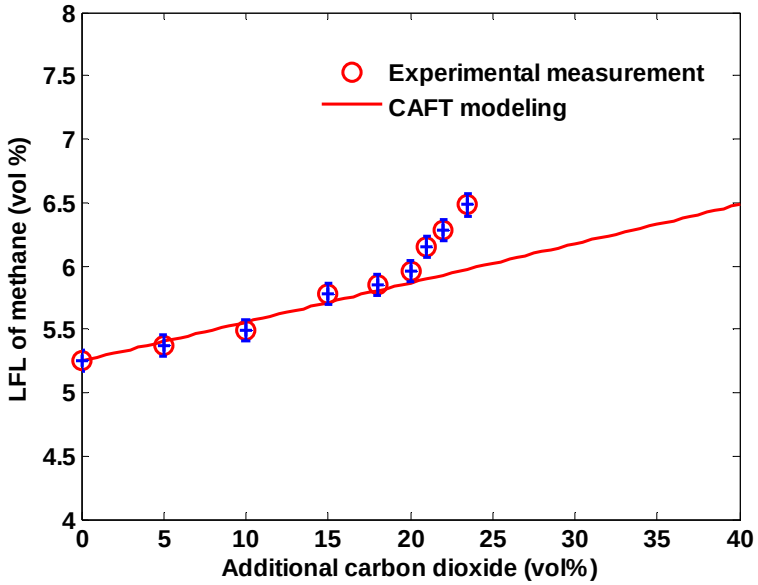

Fig. 6.7. Methane LFL with additional carbon dioxide using CAFT modeling.

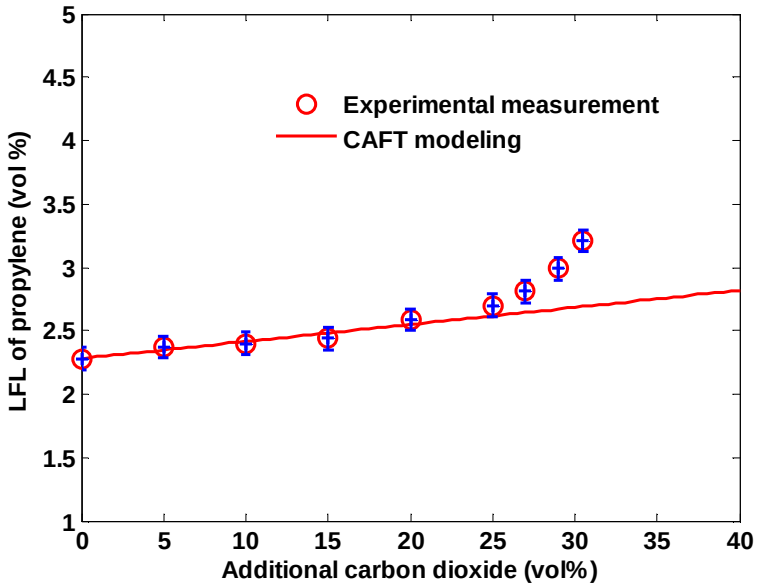

Fig. 6.8. Propylene LFL with additional carbon dioxide using CAFT modeling.

To compare the dilution effects from nitrogen and carbon dioxide, we re-express Eq. (6-5) as Eq. (6-10), and Eq. (6-9) as Eq. (6-11).

$$\gamma^{N_2} = \frac{\int_{T_0}^{T_f} C_{p,N_2} dT - \int_{T_0}^{T_f} C_{p,Air} dT}{\Delta h_c + \left[0.79\int_{T_0}^{T_f} C_{p,N_2} dT + (0.21 + a + \frac{b}{4})\int_{T_0}^{T_f} C_{p,O_2} dT - a\int_{T_0}^{T_f} C_{p,CO_2} dT - \frac{b}{2}\int_{T_0}^{T_f} C_{p,H_2O} dT \right]} \quad (6\text{-}10)$$

$$\gamma^{CO_2} = \frac{\int_{T_0}^{T_f} C_{p,CO_2} dT - \int_{T_0}^{T_f} C_{p,Air} dT}{\Delta h_c + \left[0.79\int_{T_0}^{T_f} C_{p,N_2} dT + (0.21 + a + \frac{b}{4})\int_{T_0}^{T_f} C_{p,O_2} dT - a\int_{T_0}^{T_f} C_{p,CO_2} dT - \frac{b}{2}\int_{T_0}^{T_f} C_{p,H_2O} dT \right]} \quad (6\text{-}11)$$

Clearly, Eq. (6-10) and Eq. (6-11) have the same denominator expressions, and the numerators are the difference between the inert gas heat capacity and air heat capacity. A more general equation for inert dilution effect is expressed as Eq. (6-12), where we can conclude that inert gas dilution effect on hydrocarbon LFL mainly depends on the heat capacity differences between inert gas and air.

$$\gamma^{inert-gas} = k\left(\int_{T_0}^{T_f} C_{p,inert-gas}\,dT - \int_{T_0}^{T_f} C_{p,Air}\,dT\right) \tag{6-12}$$

where, k is a constant for inert gas added to the fuel-air mixture at LFL condition:

$$k = \frac{1}{\Delta h_c + 0.79\int_{T_0}^{T_f} C_{p,N_2}\,dT + (0.21 + a + \frac{b}{4})\int_{T_0}^{T_f} C_{p,O_2}\,dT - a\int_{T_0}^{T_f} C_{p,CO_2}\,dT - \frac{b}{2}\int_{T_0}^{T_f} C_{p,H_2O}\,dT}$$

6.2.2 CAFT of binary hydrocarbon mixture with additional nitrogen

As with pure fuels, a fuel mixture burns completely at the LFL. Introduced additional nitrogen works as a heat sink. The adiabatic flame temperature remains constant with varied concentration of additional nitrogen. To estimate the adiabatic flame temperatures for fuel mixtures, Vidal [50] proposed a linear equation which is represented in Eq. (6-13).

$$T_{f,m} = x_1 \cdot T_{f,1} + x_2 \cdot T_{f,2} \tag{6-13}$$

where, $T_{f,1}$ and $T_{f,2}$ are the adiabatic flame temperatures of pure fuel 1 and pure fuel 2, which are included in Table 6.4 for all the selected pure hydrocarbons. x_1, x_2 are the molar fractions ($x_1 + x_2 = 1$) of fuel 1 and fuel 2 on the combustible basis. $T_{f,m}$ is the fuel mixture adiabatic flame temperature that can be easily calculated from the Eq. (6-13).

6.2.3. Binary hydrocarbon mixture LFL

Finally, we reapplied CAFT governing equation Eq. (6-1) to binary hydrocarbon mixture containing components fuel-1 (C_aH_b) and fuel-2 (C_mH_n), where the fuel mixture LFL (LFL_m) becomes the function of its adiabatic flame temperature ($T_{f,m}$). The fuel mixture lower flammability limit is represented in Eq. (6-14).

$$LFL_m = \frac{\sum_{prods} n_i \int_{T_0}^{T_{f,m}} C_{p_i} dT}{\Delta h_{c,,m}} \tag{6-14}$$

where, the amounts of reaction products are calculated from the reaction equation Eq. (6-15), and the result is listed in Table 6.6.

$$\left(x_1 C_a H_b + x_2 C_m H_n\right) + \left(a x_1 + m x_2 + \frac{b x_1 + n x_2}{4}\right) O_2 \rightarrow$$
$$\left(a x_1 + m x_2\right) CO_2 + \frac{b x_1 + n x_2}{2} H_2O \tag{6-15}$$

Table 6.6. Fuel mixture (C_aH_b and C_mH_n) combustion productions at LFL with additional nitrogen.

Compounds	**Amount before reaction** (mole)	**Amount after reaction** (mole)
Fuel mixture	$<LFL_m>$	
C_aH_b	x_1LFL_m	0
C_mH_n	x_2LFL_m	0
N_2 (additional)	X	X
Air	$<1–X–LFL_m>$	
O_2	$0.21(1–X–LFL_m)$	$0.21(1–X–LFL_m)–rLFL_m$
N_2	$0.79(1–X–LFL_m)$	$0.79(1–X–LFL_m)$
CO_2	0	$sLFL_m$
H_2O	0	$tLFL_m$

$$r = ax_1 + mx_2 + \frac{bx_1 + nx_2}{4}$$

$$s = ax_1 + mx_2$$

$$t = \frac{bx_1 + nx_2}{2}$$

Enthalpy of fuel mixture combustion ($\Delta h_{c,m}$) can be calculated using Eq. (6-16) based on the Hess's Law of chemical reaction [78], which states that the change of enthalpy is same for the conversion from same reactants to same products regardless of reaction taking place in one step or in a series of steps.

$$\Delta h_{c,m} = x_1 \Delta h_{c,1} + x_2 \Delta h_{c,2} \tag{6-16}$$

Now, solving for LFL_m from Eq. (6-14), we can finally get correlation of binary hydrocarbon mixture LFL_m with the additional nitrogen concentration in Eq. (6-17).

$$LFL_m^{N_2} = LFL_m + \gamma_m^{N_2} X_{N_2} \tag{6-17}$$

where, LFL_m is the binary hydrocarbon mixture LFL (Eq. (6-18)). $\gamma_m^{N_2}$ is the nitrogen dilution effect on binary hydrocarbon mixture (Eq. (6-19)). Both these two variables are the function of fuel mixture adiabatic flame temperature $T_{f,m}$.

$$LFL_m = \frac{0.79\int_{T_0}^{T_{f,m}} C_{p,N_2} dT + 0.21\int_{T_0}^{T_{f,m}} C_{p,O_2} dT}{\Delta H_{c,m} + \left(0.79\int_{T_0}^{T_{f,m}} C_{p,N_2} dT + (0.21+r)\int_{T_0}^{T_{f,m}} C_{p,O_2} dT - s\int_{T_0}^{T_{f,m}} C_{p,CO_2} dT - t\int_{T_0}^{T_{f,m}} C_{p,H_2O} dT\right)} \tag{6-18}$$

$$\gamma_m^{N_2} = \frac{0.21\left(\int_{T_0}^{T_{f,m}} C_{p,N_2} dT - 0.21\int_{T_0}^{T_{f,m}} C_{p,O_2} dT\right)}{\Delta H_{c,m} + \left(0.79\int_{T_0}^{T_{f,m}} C_{p,N_2} dT + (0.21+r)\int_{T_0}^{T_{f,m}} C_{p,O_2} dT - s\int_{T_0}^{T_{f,m}} C_{p,CO_2} dT - t\int_{T_0}^{T_{f,m}} C_{p,H_2O} dT\right)} \tag{6-19}$$

The CAFT modeling LFLs of binary hydrocarbon mixtures (methane and propane, ethane and propane, methane and ethylene, and ethylene and propylene) at different molar ratios (20%/80%, 40%/60%, 60%/40%, 80%/20%) are illustrated in Figures 6.9 – 6.12.

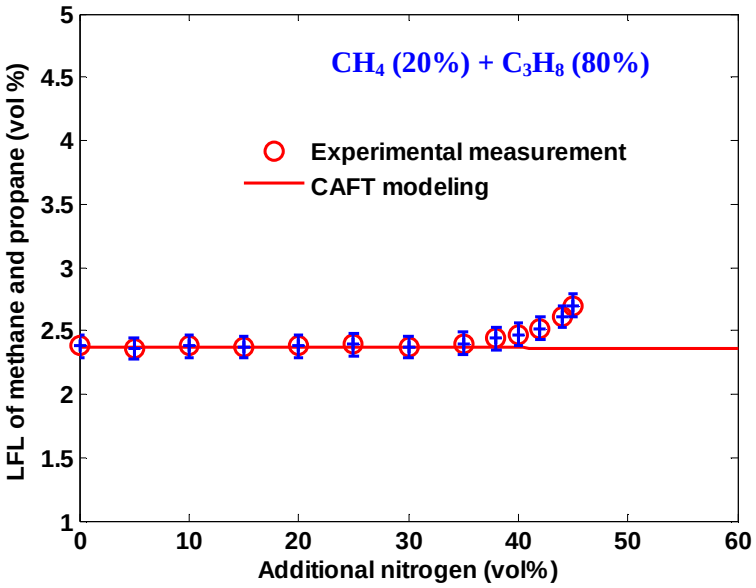

Fig. 6.9. Methane and propane LFL with additional nitrogen using CAFT modeling.

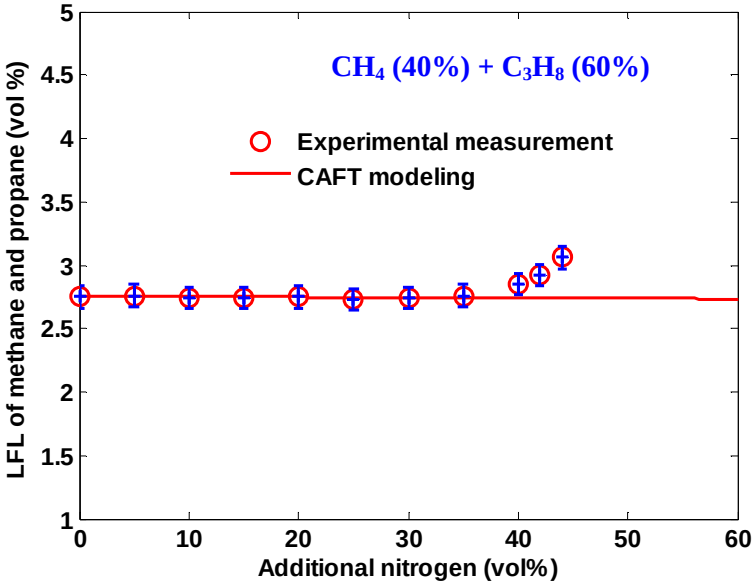

Fig. 6.9. Continued.

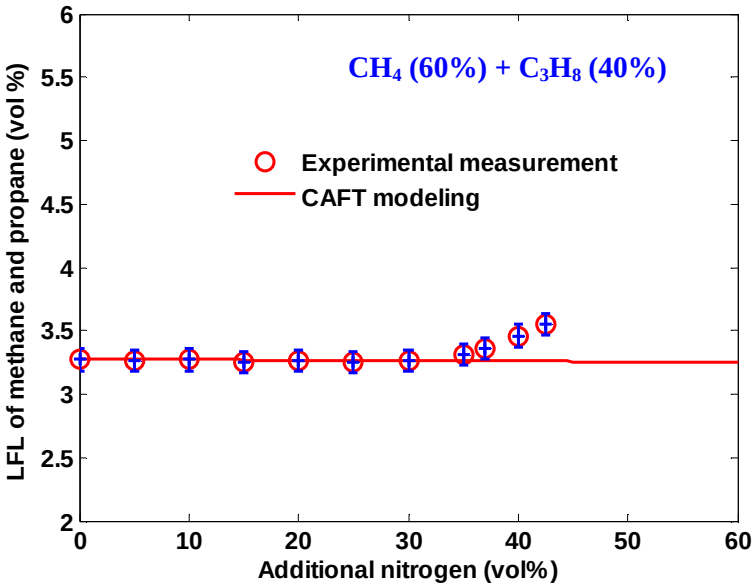

Fig. 6.9. Continued.

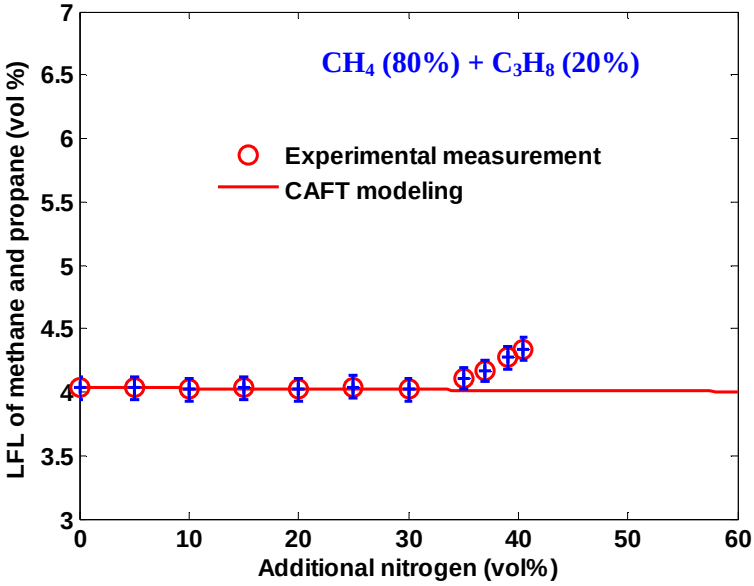

Fig. 6.9. Continued.

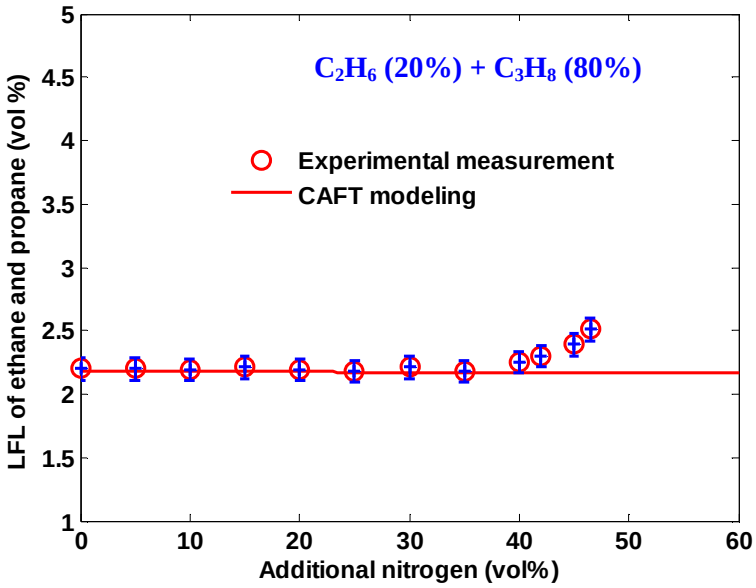

Fig. 6.10. Ethane and propane LFL with additional nitrogen using CAFT modeling.

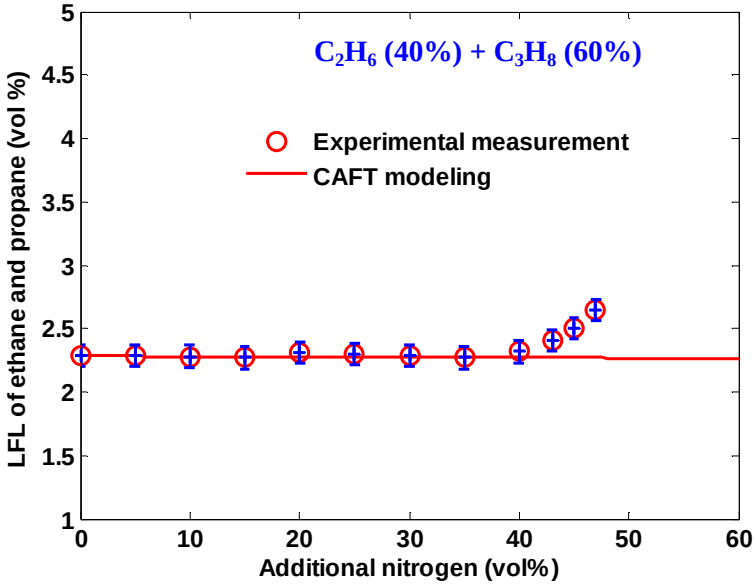

Fig. 6.10. Continued.

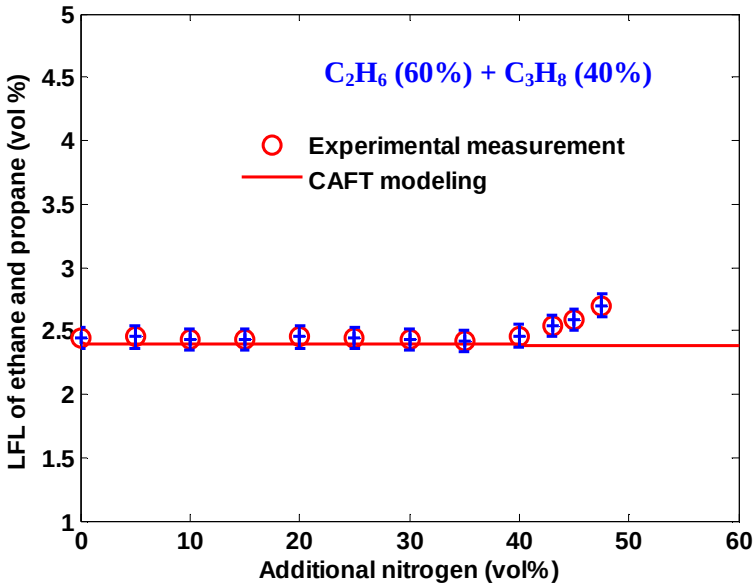

Fig. 6.10. Continued.

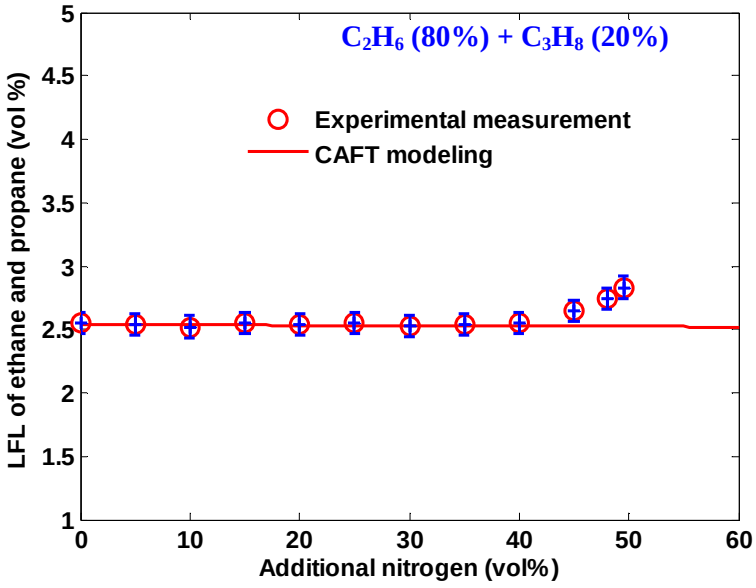

Fig. 6.10. Continued.

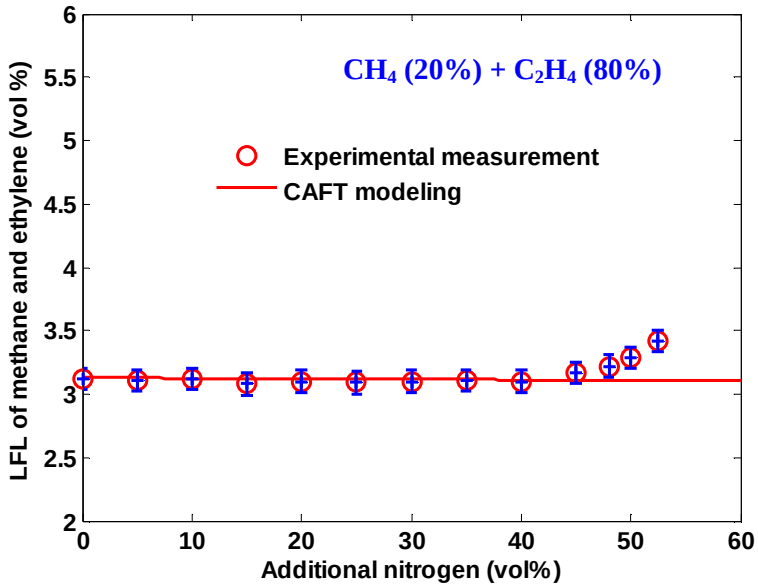

Fig. 6.11. Methane and ethylene LFL with additional nitrogen using CAFT modeling.

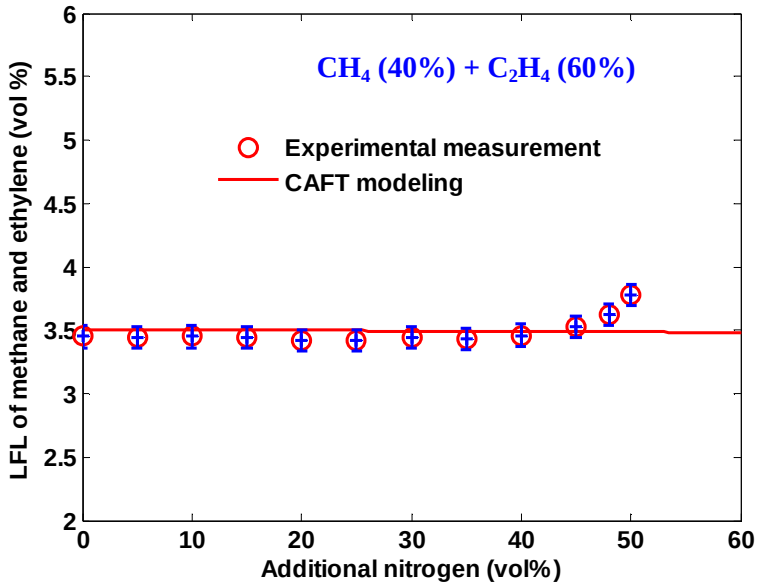

Fig. 6.11. Continued.

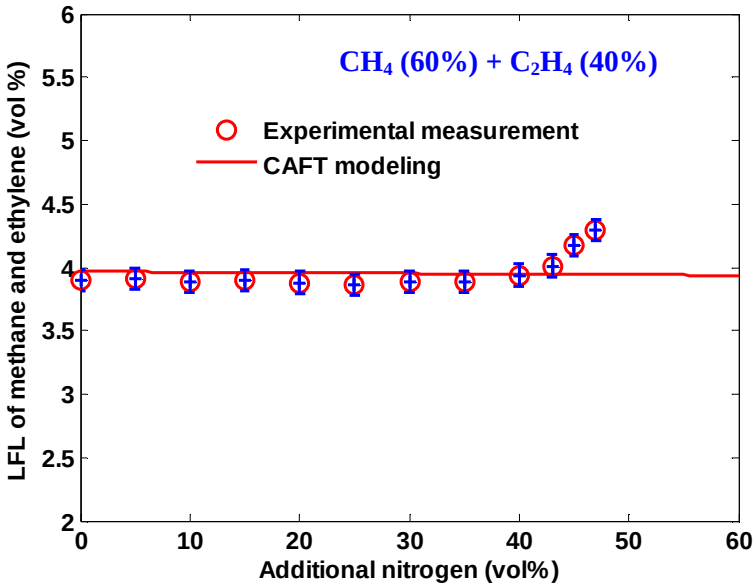

Fig. 6.11. Continued.

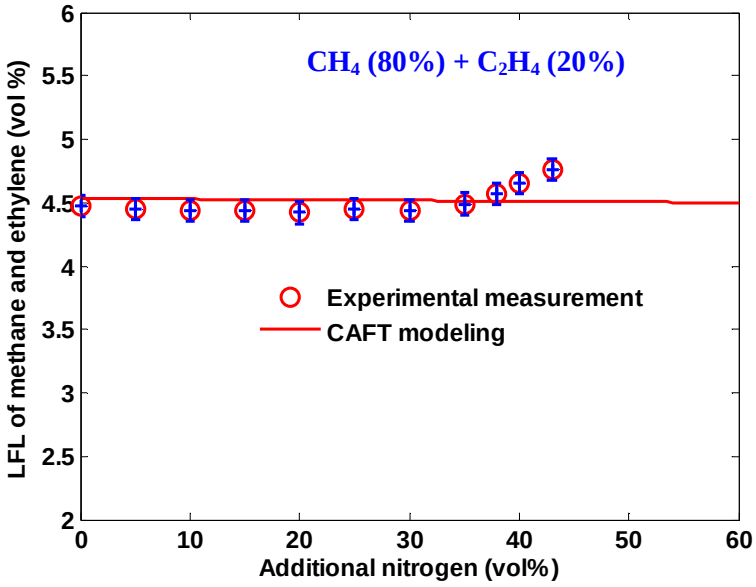

Fig. 6.11. Continued.

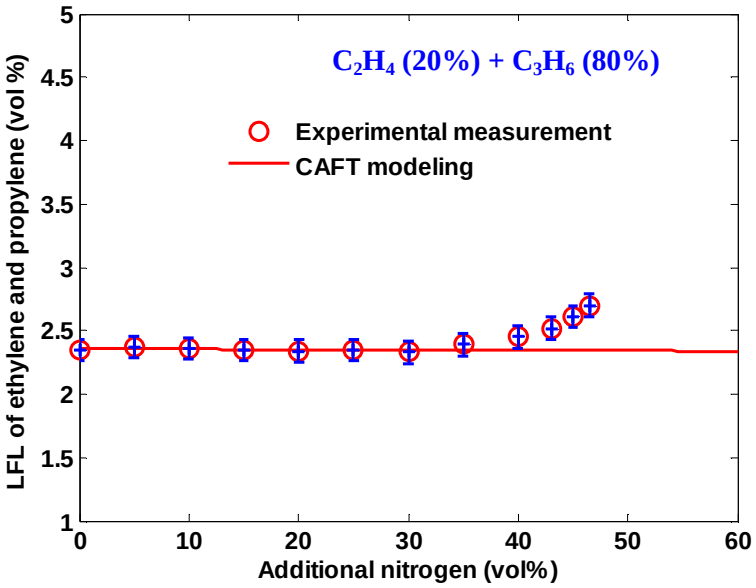

Fig. 6.12. Ethylene and propylene LFL with additional nitrogen using CAFT modeling.

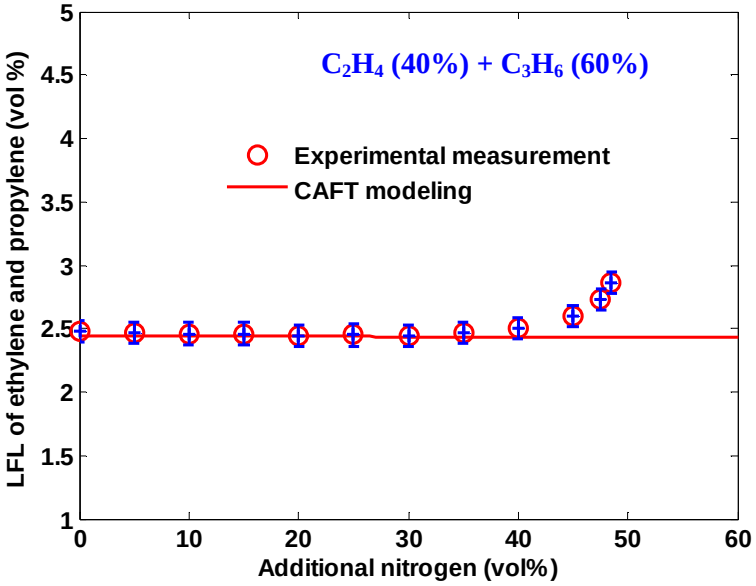

Fig. 6.12. Continued.

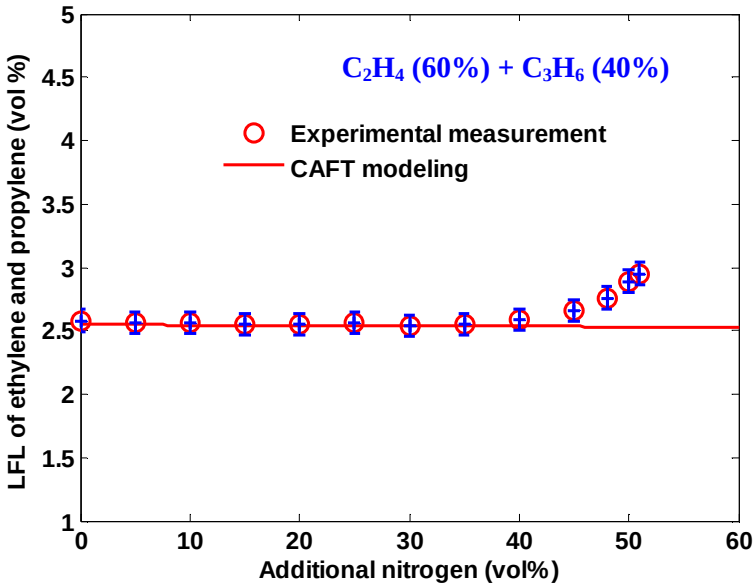

Fig. 6.12. Continued.

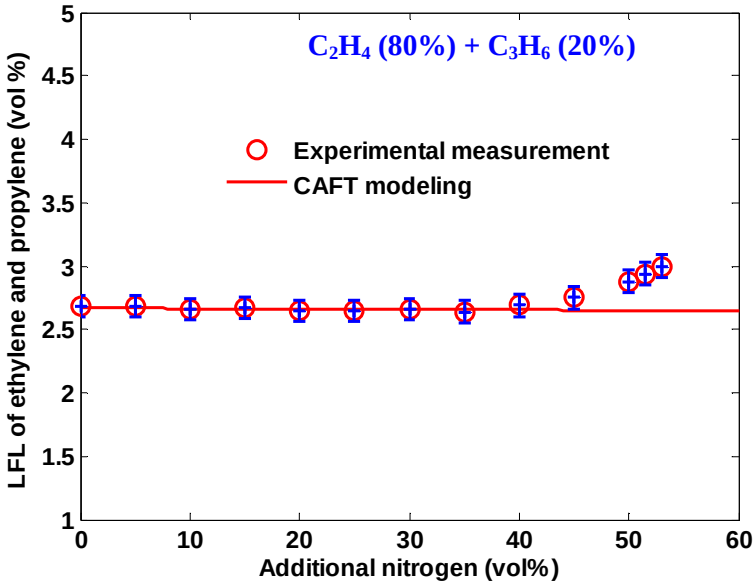

Fig. 6.12. Continued.

Similar to the pure hydrocarbons, all the CAFT modeling LFLs of selected binary hydrocarbon mixtures can fit experimental data very well except the flammability nose zone. The same proposed reason for the exception can be applied to the binary hydrocarbon mixtures: when additional nitrogen concentration increases, the oxygen environment becomes leaner and the reaction mechanism changes, which results in some incomplete combustion products, and finally the non-constant CAFT.

6.3 CAFT modeling on binary hydrocarbon mixture UFLs

At the UFL concentration, a flammable material will not undergo complete combustion since fuel is in excess; therefore, the reaction products become scattered, and H_2O, CO_2, CO, H_2 and many radicals (e.g., H, O, O_2, OH, solid C, NO, NO_2, CH_2O, and etc) are usually found. To apply CAFT modeling on fuel mixture UFL, some assumptions are presumed following Chen work [76, 77] on nitrogen dilution effect on pure hydrocarbon UFL:

1) The component of fuel is in excess and oxygen gas reacts completely with the main products of H_2O, CO_2, CO, and H_2;
2) Nitrogen works as a heat sink, addition of nitrogen into fuel/air mixture does not change the chemical reaction mechanism;
3) The adiabatic flame temperature rises are the same for all limit mixtures at the UFLs.

At adiabatic conditions, the total energy released in combustion heats reaction products; therefore, Eq. (6-1) is applied as the governing equation for CAFT modeling on UFL as well. Based on the above assumptions, the chemical reaction at UFL is given from Eq. (6-20), and the amounts of reaction products are listed in Table 6.7.

$$C_a H_b + (a - \frac{a_1}{2} + \frac{b - b_1}{4})O_2 \rightarrow (a - a_1)CO_2 + a_1 CO + \frac{b - b_1}{2} H_2O + \frac{b_1}{2} H_2 \quad (6\text{-}20)$$

Table 6.7. Pure fuel (C_aH_b) combustion productions at UFL with additional nitrogen.

Compounds	**Amount before reaction** (mole)	**Amount after reaction** (mole)
C_aH_b	UFL	UFL–0.21(1–X–UFL)k_1
N_2 (additional)	X	X
<Air>	<1–X–UFL>	
O_2	0.21(1–X–UFL)	0
N_2	0.79(1–X–UFL)	0.79(1–X–UFL)
CO	0	0.21(1–X–UFL) k_3
CO_2	0	0.21(1–X–UFL) k_2
H_2	0	0.21(1–X–UFL) k_5
H_2O	0	0.21(1–X–UFL) k_4

$$k_1 = \frac{1}{a - a_1/2 + (b - b_1)/4}$$

$$k_2 = \frac{a - a_1}{a - a_1/2 + (b - b_1)/4}$$

$$k_3 = \frac{a_1}{a - a_1/2 + (b - b_1)/4}$$

$$k_4 = \frac{(b - b_1)/2}{a - a_1/2 + (b - b_1)/4}$$

$$k_5 = \frac{b_1/2}{a - a_1/2 + (b - b_1)/4}$$

Now applying the CAFT governing equation Eq. (6-1) to pure hydrocarbon C_aH_b with and without inert gas nitrogen dilution, which are indicated as Eq. (6-21) and Eq. (6-22) respectively, we can easily obtain a simple expression (Eq. (6-23)) for the UFL of pure hydrocarbon diluted with nitrogen, where all the variables with the superscript N_2 refer to fuel mixture with nitrogen dilution.

$$n_{O_2}\Delta h_c = \sum_{prods} n_i \int_{T_0}^{T_f} C_{p,i}\,dT = (T_f - T_0)\sum_{prods} n_i \overline{C}_{p,i} \tag{6-21}$$

$$n_{O_2}{}^{N_2}\Delta h_c{}^{N_2} = \sum_{prods} n_i{}^{N_2} \int_{T_0}^{T_f{}^{N_2}} C_{p,i}\,dT = (T_f{}^{N_2} - T_0)\sum_{prods} n_i{}^{N_2}\,\overline{C}_{p,i} \tag{6-22}$$

$$UFL^{N_2} = UFL - \left(UFL + (1-UFL)\frac{\overline{C}_{P,N_2}}{\overline{C}_{p,\,fuel}} \right) X_{N_2} \tag{6-23}$$

Clearly from Eq. (6-23), the pure hydrocarbon UFL is linearly related to additional nitrogen volume concentration, with the intercept equal to UFL in air without nitrogen dilution and the indicated slope dependent on average heat capacity ratio of inert gas to fuel. Table 6.8 lists the heat capacities at constant pressure for all the selected pure hydrocarbons, and Table 6.9 lists their average heat capacities at different temperature ranges (same initial temperature 298 K, and 4 different final adiabatic flame temperatures , 1500 /1700/1900/2100 K) . Figures 6.13 – 18 show pure hydrocarbon UFLs at varied nitrogen concentrations from experimental measurement and CAFT modeling (Eq. (6-23)).

Table 6.8. Heat capacities of pure hydrocarbons.

Products	$C_P = a + b \cdot T + c \cdot T^2 + d \cdot T^3$ (J/mol•K)			
	a	$b*10^2$	$c*10^5$	$d*10^9$
CH_4	19.875	5.021	1.268	-11.004
C_2H_6	6.895	17.255	-6.402	7.28
C_3H_8	-4.042	30.456	-15.711	31.716
n-C_4H_{10}	3.954	37.126	-18.326	34.979
C_2H_4	3.950	15.628	-8.339	17.657
C_3H_6	3.151	23.812	-12.176	24.603

Table 6.9. Hydrocarbon average heat capacity at different final CAFTs.

Products	Average heat capacity $\overline{C}_P$ ((J/mol-K)			
	1500 K	**1700 K**	**1900 K**	**2100 K**
CH_4	65.22	68.39	70.72	72.06
C_2H_6	110.22	115.73	120.31	124.06
C_3H_8	157.21	164.87	171.77	178.29
n-C_4H_{10}	204.31	213.98	222.53	230.39
C_2H_4	85.57	89.46	93.04	96.50
C_3H_6	130.02	136.18	141.75	147.02

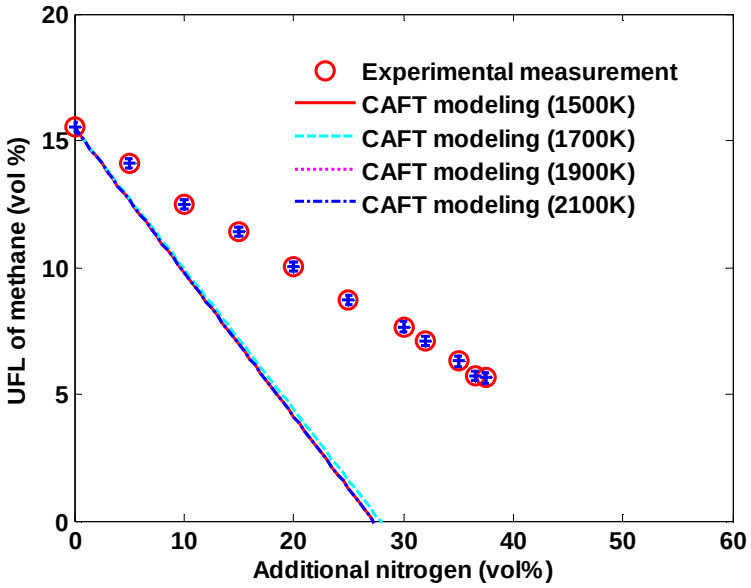

Fig. 6.13. Methane UFL with additional nitrogen using CAFT modeling.

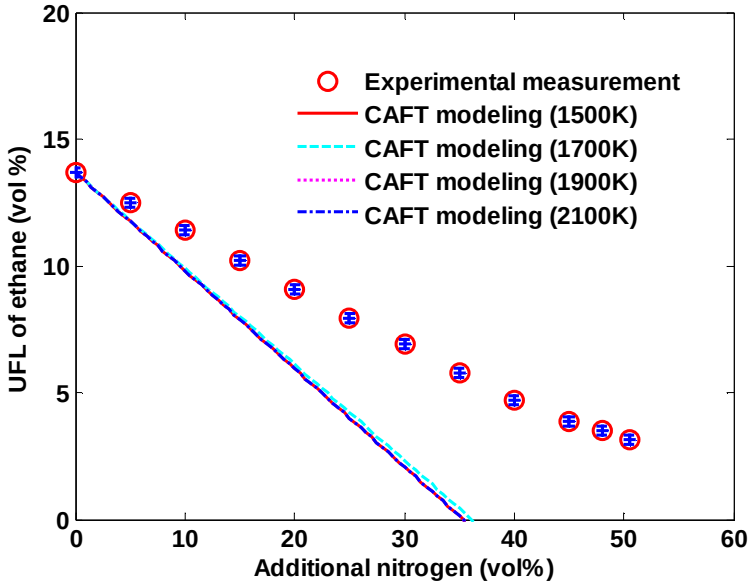

Fig. 6.14. Ethane UFL with additional nitrogen using CAFT modeling.

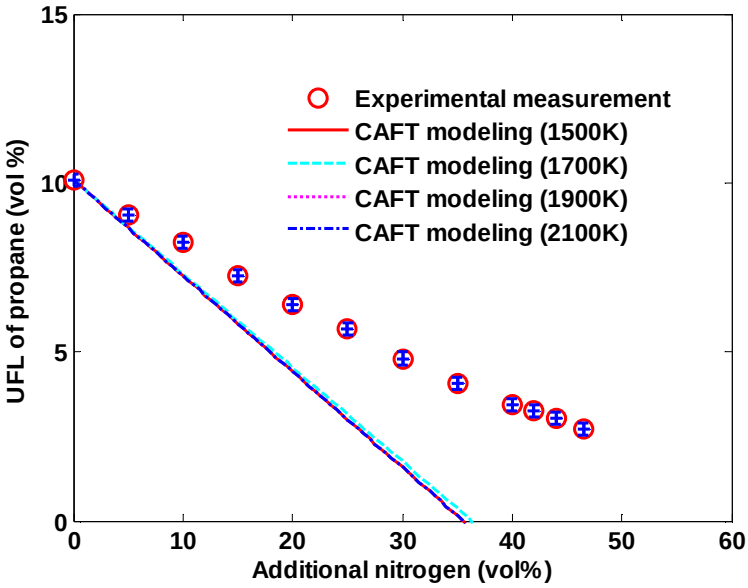

Fig. 6.15. Propane UFL with additional nitrogen using CAFT modeling.

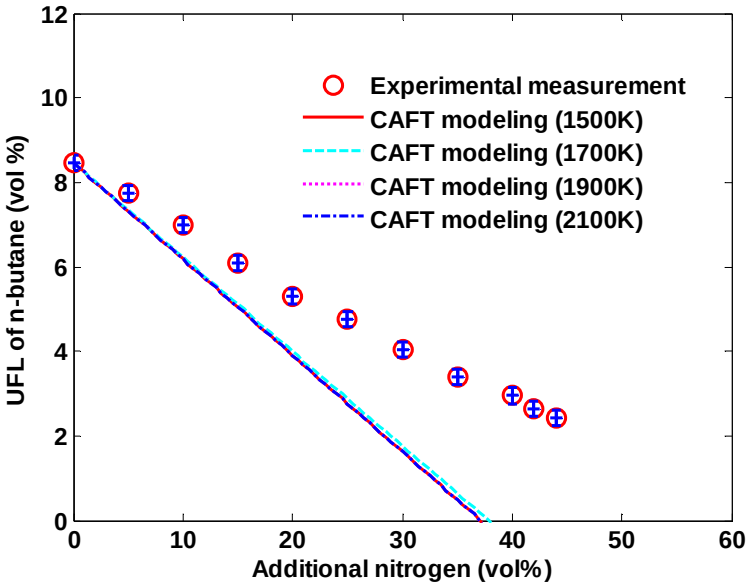

Fig. 6.16. N-butane UFL with additional nitrogen using CAFT modeling.

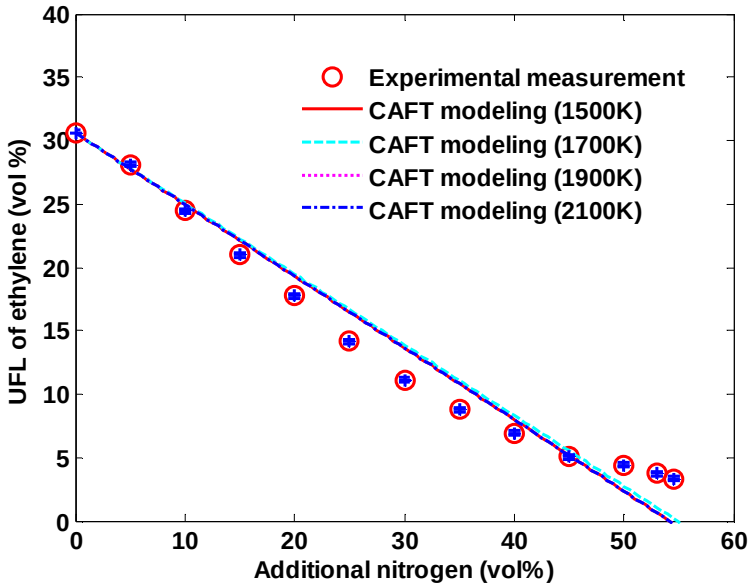

Fig. 6.17. Ethylene UFL with additional nitrogen using CAFT modeling.

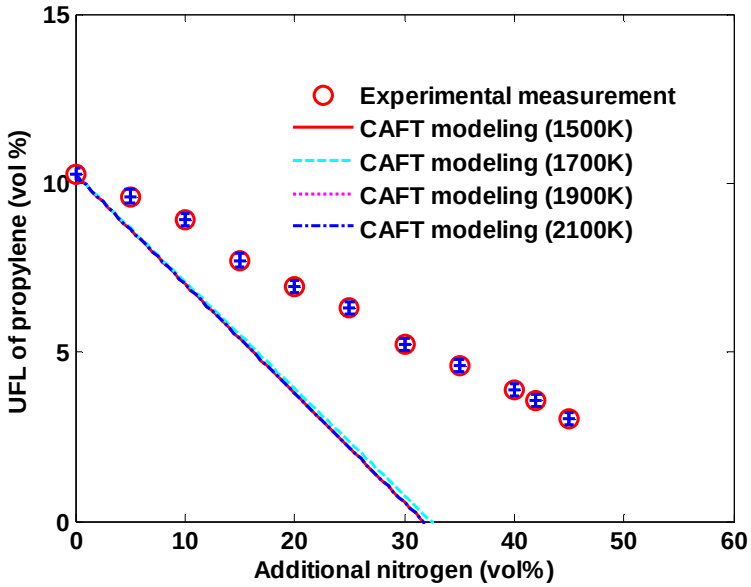

Fig. 6.18. Propylene UFL with additional nitrogen using CAFT modeling.

The big discrepancy between the modeling UFL data and the experimental results indicates that the assumptions applied to the CAFT modeling on UFL are unaccptible. As pointed out from previous research, combustion at UFL becomes unpredictable and the reaction products are far more complex than those presumed from Chen's work [76, 77]. However, if more complicated reaction products (including other radicals, e.g., H, OH, O, NO, solid C, NO, NO_2, CH_2O, and etc) are assumed but under the assumption of constant adiabatic flame temperature, the same UFL prediction equation (Eq. (6-23) can be obtained. Therefore, the assumption of constant adiabatic flame temperature at different inert gas dilution conditions cannot represent the combustion mechanism correctly.

Theoretically, CAFT modeling is based on the premise that the flammability limits are thermal-control in behavior and are not highly dependent on kinetics [79], which is true at LFL compositions, but at UFL kinetics becomes dominant. Therefore, an accurate UFL estimation requires an analysis of the thermal phenomenal together with the combustion kinetics happening at fuel rich conditions. A more detailed approach to predict UFL theoretically will be discussed later in the section of VIII: Conclusion and Future work.

CHAPTER VII

LE CHATELIER'S LAW AND FUEL MIXTURE FLAMMABILITY

7.1 Introduction

Due to a large number of practical applications involving ubiquitous fuel mixtures, accurate prediction of fuel mixture flammability limit is highly desirable. The most common method for predicting the flammability limit of fuel mixtures is the Le Chatelier's law, and especially this law works best for estimating the LFLs. Le Chatelier arrived at this 'mixing' rule through experimenting with LFLs of fuel mixtures containing methane and other lower hydrocarbons [63]. The proposed mixing rule is expressed in Eq. (2-50). In accordance with Le Chatelier's work, Kondo et al. [64] pointed out that Le Chatelier's rule can be extended to UFL estimations, as shown in Eq. (2-51), for some blended fuels with acceptable accuracy.

Because Le Chatelier's law was empirically derived, it was found not to be universally applicable, especially for UFL estimation, e.g., hydrocarbon mixtures containing unsaturated hydrocarbons [72], or the LFLs of fuel mixtures that may give rise to cool flames [13]. Also, industrial people are still confused to its feasibility at different external conditions, e. g, at non varied temperature and pressure, or fuel mixtures diluted with inert gases and different oxygen concentrations.

In this chapter, a detailed derivation was conducted on LFLs to shed light on the inherent principle residing in this rule. By assuming a constant flame temperature for

pure fuels and their constituting mixture during flame propagation, a theoretical evaluation of Le Chatelier's rule was presented. Results showed that this rule can be extended to fuel mixture with dilution of inert gases and different oxygen concentrations for LFL estimations, and particularly to the non-extreme initial conditions. Unlike the LFL, generalizations of this rule at UFL turn out to be impossible when using the same reaction mechanism. This is because of the high complexity of combustion kinetics and interacting physics of convection flow at the upper flammability limits. Moreover, thermal control is a generally accepted principle to govern the combustion reaction at LFL; however, we found that it is not necessarily valid for all fuels, such as hydrogen. The findings from this study can be used as guidelines to maximize safety in the process design and operational procedures involving flammable chemicals.

Mashuga conducted a theoretical derivation of Le Chatelier's law based on the following assumptions [80]:

a) Constant product heat capacities;
b) Constant mole number of total reactants and products;
c) Constant combustion kinetics of the pure species independent of the presence of other combustibles;
d) Constant adiabatic temperature rise at the flammability limit for all combustible species.

All these assumptions, however, cannot tackle all the intrinsic principles characterizing the combustion at flammability limits. For example, heat loss can affect experimental flammability limits, and it becomes indispensable to quantify flammability

limits when the apparatus quenching effect becomes apparent, for example, in the case of cylindrical vessels with I.D. less than 60 mm. Takahashi [15] observed the changes in flammability limit when conducting tests with apparatus of different geometries; methane's lower flammability limit in a 50 mm x 400 mm cylindrical reaction vessel was found to be 4.7 vol%, while 5.0 vol% was obtained when the apparatus dimension was changed to 200 mm x 400 mm. It is important to point out that Le Chatelier's law was originally developed from experiments using a glass tube of 30 mm in diameter and 300 mm long, which implies that the tendency for heat loss is inevitable regardless of the apparatus geometry and thus, and adiabatic reaction condition is not necessary for this rule derivation. Meanwhile, constant property assumptions, e.g., heat capacity and number of moles of gas, are not inherently suitable for some fuels with a LFL over 10 vol% (e.g., carbon monoxide). Additionally, the combustion reaction under the fuel-lean condition often completes in a fraction of a second, and this reaction can easily achieve equilibrium status. Therefore, at LFL, an equilibrium process becomes dominant and the reaction kinetics can be neglected [79].

In this section, a new approach was conducted to derive Le Chatelier's law with the only assumption of constant adiabatic flame temperature. Moreover, this law's applications with different inert additions, at varied oxygen concentrations and non-ambient conditions were verified below.

The starting point for deriving Le Chatelier's rule is the principle of energy conservation, which can be represented in Eq. (7-1) for combustion taking place at flammability limits,

$$\Delta H = H_f - H_i = Q + W_s + \int VdP \tag{7-1}$$

where, ΔH is the change in enthalpy for a reaction system. H_f and H_i are the final and initial enthalpies, respectively; W_s is the shaft work acting on the system; Q is the heat exchange between the reaction system and its surroundings.

The total heat exchange is dependent on the apparatus configuration. Heat conduction is usually ignored compared with heat heat convection (Q_c) and heat radiation (Q_r), which are associated with heat losses ranging from burnt gas to unburnt gas. Normally there is no shaft work input into the flammability apparatus. When combustion happens at the flammability limit, the reaction system's pressure can be treated as a constant. This is because at this condition, combustion becomes weak and only partial fuel participates in the reaction, hence the last term in Eq. (7-1) can be set to zero. The enthalpy change (ΔH) can be subdivided into two parts: isothermal combustion enthalpy change (ΔH_c) at initial temperature (T_0), and the reaction products' enthalpy change (ΔH_h) from the initial temperature to the final flame temperature (T_f) as shown in Eq. (7-2). Combining all those variables together, Eq. (7-1) can be extended to Eq. (7-3).

$$\Delta H_h = \sum_{prods} n_j \int_{T_0}^{T_f} C_{P_j} dT \tag{7-2}$$

$$\Delta H_c + \sum_{prods} n_j \int_{T_0}^{T_f} C_{P_j} dT = (Q_c + Q_r) \tag{7-3}$$

where, ΔH_c is empirically negative for exothermic combustion. Heat losses (Q_r and Q_c) from burnt gas to the surroundings are to be set to negative. n_j is the mole number of product j.

7.2 Le Chatelier's law on LFL

For simplicity, we developed the derivation starting with a binary fuel mixture of hydrocarbons, $C_{a1}H_{b1}$ and $C_{a2}H_{b2}$, at ambient conditions (room temperature and atmospheric pressure). At the concentrations near the LFL, it was assumed that fuel combustion proceeds promptly with almost complete reaction, and the end products mainly include CO_2 and H_2O. It is noteworthy to mention that flame temperatures near the limits are less than 1650 K for most fuels and dissociation products, and thus can be made negligible [81]. Therefore, the reaction products of pure fuels $C_{a1}H_{b1}$ and $C_{a2}H_{b2,}$ as well as their mixture for 1 mole fuel/air mixture, can be estimated using Eqs. (7-4), (7-5), and (7-6), respectively. LFL_1, LFL_2, and LFL_m are the LFLs of pure fuels $C_{a1}H_{b1}$, $C_{a2}H_{b2}$, and the mixture of $C_{a1}H_{b1}$and $C_{a2}H_{b2}$ with molar ratios of y_1 for component $C_{a1}H_{b1}$ and y_2 for $C_{a2}H_{b2}$ (y_1+y_2=1).

$$\begin{aligned}&(LFL_1)C_{a_1}H_{b_1}+(1-LFL_1)Air\rightarrow\\&(LFL_1\times a_1)CO_2+\left(\frac{b_1}{2}\times LFL_1\right)H_2O+0.79(1-LFL_1)N_2+\\&\left[0.21(1-LFL_1)-(a_1\times LFL_1)-\left(\frac{b_1}{4}\times LFL_1\right)\right]O_2\end{aligned}\qquad (7\text{-}4)$$

$$
\begin{aligned}
&(LFL_2)C_{a_2}H_{b_2} + (1 - LFL_2)Air \rightarrow \\
&(LFL_2 \times a_2)CO_2 + \left(\frac{b_2}{2} \times LFL_2\right)H_2O + 0.79(1 - LFL_2)N_2 + \\
&\left[0.21(1 - LFL_2) - (a_2 \times LFL_2) - \left(\frac{b_2}{4} \times LFL_2\right)\right]O_2
\end{aligned}
\tag{7-5}
$$

$$
\begin{aligned}
&\left[(y_1 \times LFL_m)C_{a_1}H_{b_1} + (y_2 \times LFL_m)C_{a_2}H_{b_2}\right] + (1 - LFL_m)Air \rightarrow \\
&LFL_m(y_1a_1 + y_2a_2)CO_2 + LFL_m\left(\frac{y_1b_1 + y_2b_2}{2}\right)H_2O + 0.79(1 - LFL_m)N_2 \\
&+ \left[0.21(1 - LFL_m) - LFL_m(y_1a_1 + y_2a_2) - LFL_m\left(\frac{y_1b_1 + y_2b_2}{4}\right)\right]O_2
\end{aligned}
\tag{7-6}
$$

Now, putting together all the reaction products into Eq. (7-3) and rearranging it for solving isothermal combustion enthalpy change ΔH_c for 1 mole of fuel/air mixture using the average heat capacities, we can obtain Eqs. (7-7), (7-8), and (7-9).

$$
\begin{aligned}
&\Delta H_{c_1} = LFL_1 \times \Delta h_{c_1} = LFL_1 \times (q_{c_1} + q_{r_1}) - \\
&(T_{f_1} - T_0)\left(n_{CO_2,1}\widehat{C}_{P_{CO_2},1} + n_{H_2O,1}\widehat{C}_{P_{H_2O},1} + n_{N_2,1}\widehat{C}_{P_{N_2},1} + n_{O_2,1}\widehat{C}_{P_{O_2},1}\right)
\end{aligned}
\tag{7-7}
$$

$$
\begin{aligned}
&\Delta H_{c_2} = LFL_2 \times \Delta h_{c_2} = LFL_2 \times (q_{c_2} + q_{r_2}) - \\
&(T_{f_2} - T_0)\left(n_{CO_2,2}\widehat{C}_{P_{CO_2},2} + n_{H_2O,2}\widehat{C}_{P_{H_2O},2} + n_{N_2,2}\widehat{C}_{P_{N_2},2} + n_{O_2,2}\widehat{C}_{P_{O_2},2}\right)
\end{aligned}
\tag{7-8}
$$

$$
\begin{aligned}
&\Delta H_{c_m} = LFL_m \times \Delta h_{c_m} = LFL_m \times (q_{c_m} + q_{r_m}) \\
&- (T_{f_m} - T_0)\left(n_{CO_2,m}\widehat{C}_{P_{CO_2},m} + n_{H_2O,m}\widehat{C}_{P_{H_2O},m} + n_{N_2,m}\widehat{C}_{P_{N_2},m} + n_{O_2,m}\widehat{C}_{P_{O_2},m}\right)
\end{aligned}
\tag{7-9}
$$

where, Δh_c is the enthalpy change of the combustion in unit of energy per molar fuel; q_c and q_r are heat losses through convection and radiation in unit of energy per molar fuel;

n_j is the reaction product obtained from Eqs. (7-4), (7-5) and (7-6); $\widehat{C}_P$ is the average heat capacity at the temperature range of T_0 through T_f; subscripts 1, 2, and m indicate the reaction systems of pure fuel $C_{a1}H_{b1}$ and $C_{a2}H_{b2}$, and the mixture of $C_{a1}H_{b1}$and $C_{a2}H_{b2}$; the enthalpy of combustion Δh_{c_m} can be calculated using Eq. (7-10) based on the Hess's Law of chemical reaction [78], which states the reaction enthalpy change is constant for the conversion from the same reactants to the same products regardless of reaction taking place in one step or in a series of steps.

$$\Delta h_{c_m} = y_1 \Delta h_{c_1} + y_2 \Delta h_{c_2} \tag{7-10}$$

Solving for Δh_{c_1}, Δh_{c_2} and Δh_{c_m} from Eqs. (7-7), (7-8) and (7-9), and then putting them into Eq. (7-10), we can finally obtain Eq. (7-11), which was derived only under the assumption of constant flame temperatures for pure fuels $C_{a1}H_{b1}$, $C_{a2}H_{b2}$, and the mixture of $C_{a1}H_{b1}$and $C_{a2}H_{b2}$.

$$\frac{\left[LFL_m\left(q_{c_m}+q_{r_m}\right)-\widehat{C}_{P_{Air}}\left(T_{f_m}-T_0\right)\right]}{LFL_m} = \frac{y_1\left[LFL_1\left(q_{c_1}+q_{r_1}\right)-\widehat{C}_{P_{Air}}\left(T_{f_1}-T_0\right)\right]}{LFL_1}+\frac{y_2\left[LFL_2\left(q_{c_2}+q_{r_2}\right)-\widehat{C}_{P_{Air}}\left(T_{f_2}-T_0\right)\right]}{LFL_2} \tag{7-11}$$

where, $\widehat{C}_{P_{Air}}\ (=0.79\widehat{C}_{P_{N_2}}+0.21\widehat{C}_{P_{O_2}})$ is the average heat capacity of air at the temperature range of T_0 through T_f.

Heat losses per mole of fuel/air mixture $LFL\left(q_c+q_r\right)$, through convection and radiation, can be estimated approximately using Eqs. (7-12) and (7-13), respectively.

$$Q_c = \alpha h A_s (T_f - T_\infty)\Delta t \tag{7-12}$$

$$Q_r = \alpha \sigma A_s \left(\varepsilon_g T_f^4 - \alpha_g T_\infty^4\right)\Delta t \tag{7-13}$$

where, h is the convective heat transfer coefficient, which is greatly dependent on the temperature gradient between the reaction system and its surroundings, and can be set constant for the reaction system of pure fuels as well as fuel mixtures when the final flame temperature is constant. A_s is the heat exchange surface area. For one mole of different fuel/air mixtures at the same pressure and temperature, they occupy the same volume space. When a certain flammability criterion is applied, the flame propagation pathway becomes defined. For example, on one particular criterion, the flame propagation pathway has been defined as a predefined travel distance along the cylindrical vessels [13, 67]; the experimental methods proposed by ASHRAE require the flame to reach an arc of vessel wall, subtending an angle larger than 90° as measured from ignition point in spherical vessels [82, 83]; therefore, the heat exchange surface area can be reasonably assumed to be constant for the same volumes of fuel/air mixtures (pure fuel in air and fuel mixture in air). Δt is the flame propagation duration, and was defined in this paper as the time needed to cover the flame propagation from ignition to fire extinguishment. When a certain flammability apparatus and a criterion are selected, it is mainly affected by fuel burning velocity that can be treated as a constant value at flammability limits. Zhao [67] measured the flame propagation time in a cylindrical vessel and obtained near-constant values for hydrocarbons at their LFLs. α is an efficiency factor with respect to the heat exchange surface area, which expands gradually

with flame propagation; α is assumed to be constant for the same experimental conditions. σ is the Stefan-Boltzmann constant. ε_g, gas emissivity, is presumed constant for different fuel/air mixtures using the same flammability criterion and apparatus and it mainly depends on the reaction system's temperature and pressure, the configuration of flammability apparatus, and the molar fraction of non-transparent products to radiation (*e.g.*, carbon dioxide, water). At LFLs with same experimental conditions and the constant flame temperature assumption, all the emissivity-related parameters can be treated equally. The effect of heat absorption can be neglected because the value of $\alpha_g T_\infty^4$ is much smaller than that of $\varepsilon_g T_f^4$. Combining the aforementioned parameters together at the constant flame conditions, we can get Eq. (7-14).

$$LFL_m\left(q_{c_m}+q_{r_m}\right)=LFL_1\left(q_{c_1}+q_{r_1}\right)=LFL_2\left(q_{c_2}+q_{r_2}\right) \tag{7-14}$$

Substituting Eq. (7-14) into Eq. (7-11), we can finally obtain Le Chatelier's law for binary hydrocarbon mixture at the ambient conditions (Eq. (7-15)).

$$\frac{1}{LFL_m}=\frac{y_1}{LFL_1}+\frac{y_2}{LFL_2} \tag{7-15}$$

In order to develop an estimating equation that is widely acceptable, the fuel mixtures are assumed to consist of the components with the formula of $C_aH_bO_cN_dX_eS_f$, where 'X' is a halogen atom. At LFL, the combustion process is controlled by the "near equilibrium" chemical kinetics, and the products mainly contain CO_2, H_2O, NO_2 (or N_2), SO_2 (or H_2SO_4), and HX [8, 84-86]. Furthermore, Martel also [85] pointed out that the

products of NO_2 and SO_2 should be considered a priority for obtaining accurate prediction of the LFL. Finally, the chemical reaction can be expressed as Eq. (16) for a fuel $C_aH_bO_cN_dX_eS_f$ combusting at LFLs.

$$\begin{aligned}&(LFL)C_aH_bO_cN_dX_eS_f + (1-LFL)Air \rightarrow (LFL\times a)CO_2 + (LFL\times f)SO_2 \\ &+ (LFL\times e)HX + \left(\frac{b-e}{2}\times LFL\right)H_2O + (LFL\times d)NO_2 \\ &+ 0.79(1-LFL)N_2 + \left[0.21(1-LFL) - \left[\left(a + f + d + \frac{b-e}{4} - \frac{c}{2}\right)\times LFL\right]\right]O_2\end{aligned} \tag{7-16}$$

Similar to the operation above, substituting all the reaction products of pure fuels and the mixture into Eq. (7-3), we can get the same expression as Eq. (7-11) and eventually obtain the formula of Le Chatelier's law under the assumption of constant combustion flame temperature.

When fuel mixture is diluted with inert gas and at the concentration near its LFL, same to fuel mixture in air without the inert gas, fuel combustion can proceed with almost complete reaction with the main end products of CO_2, H_2O, and the left air and the unreacted inert gas. At LFL the flame temperature is less than 1650 K for most fuels and the dissociation products are negligible, including the added inert gas [81]; meanwhile, as indicated from Chapter V, inert gas will not affect fuel combustion mechanism outside of the flammability nose zone. Therefore, the added inert gas can be treated as a heat sink. For fuel 1 $C_{a1}H_{b1}$, fuel 2, $C_{a2}H_{b2}$, and the fuel mixture of $C_{a1}H_{b1}$ and $C_{a2}H_{b2}$ with additional nitrogen introduced, the reaction productions be estimated using Eqs. (7-17), (7-18), and (7-19), respectively.

$$\begin{aligned}&\left(LFL_1^{N_2}\right)C_{a_1}H_{b_1}+(X)N_2+\left(1-X-LFL_1^{N_2}\right)Air\rightarrow\\&\left(LFL_1^{N_2}\times a_1\right)CO_2+\left(\frac{b_1}{2}\times LFL_1^{N_2}\right)H_2O+\left[X+0.79\left(1-X-LFL_1^{N_2}\right)\right]N_2\\&+\left[0.21\left(1-X-LFL_1^{N_2}\right)-\left(a_1\times LFL_1^{N_2}\right)-\left(\frac{b_1}{4}\times LFL_1^{N_2}\right)\right]O_2\end{aligned}\tag{7-17}$$

$$\begin{aligned}&\left(LFL_2^{N_2}\right)C_{a_2}H_{b_2}+(X)N_2+\left(1-X-LFL_2^{N_2}\right)Air\rightarrow\\&\left(LFL_2^{N_2}\times a_2\right)CO_2+\left(\frac{b_2}{2}\times LFL_2^{N_2}\right)H_2O+\left[X+0.79\left(1-X-LFL_2^{N_2}\right)\right]N_2\\&+\left[0.21\left(1-X-LFL_2^{N_2}\right)-\left(a_2\times LFL_2^{N_2}\right)-\left(\frac{b_2}{4}\times LFL_2^{N_2}\right)\right]O_2\end{aligned}\tag{7-18}$$

$$\begin{aligned}&\left[\left(y_1\times LFL_m^{N_2}\right)C_{a_1}H_{b_1}+\left(y_2\times LFL_m^{N_2}\right)C_{a_2}H_{b_2}\right]+(X)N_2+\left(1-X-LFL_m^{N_2}\right)Air\rightarrow\\&LFL_m^{N_2}\left(y_1a_1+y_2a_2\right)CO_2+LFL_m^{N_2}\left(\frac{y_1b_1+y_2b_2}{2}\right)H_2O\\&+\left[X+0.79\left(1-X-LFL_m^{N_2}\right)\right]N_2\\&+\left[0.21\left(1-X-LFL_m^{N_2}\right)-LFL_m^{N_2}\left(y_1a_1+y_2a_2\right)-LFL_m^{N_2}\left(\frac{y_1b_1+y_2b_2}{4}\right)\right]O_2\end{aligned}\tag{7-19}$$

where $LFL_1^{N_2}$, $LFL_2^{N_2}$, and $LFL_m^{N_2}$ are the LFLs with additional nitrogen for fuel 1, $C_{a1}H_{b1}$, fuel 2, $C_{a2}H_{b2}$, and the fuel mixture of $C_{a1}H_{b1}$and $C_{a2}H_{b2}$. y_1 and y_2 are the molar ratios of fuel 1 and fuel 2 on the combustible basis ($y_1+y_2=1$). X is the additional nitrogen volume concentration.

Now, putting all the reaction productions into Eq. (7-3) and rearranging it for solving isothermal combustion enthalpy change ΔH_c for 1 mole of fuel/air mixture using the average heat capacities, we can obtain the same Eqs. (7-7), (7-8), and (7-9) as before. Next, solving for Δh_{c_1}, Δh_{c_2} and Δh_{c_m} from Eqs. (7-7), (7-8) and (7-9), and then putting

them into Eq. (7-10), we can finally obtain Eq. (7-20), which was again under the assumption of constant flame temperatures.

$$\frac{\left\{LFL_m^{N_2}\left(q_{c_m}+q_{r_m}\right)-\left(T_{f_m}-T_0\right)\left[\hat{C}_{P_{Air}}+X\left(\hat{C}_{P_{N_2}}-\hat{C}_{P_{Air}}\right)\right]\right\}}{LFL_m^{N_2}}=$$
$$\frac{y_1\left\{LFL_1^{N_2}\left(q_{c_1}+q_{r_1}\right)-\left(T_{f_1}-T_0\right)\left[\hat{C}_{P_{Air}}+X\left(\hat{C}_{P_{N_2}}-\hat{C}_{P_{Air}}\right)\right]\right\}}{LFL_1^{N_2}} \tag{7-20}$$
$$+\frac{y_2\left\{LFL_2^{N_2}\left(q_{c_2}+q_{r_2}\right)-\left(T_{f_2}-T_0\right)\left[\hat{C}_{P_{Air}}+X\left(\hat{C}_{P_{N_2}}-\hat{C}_{P_{Air}}\right)\right]\right\}}{LFL_2^{N_2}}$$

Clearly, under the assumption of constant flame temperature, when the same flammability criterion and flammability apparatus are applied to pure fuels, $C_{a1}H_{b1}$and $C_{a2}H_{b2}$, and the fuel mixture of $C_{a1}H_{b1}$and $C_{a2}H_{b2}$ with the same additional nitrogen contents, heat losses can be treated as a constant, say, Eq. (7-21). Finally, Eq. (7-20) can be simplified as Eq. (7-22), the Le Chatelier's law applied to fuel mixture with inert gas dilution. Tables 7.1 – 7.4 show the LFLs of fuel mixtures at different additional nitrogen concentrations from experimental observations and Le Chatelier's law predictions.

$$LFL_m^{N_2}\left(q_{c_m}+q_{r_m}\right)=LFL_1^{N_2}\left(q_{c_1}+q_{r_1}\right)=LFL_2^{N_2}\left(q_{c_2}+q_{r_2}\right) \tag{7-21}$$

$$\frac{1}{LFL_m^{N_2}}=\frac{y_1}{LFL_1^{N_2}}+\frac{y_2}{LFL_2^{N_2}} \tag{7-22}$$

Table 7.1. LFLs of methane and propane with nitrogen dilution from experimental observations and Le Chatlier's law.

Fuel mixtures	N2* (vol %)	LFL (exp.) (vol %)	LFL (calc.) (vol %)	Dev.	|Dev. %|
$CH_4 + C_3H_8$ (20% / 80%)	5	2.36	2.38	0.02	0.85
	10	2.38	2.35	0.03	1.26
	15	2.37	2.37	0.00	0.00
	20	2.38	2.37	0.01	0.42
	25	2.39	2.34	0.05	2.09
	30	2.37	2.35	0.02	0.84
	35	2.40	2.34	0.06	2.50
$CH_4 + C_3H_8$ (40% / 60%)	5	2.76	2.75	0.01	0.18
	10	2.74	2.73	0.01	0.34
	15	2.74	2.74	0.00	0.00
	20	2.75	2.74	0.01	0.32
	25	2.73	2.72	0.01	0.39
	30	2.74	2.73	0.01	0.34
	35	2.76	2.72	0.04	1.36
$CH_4 + C_3H_8$ (60% / 40%)	5	3.26	3.28	0.02	0.49
	10	3.27	3.25	0.02	0.63
	15	3.25	3.26	0.01	0.36
	20	3.26	3.26	0.00	0.00
	25	3.25	3.24	0.01	0.39
	30	3.26	3.25	0.01	0.32
	35	3.31	3.26	0.05	1.61
$CH_4 + C_3H_8$ (80% / 20%)	5	4.03	4.04	0.01	0.26
	10	4.02	4.01	0.01	0.21
	15	4.03	4.02	0.01	0.16
	20	4.02	4.02	0.00	0.00
	25	4.04	4.00	0.04	1.01
	30	4.02	4.01	0.01	0.21
	35	4.11	4.05	0.06	1.42

N_2*: additional nitrogen added; exp.: experiment; calc.: Le Chatelier's law

Table 7.2. LFLs of ethane and propane with nitrogen dilution from experimental observations and Le Chatlier's law.

Fuel mixtures	N2* (vol %)	LFL (exp.) (vol %)	LFL (calc.) (vol %)	Dev.	|Dev. %|
$C_2H_6 + C_3H_8$ (20% / 80%)	5	2.19	0.01	0.44	2.19
	10	2.17	0.02	0.79	2.17
	15	2.18	0.03	1.41	2.18
	20	2.18	0.01	0.33	2.18
	25	2.16	0.02	0.80	2.16
	30	2.17	0.04	1.87	2.17
	35	2.15	0.03	1.32	2.15
	40	2.23	0.02	0.96	2.23
$C_2H_6 + C_3H_8$ (40% / 60%)	5	2.29	2.30	0.01	0.46
	10	2.28	2.29	0.01	0.26
	15	2.27	2.29	0.02	0.77
	20	2.31	2.30	0.01	0.60
	25	2.3	2.28	0.02	1.05
	30	2.29	2.28	0.01	0.55
	35	2.27	2.26	0.01	0.32
	40	2.32	2.32	0.00	0.00
$C_2H_6 + C_3H_8$ (60% / 40%)	5	2.45	2.42	0.03	1.12
	10	2.43	2.41	0.02	0.75
	15	2.43	2.41	0.02	0.92
	20	2.45	2.42	0.03	1.15
	25	2.44	2.40	0.04	1.58
	30	2.43	2.40	0.03	1.34
	35	2.42	2.39	0.03	1.38
	40	2.46	2.43	0.03	1.25
$C_2H_6 + C_3H_8$ (80% / 20%)	5	2.54	2.56	0.02	0.72
	10	2.52	2.55	0.03	1.28
	15	2.55	2.54	0.01	0.35
	20	2.54	2.56	0.02	0.88
	25	2.55	2.54	0.01	0.31
	30	2.53	2.53	0.00	0.00
	35	2.54	2.52	0.02	0.60
	40	2.55	2.54	0.01	0.24

N_2*: additional nitrogen added; exp.: experiment; calc.: Le Chatelier's law

Table 7.3. LFLs of methane and ethylene with nitrogen dilution from experimental observations and Le Chatlier's law.

Fuel mixtures	N2* (vol %)	LFL (exp.) (vol %)	LFL (calc.) (vol %)	Dev.	|Dev. %|
$CH_4 + C_2H_4$ (20% / 80%)	5	3.11	3.09	0.02	0.66
	10	3.12	3.07	0.05	1.66
	15	3.08	3.11	0.03	0.90
	20	3.10	3.09	0.01	0.40
	25	3.09	3.08	0.01	0.42
	30	3.10	3.06	0.04	1.34
	35	3.11	3.11	0.00	0.00
$CH_4 + C_2H_4$ (40% / 60%)	5	3.44	3.45	0.01	3.44
	10	3.45	3.42	0.03	3.45
	15	3.44	3.46	0.02	3.44
	20	3.42	3.44	0.02	3.42
	25	3.42	3.43	0.01	3.42
	30	3.44	3.41	0.03	3.44
	35	3.43	3.47	0.04	3.43
$CH_4 + C_2H_4$ (60% / 40%)	5	3.91	3.90	0.01	0.37
	10	3.89	3.87	0.02	0.51
	15	3.90	3.90	0.00	0.00
	20	3.88	3.89	0.01	0.14
	25	3.86	3.87	0.01	0.38
	30	3.89	3.86	0.03	0.71
	35	3.89	3.93	0.04	1.09
$CH_4 + C_2H_4$ (80% / 20%)	5	4.45	4.48	0.03	0.67
	10	4.44	4.45	0.01	0.27
	15	4.44	4.48	0.04	0.86
	20	4.42	4.46	0.04	0.96
	25	4.45	4.45	0.00	0.00
	30	4.44	4.45	0.01	0.16
	35	4.49	4.54	0.05	1.04

N_2*: additional nitrogen added; exp.: experiment; calc.: Le Chatelier's law

Table 7.4. LFLs of ethylene and propylene with nitrogen dilution from experimental observations and Le Chatlier's law.

Fuel mixtures	N2* (vol %)	LFL (exp.) (vol %)	LFL (calc.) (vol %)	Dev.	|Dev. %|
$C_2H_4 + C_3H_6$ (20% / 80%)	5	2.37	2.37	0.00	0.00
	10	2.36	2.39	0.03	1.31
	15	2.35	2.36	0.01	0.52
	20	2.34	2.34	0.00	0.00
	25	2.35	2.36	0.01	0.34
	30	2.33	2.34	0.01	0.33
	35	2.39	2.45	0.06	2.37
	40	2.45	2.58	0.13	5.49
$C_2H_4 + C_3H_6$ (40% / 60%)	5	2.47	2.46	0.01	0.28
	10	2.46	2.48	0.02	0.71
	15	2.46	2.46	0.00	0.00
	20	2.44	2.44	0.00	0.00
	25	2.45	2.45	0.00	0.00
	30	2.44	2.43	0.01	0.30
	35	2.47	2.53	0.06	2.36
	40	2.5	2.63	0.13	5.23
$C_2H_4 + C_3H_6$ (60% / 40%)	5	2.56	2.57	0.01	0.23
	10	2.56	2.57	0.01	0.42
	15	2.55	2.57	0.02	0.82
	20	2.55	2.55	0.00	0.00
	25	2.56	2.56	0.00	0.00
	30	2.54	2.54	0.00	0.00
	35	2.55	2.62	0.07	2.58
	40	2.59	2.68	0.09	3.43
$C_2H_4 + C_3H_6$ (80% / 20%)	5	2.68	2.68	0.00	0.00
	10	2.66	2.67	0.01	0.42
	15	2.67	2.69	0.02	0.74
	20	2.65	2.67	0.02	0.74
	25	2.65	2.67	0.02	0.67
	30	2.66	2.65	0.01	0.47
	35	2.64	2.71	0.07	2.63
	40	2.69	2.73	0.04	1.43

N_2*: additional nitrogen added; exp.: experiment; calc.: Le Chatelier's law

Now, substituting "INT" as a general inert gas for N_2 in Eqs. (7-17), (7-18) and (7-19), we can get the correlated equation of fuel 1 $C_{a1}H_{b1}$, fuel 2 $C_{a2}H_{b2}$, and the fuel mixture composed of $C_{a1}H_{b1}$ and $C_{a2}H_{b2}$, Eq. (7-23), similarly under the assumption of constant flame temperature.

$$\begin{aligned}\frac{\left\{LFL_m^{INT}\left(q_{c_m}+q_{r_m}\right)-\left(T_{f_m}-T_0\right)\left[\widehat{C}_{P_{Air}}+X\left(\widehat{C}_{P_{INT}}-\widehat{C}_{P_{Air}}\right)\right]\right\}}{LFL_m^{INT}} = \\ \frac{y_1\left\{LFL_1^{INT}\left(q_{c_1}+q_{r_1}\right)-\left(T_{f_1}-T_0\right)\left[\widehat{C}_{P_{Air}}+X\left(\widehat{C}_{P_{INT}}-\widehat{C}_{P_{Air}}\right)\right]\right\}}{LFL_1^{INT}} \\ +\frac{y_2\left\{LFL_2^{INT}\left(q_{c_2}+q_{r_2}\right)-\left(T_{f_2}-T_0\right)\left[\widehat{C}_{P_{Air}}+X\left(\widehat{C}_{P_{INT}}-\widehat{C}_{P_{Air}}\right)\right]\right\}}{LFL_2^{INT}}\end{aligned} \quad (7\text{-}23)$$

where LFL_1^{INT}, LFL_2^{INT}, and LFL_m^{INT} are the LFLs with dilution of inert gas for fuel 1, $C_{a1}H_{b1}$, fuel 2, $C_{a2}H_{b2}$, and the fuel mixture of $C_{a1}H_{b1}$and $C_{a2}H_{b2}$. y_1 and y_2 are the molar ratios of fuel 1 and fuel 2 on the combustible basis ($y_1+y_2=1$). X is the inert gas volume concentration.

Similarly as above operation, Eq. (7-23) can be simplified as Eq. (7-24) under the assumption of constant flame temperature with the same flammability criterion and flammability apparatus.

$$\frac{1}{LFL_m^{INT}}=\frac{y_1}{LFL_1^{INT}}+\frac{y_2}{LFL_2^{INT}} \quad (7\text{-}24)$$

To verify Le Chatelier's application to LFL with varied oxygen concentrations, we treat this condition separately as two categories: (i) oxygen-lean ambience (oxygen

concentration is less than that in air); and (ii) oxygen-rich ambience (oxygen concentration is higher than that in air). Apparently, oxygen-lean ambience is equivalent to the condition of fuel in air with additional nitrogen introduction, and the feasibility of Le Chatelier's law was verified above. At oxygen-rich ambience, oxygen is sufficient and the excess oxygen acts as a heat sink only. The final reaction products with sufficient oxygen can be characterized using Eqs. (7-25), (7-26), (7-27), respectively, for fuel 1 $C_{a1}H_{b1}$, fuel 2 $C_{a2}H_{b2}$, and the fuel mixture of $C_{a1}H_{b1}$ and $C_{a2}H_{b2}$.

$$\begin{aligned}&\left(LFL_1^{O_2}\right)C_{a_1}H_{b_1}+(X)O_2+\left(1-X-LFL_1^{O_2}\right)Air\rightarrow\\&\left(LFL_1^{O_2}\times a_1\right)CO_2+\left(\frac{b_1}{2}\times LFL_1^{O_2}\right)H_2O+0.79\left(1-X-LFL_1^{O_2}\right)N_2\\&+\left[0.21\left(1-X-LFL_1^{O_2}\right)+X-\left(a_1\times LFL_1^{O_2}\right)-\left(\frac{b_1}{4}\times LFL_1^{O_2}\right)\right]O_2\end{aligned}\tag{7-25}$$

$$\begin{aligned}&\left(LFL_2^{O_2}\right)C_{a_2}H_{b_2}+(X)O_2+\left(1-X-LFL_2^{O_2}\right)Air\rightarrow\\&\left(LFL_2^{O_2}\times a_2\right)CO_2+\left(\frac{b_2}{2}\times LFL_2^{O_2}\right)H_2O+0.79\left(1-X-LFL_2^{O_2}\right)N_2\\&+\left[0.21\left(1-X-LFL_2^{O_2}\right)+X-\left(a_2\times LFL_2^{O_2}\right)-\left(\frac{b_2}{4}\times LFL_2^{O_2}\right)\right]O_2\end{aligned}\tag{7-26}$$

$$\begin{aligned}&\left[\left(y_1\times LFL_m^{O_2}\right)C_{a_1}H_{b_1}+\left(y_2\times LFL_m^{O_2}\right)C_{a_2}H_{b_2}\right]+(X)O_2+\left(1-X-LFL_m^{O_2}\right)Air\rightarrow\\&LFL_m^{O_2}\left(y_1a_1+y_2a_2\right)CO_2+LFL_m^{O_2}\left(\frac{y_1b_1+y_2b_2}{2}\right)H_2O+0.79\left(1-X-LFL_m^{N_2}\right)N_2\\&+\left[0.21\left(1-X-LFL_m^{O_2}\right)+X-LFL_m^{O_2}\left(y_1a_1+y_2a_2\right)-LFL_m^{O_2}\left(\frac{y_1b_1+y_2b_2}{4}\right)\right]O_2\end{aligned}\tag{7-27}$$

where $LFL_1^{O_2}$, $LFL_2^{O_2}$, and $LFL_m^{O_2}$ are the LFLs with dilution of inert gas for fuel 1 $C_{a1}H_{b1}$, fuel 2 $C_{a2}H_{b2}$, and the fuel mixture of $C_{a1}H_{b1}$and $C_{a2}H_{b2}$. y_1 and y_2 are the molar ratios of fuel 1 and fuel 2 on the combustible basis ($y_1+y_2=1$). X is the additional oxygen volume concentration.

With the same operations as above, we can obtain Eq. (7-28) by combining Eqs. (7-7), (7-8), (7-9), (7-10), (7-25), (7-26), and (7-27) together. Eq. (7-28) can be simplified as Eq. (7-29) under the same assumption of constant flame temperature with the same flammability criterion and flammability apparatus.

$$\begin{aligned}\frac{\left\{LFL_m^{O_2}\left(q_{c_m}+q_{r_m}\right)-\left(T_{f_m}-T_0\right)\left[\hat{C}_{P_{Air}}+X\left(\hat{C}_{P_{O_2}}-\hat{C}_{P_{Air}}\right)\right]\right\}}{LFL_m^{O_2}} = \\ \frac{y_1\left\{LFL_1^{O_2}\left(q_{c_1}+q_{r_1}\right)-\left(T_{f_1}-T_0\right)\left[\hat{C}_{P_{Air}}+X\left(\hat{C}_{P_{O_2}}-\hat{C}_{P_{Air}}\right)\right]\right\}}{LFL_1^{O_2}} \\ +\frac{y_2\left\{LFL_2^{O_2}\left(q_{c_2}+q_{r_2}\right)-\left(T_{f_2}-T_0\right)\left[\hat{C}_{P_{Air}}+X\left(\hat{C}_{P_{O_2}}-\hat{C}_{P_{Air}}\right)\right]\right\}}{LFL_2^{O_2}}\end{aligned} \tag{7-28}$$

$$\frac{1}{LFL_m^{O_2}}=\frac{y_1}{LFL_1^{O_2}}+\frac{y_2}{LFL_2^{O_2}} \tag{7-29}$$

When combustible mixtures are initially at non-ambient conditions, a similar derivation can be performed, as above, at ambient conditions. Clearly, Eq. (7-3) still works as a governing equation because it originates from the energy conservation law. In accordance to Hess's law of chemical reaction, Eq. (7-10) would remain valid regardless of the reactants' original conditions. Although the LFL changes with initial temperature considerably, there exists a constant threshold temperature, *i.e.*, the lower flammability

limit temperature below which flame cannot propagate [49]. Therefore, dissociation of products becomes negligible at non-ambient conditions, as well as at ambient conditions. Similarly, at the LFL conditions, reaction is often thermally controlled. When the reactants' initial temperature is not too high (so that decomposition can be ignored), nor too low and without phase transition, Eqs. (7-11), (7-20), (7-23) and (7-28) still work under the assumption of constant flame temperature. Heat losses through convection and radiation are mainly dependent on the final conditions of the reaction system; especially the flame temperature and the heat transfer parameters, *e.g.,* heat exchange coefficient, h and gas emissivity, ε_g, which are more dependent on temperature than pressure. Therefore, by using the same flammability detection criteria and the same flammability apparatus with the constant flame temperature assumption, Eq. (7-14) and (7-21) can also be extended for the non-ambient conditions. Compared to temperature, pressure usually has little effect on the lower flammability limit, as shown by a very sharp cut-off at elevated pressures for lean fuel. Eventually, we can further confirm Le Chatelier's law application for the initial fuel/air reaction system when it is not at extreme conditions. Moreover, the uncertainties occurring in the aforementioned can be reduced by cancelling some terms in the product equation because they are simultaneously present in the reaction systems with pure fuels and fuel mixtures, *e.g.,* the left sides of Eqs. (7-11), (7-20), (7-23) and (7-28) are related to pure fuels and its right side to the fuel mixtures at different conditions, say, fuel mixture in air, fuel mixture in air with additional nitrogen, fuel mixture with a common inert gas, and fuel mixture with excess oxygen. As an example, Table 7.5 shows the LFLs of carbon monoxide/n-butane

mixtures through experiments and calculation using Le Chatelier's rule at atmospheric pressure, but with different initial temperatures [87], which indicates that Le Chatelier's rule can predict experimental data well at the non-ambient conditions.

For fuel mixtures containing three or more combustible components at ambient and non-ambient conditions, a similar derivation procedure can be developed, with more relevant variables and numbers to be added to the corresponding equations. Finally, the general formula of Le Chatelier's law can be expressed as Eq. (7-15) for the LFL of fuel mixture in air, Eq. (7-18) for the LFL of fuel mixture in air with additional nitrogen introduction, (7-24) for the LFL of fuel mixture with an inert gas, and (7-29) for the LFL of fuel mixture with excess oxygen.

Table 7.5. Lower flammability limits of carbon monoxide and n-butane mixtures at different initial temperatures.

Fuel mixtures		**Temperature** (°C)	**LFL_{exp}** (vol%)	**LFL_{cal}** (vol%)
CO	C_4H_{10}			
69.5%	30.5%	25	4.30	4.41
61.7%	38.3%	215	3.00	3.13
63.1%	36.9%	320	2.82	2.87

7.3 Le Chatelier's law on UFL

Similarly, Eqs. (7-3) and (7-10) are also required as the governing equations for Le Chatelier's law verification at LFL. Under fuel-rich conditions, combustion is incomplete with unspecified products, thus, the effective molar heat of combustion ΔH_c

may decrease rapidly as the fuel concentration increases toward the UFL. Chen [76, 77] pointed out that at UFLs, most hydrocarbons will undergo an incomplete combustion with the main products of CO_2, H_2O, H_2, and CO, and the chemical reaction equation can be expressed as Eq. (7-30).

$$C_aH_b + \left(a - \frac{a_1}{2} + \frac{b-b_1}{4}\right)O_2 \rightarrow a_1CO + (a-a_1)CO_2 + \frac{b_1}{2}H_2 + \frac{b-b_1}{2}H_2O \qquad (7\text{-}30)$$

where, a_1 is the mole of CO and $b_1/2$ is the mole of H_2 that is produced under the assumption that one mole of a hydrocarbon, C_aH_b, is burnt.

If the chemical reaction in Eq. (7-30) is applied to the hydrocarbon mixture, C_aH_b/C_mH_n, for estimating the UFL, then Le Chatelier's law can be approximated in Eq. (2-51). However, the resulting predictions from Le Chatelier's law become unacceptably inaccurate when they are compared with experimental observations for hydrocarbon mixtures containing unsaturated hydrocarbons [72]. This is because the thermal variables alone are not sufficient to describe the combustion behavior at the UFL. At the LFL, the combustion reaction is thermally controlled, whereas the kinetic reaction control is dominant at the upper flammability limit [79]. The presence of other fuels more or less disturbs the combustion reactions of any fuel in blended gases, especially at UFL conditions [27]. For example, the UFL for the experimental CO/H_2 mixture deviates dramatically from the corresponding values calculated using Le Chatelier's law for the mixture containing small concentrations of hydrogen. This is because the radicals from

hydrogen, primarily OH, can significantly affect the oxidation rate of carbon monoxide [88].

Previous works have done to investigate the nature of the UFL phenomenon from the viewpoint of chain theory of combustion [89], which defines the flammability limits using a competition of chain-branching and chain-termination reactions in a flame front. However, the high complexity of chemical kinetics of combustion, such as: drastically varied oxidation mechanisms at different temperatures [90], cool flame [91] and soot formation [92] at different initial conditions and several hundred elementary chemical reactions [93], makes theoretical derivation of Le Chatelier's rule and generalization of this rule at UFLs impossible. Additionally, unlike the LFLs, which are relatively constant at high pressure and temperature, the UFLs can vary over a wide range of fuel concentrations at high pressure and temperature [94].

7. 4. Discussion

In this work, derivation of Le Chatelier's rule was conducted under the assumption of constant flame temperature, which was proved to be an inherently valid conclusion, especially at LFLs. The Burgess and Wheeler law states that the heat liberated by a mole of lean limit mixture is nearly constant (about 11.0 kcal/mol) for most hydrocarbons burning in the air [95], and the heat releases from some organic compounds containing one atom of nitrogen are around 11.2 kcal/mol at lower flammability limits [86]. It is commonly admitted that the main combustion products of lean fuel mixtures are left air. Therefore, based on these results, the adiabatic flame

temperatures turn out to be close to each other for most fuels at LFLs. By using the kinetic mechanism of flammability limit, Law and Egolfopoulos pointed that at the lower flammability limit the dominant chain branching reactions, $H+O_2 \rightarrow O+OH$, and the dominant chain termination reaction, $H+O_2 \rightarrow HO_2+M$, are the same for all hydrocarbon/air mixtures. As a result, the lower flammability limit is expected to occur at the same adiabatic flame temperature [96].

7.5 Conclusion

In this chapter, Le Chatelier's law was derived based on energy conservation, where the detailed work focuss on the LFL. Only one assumption was used for Le Chatelier's derivation: a constant flame temperature for pure fuels and the fuel mixtures during the flame propagation. Because of the high complexity of chemical kinetics of combustion at the UFLs, generalization of this law on UFL turns out to be impossible when applying the same reaction mechanism as did at LFL.

Because the same reaction mechanism in LFL condition can be applied to the fuel mixture diluted with inert gas or varied oxygen concentrations, we verified that Le Chatelier's law remains valid at these conditions. Specifically, when the reaction system's initial temperature is neither too high (decomposition can be neglected) nor too low (no phase transition occurs), then Le Chatelier's rule still remains valid. Usually the LFL is depicted by a sharp cut-off at elevated pressures for lean fuel, thus it would be more accurate to use Le Chatelier's law at elevated pressure than at elevated temperature

because the reaction mechanism is significantly dependent on temperature rather than pressure.

CHAPTER VIII

CONCLUSIONS AND FUTURE WORK

8.1 Summary and conclusions

In this research, the LFLs and UFLs of binary hydrocarbon mixtures in air at ambient conditions (room temperature and 1 atmospheric pressure) were measured. The obtained experimental data include LFLs and UFLs with and without inert gas dilutions (nitrogen as an example was applied). The tested binary hydrocarbon mixtures include the some of the combinations of low-carbon hydrocarbons, methane, ethane, propane, n-butane, ethylene, propylene, and acetylene. The employed flammability apparatus is a cylindrical two-end-closed vessel with the geometry of I.D. 10.52 cm and length 100 cm. The applied flammability detection criterion is named as the thermal criterion, by which a certain flame propagation distance, 75 cm, is selected as the standard of continuous flame propagation. To determine the flammability limits (LFL and UFL), a series of experiments were conducted at different fuel concentrations, and at every concentration point, the probability of continuous flame propagation was recorded. Finally, flammability limits were estimated by choosing the fuel concentration with 50% probability of continuous flame propagation.

By comparing experimental data with the predictions from Le Chatelier's Law for binary hydrocarbon mixtures without inert gas dilution, we obtained the following conclusions: (i) all the LFLs of fuel mixtures can be fit by Le Chatelier's law within the

experimental uncertainties; (ii) the law-predicted UFLs of fuel mixtures which contain two saturated hydrocarbons can roughly represent Le Chatelier's law; (iii) however, for UFLs of fuel mixtures containing at least one unsaturated components, Le Chatelier's law fails to work. The way to modify Le Chatelier's law is to add powers to the percentage concentrations of fuels. The certain values of added powers are based on the maximum R-square principle. For different fuel combinations, the powering values were different and there seems no direct connection among them.

Nitrogen dilution effects on binary hydrocarbon mixture include the variations of LFL and UFL at different additional nitrogen concentrations, and the minimum inerting concentrations (MICs). The experimental results indicate that LFLs of binary hydrocarbon mixtures remain almost constant with addition of nitrogen, while UFLs decrease dramatically. Approximately, all the binary hydrocarbon mixture LFLs are linearly related to the additional nitrogen concentrations except the flammability nose zone, which is similar to the fuel UFLs of fuel mixtures without containing no ethylene. A quantified characterization of LFL with the additional nitrogen can be linearly regressed for all the selected hydrocarbons (methane, ethane, propane, n-butane, ethylene, propylene) and the combined binary mixtures. Modification of Le Chatelier's law with nitrogen dilution was conducted through the definition of inert gas dilution coefficient. The nitrogen dilution coefficient on LFL is defined as the slope of the linear fitting line from the selected pure hydrocarbons. A fuel mixture LFL can be estimated from pure fuel properties. The nitrogen dilution coefficient on fuel mixture LFL can be optimized as the summation of the reciprocal of the pure fuel's dilution coefficient with

a volume composition weighting factor. The quantitative relationship of fuel mixture UFL with the added nitrogen is approximated to be linear except mixtures containing ethylene, and the similar operation was conducted to determine the nitrogen dilution effect on the UFL of pure hydrocarbons and binary hydrocarbon mixtures without ethylene. For fuel mixtures having ethylene, a relation of the square root of UFL with additionally introduced nitrogen is linearly illustrated. The MIC occurs at the converging point of the LFL and UFL with dilution of inert gases. An equal relation between them can be applied to calculate the MIC as a function of the fuel mixture LFL, UFL and the dilution coefficient.

CAFT modeling for nitrogen dilution effect on binary hydrocarbon mixtures was performed as well. This model includes a three-step procedure: (i) estimate the calculated adiabatic flame temperature of pure fuel; (ii) estimate the calculated adiabatic flame temperature of fuel mixture; and (iii) estimate the flammability limits of fuel mixture at different additional nitrogen concentrations. With certain assumptions including the constant adiabatic flame temperature regardless of additional nitrogen introduction and the heat sink property of added nitrogen, CAFT modeling was proved to be a powerful method to estimate the LFLs of fuel mixtures with additional nitrogen (except the flammability nose zone). Particularly, nitrogen dilution of LFL of fuel mixture is dependent on the heat capacities of nitrogen and oxygen. At the range of initial room temperature through final adiabatic flame temperature, nitrogen heat capacity is almost equal to that of oxygen. Therefore, the LFLs of all the selected hydrocarbons nearly stay constant, which is consistent with experimental observations

except the flammability nose zones. Because combustion mechanism at UFL conditions is different from that at LFL conditions, CAFT modeling loses its efficiency when the same assumptions were applied to the UFL case. The most possible reason is that the calculated flame temperature changes at different additional nitrogen concentrations.

Because Le Chatelier's law is the simplest and the most popularly used approach to estimate fuel mixture flammability limits. A theoretical derivation was proceeded and its applicability was verified at different conditions, e.g, fuel mixture with inert gas dilution, fuel mixture at varied oxygen concentrations, and at non-ambient initial status for fuel mixture system. The deriving work focused on LFL with the only assumption of constant flame temperature for pure fuels and the fuel mixtures during the flame propagation. Because of the high complexity of chemical kinetics of combustion at the UFLs, generalization of this law on UFL turns out to be impossible when applying the same reaction mechanism as did at LFL. This theoretical process indicated that Le Chatelier's law remains valid with inert gas dilution and at varied oxygen concentrations. Specifically, when the reaction system's initial temperature is neither too high (decomposition can be neglected) nor too low (no phase transition occurs), Le Chatelier's law still remains valid.

8.2 Future work

8.2.1 New flammability apparatus

So far, all the presented flammability data in this research focus on the ambient conditions, and the flammability apparatus available in this research was limited to ambient conditions, or those at low pressure and room temperature. However, the flammability properties at non–ambient conditions (e.g., different temperature and pressure) are extremely sought after for the chemical process industries. Because flammability limit is not an intrinsically fundamental property, experimental flammability always has the priority over the modeling prediction for accurate flammability purpose. Moreover, a more comprehensively numerical or theoretical analysis based on experimental flammability data requires a larger database including those at ambient as well as non-ambient conditions.

An innovative flammability apparatus is proposed in Figure 8.1. For a high temperature and pressure flammability feasibility, an 8 little spherical reaction vessel with maximum temperature and pressure up to 350 °C and 350 MPa is proposed here from Goethals work [97]. A high quality heater with reliable controls (e.g., heating rate) will be used to heat and control the fuel/air temperature inside the reaction vessel. To favor gas mixing in the reaction vessel, a magnetic stirring bar will be installed to create turbulence and speed stirring. Gas components can be loaded into the vessel through gas loading manifold, which is connected to different gas cylinders, and liquid components will be injected through the liquid syringe pump. The temperature and pressure gauges, including gas loading, fuel/air initial status settling, dynamic temperature and pressure

tracking, and the maximum temperature and pressure, are conducted through high-performance temperature and pressure sensors, which are located inside and outside of the reaction vessel.

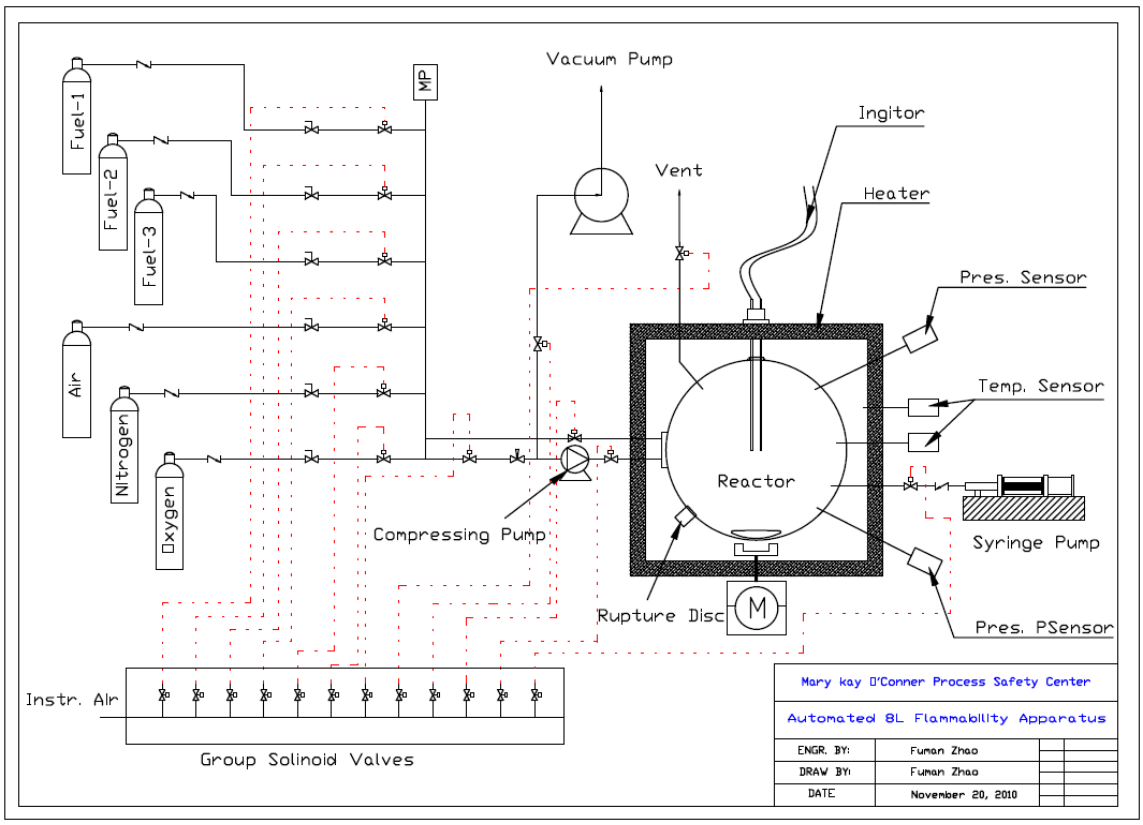

Fig. 8.1. Schematic representation of the new flammability apparatus.

Igniter system used in this new proposal is similar to that outlined in ASTM E 918-83 with the capable of inputting 10 J of energy. For a high efficiency purpose, here a multiple ignition source is proposed with 6 pieces of fuel wires. The ignition source is

a 10 mm piece of AWG 40 tinned copper wire, which is vaporized by a 500 VA isolation transformer at 115 V AC switched on with a zero-crossing solid state relay, and the current is delivered beginning at the zero point of each AC cycle. Figure 8.2 shows the igniter system circuitry.

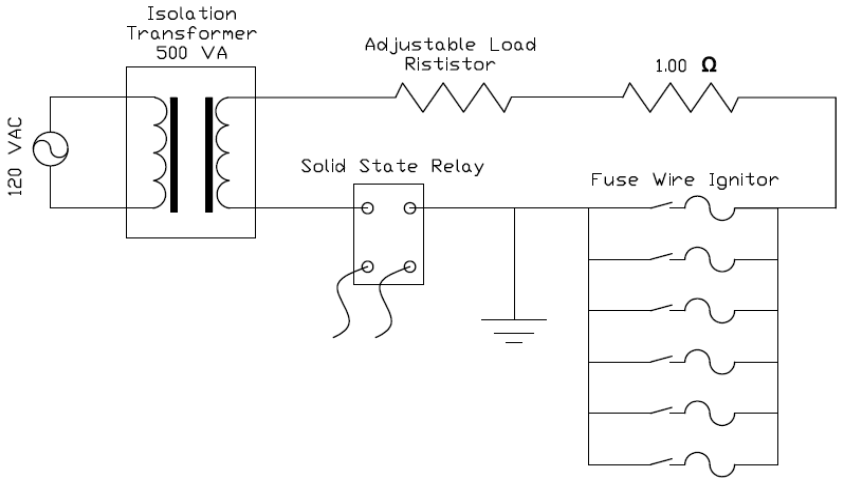

Fig. 8.2. Ignition system circuitry.

Additionally, the new flammability apparatus is proposed to be automated. That can be realized by using the actuated parts (e.g., solenoid valves, actuated valves) and LabVIEW controls for automatic data acquisition, and automatic operation including gas feeding, fuel mixture ignition, reaction product purging and venting.

The flammability detection criterion is the partial pressure rise. A 7% pressure rise is applied from the ASTM flammability testing standard, but it is fit for 1 L reaction vessel. Crowl [98] suggested a pressure rise range 5% -10 % for flammability limit

detection. The definite pressure rise value will be finally determined through experimental calibration using this apparatus.

8.2.2 Combustion simulation at UFL using CHEMKIN-CFD

As indicated from our current findings from this research, combustion at UFL condition becomes extremely complicated, and it turn out to be impossible to predict UFL accurately using simple reaction mechanism assumptions. To obtain accurate flammability data, experimental flammability are preferable; however, experimental measurement is always effort intensive, because flammability limit value changes with the external and internal test conditions, e.g., temperature, pressure, and also there exist numerous fuel mixtures. Therefore, a proper combustion program for UFL simulation is strongly sought after.

Theoretically, flammability limit is a heat balance feature with a critical flame temperature when flame propagates further. Specifically, the generated heat from combustion is absorbed by surroundings to raise the unreacted gas attached to flame front to the critical temperature, over which flame can propagate continuously. Therefore, a fundamental approach to solve UFL problem is to characterize fuel oxidation kinetics over a certain temperature range, as well as the dynamics of heat and mass transfer processes in a developing flame.

Modern chemical reaction program, CHEMKIN is already providing unparalleled simulation accuracy for commercial combustion and materials processing industries;

however, its accuracy is limited to some certain conditions, for example, a non-stable combustion. Combustion at flammability limits is a non-stable combustion, when reactor quenching effect becomes indispensible, the flammability limit from CHEMKIN simulation will deviate from experimental observation significantly.

The popularly used CFD simulation has many powerful benefits, but it is not well equipped to handle the accurate reaction mechanisms because it forces designers to sacrifice chemical accuracy for accuracy in geometry and flow. Typical CFD solutions can only handle global (single-step) reactions or a set of severely reduced chemical reaction steps.

Software CHEMKIN-CFD is a new, joint software program, and designed to couple detailed chemistry with third-party CFD codes. It extends the power of CHEMKIN into CFD, enabling the introduction of more accurate chemistry into reacting, fluid flow simulations. It possesses the capabilities to calculate kinetics and transport problems simultaneously other than only stiff differential equations.

Because the posed power from CHEMKIN-CFD and the combustion properties at flammability limits, it is extremely feasible to use CHEMKIN-CFD to predict UFL at different conditions.

REFERENCES

[1] B. Friedrich, The Explosion of TWA Flight 800, Chelsea House, Philadelphia, PA, (2002).

[2] G.D. De Smedt, D. De Corte, R. Notele, J. Berghmans, Comparison of two standard test methods for determining explosion limits of gases at atmospheric conditions, Journal of Hazardous Materials, A70 (1999) 105-113.

[3] J. Bond, Sources of Ignition, Butterworth-Heinemann Ltd, London, (1991).

[4] M.G. Zabetakis, Flammability characteristics of combustible gases and vapors, Bulletin 627, Bureau of Mines, Pittsburgh, PA, (1965).

[5] J.M. Kuchta, Investigation of fire and explosion accidents in the chemical, mining, and fuel-related industrial—A manual, Bulletin 680, Bureau of Mines, Pittsburgh, PA, (1985).

[6] G.A. Melhem, A detailed method for estimating mixture flammability limits using chemical equilibrium, Process Safety Progress, 16 (1997) 203-218.

[7] C.M. Shu, P.J. Wen, R.H. Chang, Investigations on flammability models and zones for o-xylene under various initial pressure, temperatures and oxygen concentrations, Thermochimica Acta, 392 (2002) 271-387.

[8] V. Babrauskas, Ignition Handbook, Fire Science and Technology Inc., Issaquah, WA, (2003).

[9] M.S. Mannan, Lees' Loss Prevention in the Process Industries, 3rd ed., Elsevier, Boston, (2005).

[10] C.V. Mashuga, D.A. Crowl, Application of the flammability diagram for evaluation of fire and explosion hazards of flammable vapors, Process Safety Progress, 17 (1998) 176-183.

[11] S. Besnard, Full flammability test of gases and gas mixtures in air, CERN Report, European Organization for Nuclear Research, (1996).

[12] L.G. Britton, Two hundred years of flammable limits, Process Safety Progress, 21 (2002) 1-11.

[13] H.F. Coward, G.W. Jones, Limits of flammability of gases and vapors, Bulletin 503, Bureau of Mines, Pittsburgh, PA, (1952).

[14] Y. Shoshin, L. Tecce, J. Jarosinski, Experimental and computational study of lean limit methane-air flame propagating upward in a 24 mm diameter tube, Combustion Science and Technology, 180 (2008) 1812-1828.

[15] A. Takahashi, Y. Urano, K. Tokuhashi, S. Kondo, Effect of vessel size and shape on experimental flammability limit of gases, Journal of Hazardous Materials, A105 (2003) 27-37.

[16] F. Clowes, B. Redwood, Detection and estimation of inflammable gas and vapor in air, Crosby Lockwood, London, (1896).

[17] G.W. Jones, W.P. Yant, L.B. Berger, The explosivity of hydrogen sulfide in air, Industrial & Engineering Chemistry Research, 16 (1924) 353-355.

[18] A.G. White, Limits for the propagation of flame in inflammable gas-air mixtures, Journal of Chemical Society, 125 (1924) 2387-2396.

[19] D. Conrad, T. Grewer, B. Hentschel, T. Redeker, Development of a standard method for flammability limits of vapor-air mixtures, 7th Int. Symposium on Loss Prevention and Safety Promotion in the Process Ind., European Federation of Chemical Engineering, Italy, (1992).

[20] M.G. Zabetakis, J. K. Richmond, The determination and graphic presentation of the limits of flammability of complex hydrocarbon fuels at low temperature and pressure, 4th symposium (international) on combustion, Williams & Wilkins Co., Baltimore, MD., (1953) 121-126.

[21] American Society for Testing and Materials, ASTM E681-09, Standard test method for concentration limits of flammability of chemicals (vapors and gases), ASTM International, West Conshohocken, PA, (2009).

[22] American Society for Testing and Materials, ASTM E918-83, Standard practice for determining limits of flammability of chemicals at elevated temperature and pressure, ASTM International, West Conshohocken, PA, (2005).

[23] American Society for Testing and Materials, ASTM E2079-07, Standard test methods for limiting oxygen (oxidant) concentration in gases and vapors, ASTM International, West Conshohocken, PA, (2007).

[24] American Society of Heating, Refrigerating and Air-conditioning Engineers (ASHRAE), Number designation and safety classification of refrigerants—third public review, BSR/ASHRAE Addendum “p” to ANSI/ASHRAE 34-1992, Atlanta, GA, (2000).

[25] V. Schroder, M. Molnarne, Flammability of gas mixtures Part 1: fire potential, Journal of Hazardous Materials, A121 (2005) 37-44.

[26] Y. Ju, H. Guo, K. Maruta, Determination of burning velocity and flammability limit of methane/air mixture using counterflow flames, Journal of Applied Physics, 38 (1999) 961-967.

[27] S. Kondo, K. Takizawa, A Takahashi, K. Tokuhashi, A. Sekiya, A study on flammability limits of fuel mixtures, Journal of Hazardous Materials, 155.3 (2008) 440-448.

[28] G. Ciccarelli, D. Jackson, J. Verreault, Flammability limits of NH3–H2–N2–air mixtures at elevated initial temperatures, Combustion and Flame, 144 (2006) 53-63.

[29] M. Hertzberg, The theory of flammability limits: conductive-convective wall losses and thermal quenching, RI 8469, US Bureau of Mines, Pittsburgh, PA, (1980).

[30] M. Hertzberg, The theory of flammability limits: radiative losses and selective diffusional demixing, RI 8607, US Bureau of Mines, Pittsburgh, PA, (1982).

[31] C.J. Hilado, A method for estimating limits of flammability, Journal of fire and flammability, 6 (1975) 130-139.

[32] A.A. Shimy, Calculating flammability characteristics of combustible gases and vapors, Fire Technology, 6 (1970) 135-139.

[33] V.T. Monakhov, Methods for studying the flammability of substances, National Bureau of Standards by Amerind Publishing Co., New Delhi, India, (1985).

[34] T. Suzuki, K. Koide, Empirical relationship between lower flammability limits and standard enthalpies of combustion of organic compounds, Fire and Materials, 18.5 (1994) 333-336.

[35] T. Suzuki, K. Koide, Correlation between upper flammability limits and thermochemical properties of organic compound, Fire and Materials, 18.6 (1994) 393-397.

[36] T. Suzuki, M. Ishida, Neural network techniques applied to predict flammability limits of organic compounds, Fire and Materials, 19.4 (1995) 179-189.

[37] W. Moller, P. Schulz, T. Redeker, Procedure for estimating flash points and lower explosions limits, Physikalisch-Technische Bundestanstalt Thermodynamik, PTB Report W-55, (1993).

[38] D. Dalmazzone, J.C. Laforest, J.M. Petit, Application of thermochemical energy hazard criteria to the prediction of lower flammability limits of hydrocarbons in air, Oil & Gas Science and Technology, 56.4 (2001) 365-372.

[39] F. Funk, Calculation of the lower explosivity limit of combustible gases and vapors, ChemTech, 26.12 (1974) 779-780.

[40] F.Y. Hshieh, Predicting heats of combustion and lower flammability limits of organosilicon compounds, Fire and Materials, 23.2 (1999) 78-89.

[41] F.Y. Hshieh, D.B. Hirsch, H.D. Beeson, Upper flammability limits of some organosilicon compounds, Fire and Materials, 28.6 (2004) 459-465.

[42] M. Miloshev, D. Vulchev, Z. Zdravchev, Relation between the concentration limits of flammability and physicochemical indexes of hydrocarbons, Godishnik na Visshiya Khimiko-Tekhnologicheski Institut, Sofiya, 27.3 (1982) 92-107.

[43] A.G. White, Limits for the propagation of flame in inflammable gas–air mixtures. Part III: The effect of temperature on the limits. Journal of the Chemical Society, 127 (1925) 672–684.

[44] A. Edgerton, J. Powling, The limits of flame propagation at atmospheric pressure II: the influence of changes in the physical properties, Proceedings of Royal Society, 193A (1948) 190-209.

[45] D.R. Stull, Fundamentals of fire and explosion, American Institute of Chemical Engineers, Now York, AIChE monograph series 73.10 (1977).

[46] J.G. Hansel, J. W. Mitchell, H. C. Klotz, Predicting and controlling flammability of multiple inert mixtures, Air Products and Chemicals, Inc. Prepared for Presentation at AIChE 25th Loss Prevention Symposium, Pittsburgh, PA (1991).

[47] C.V. Mashuga, D.A. Crowl, Flammability zone prediction using calculated adiabatic flame temperatures, Process Safety Progress, 18.3 (1999) 127-134.

[48] M.R. Brooks, D.A. Crowl, Flammability envelopes for methanol, ethanol, acetonitrile and toluene, Journal of Loss Prevention in the Process Industries, 20 (2007) 144-150.

[49] Y.N. Shebeko, W. Fan, I.A. Bolodian, V.Y. Navzenya, An analytical evaluation of flammability limits of gaseous mixtures of combustible-oxidizer-diluent, Fire Safety Journal, 37 (2002) 549-568.

[50] M. Vidal, W. Wong, W. J. Rogers, M.S. Mannan, Evaluation of lower flammability limits of fuel-air-diluent mixtures using calculated adiabatic flame temperature, Journal of Hazardous Materials, 130 (2006) 21-27.

[51] S.W. Benson, J.H. Buss, Additivity rules for the estimation of molecular properties. Thermodynamic Properties, the Journal of Chemical Physics, 29.3 (1958) 546-572.

[52] M.R. Reid, J.M. Prausnitz, B.E. Polling, The properties of gases and liquids, McCraw-Hill, Inc., New York, (1987).

[53] T.A. Albahri, Flammability characteristics of pure hydrocarbons, Chemical Engineering Science, 58 (2003) 3629-3641.

[54] W.H. Seaton, Group contribution method for predicting the lower and upper flammable limits of vapors in air, Journal of Hazardous Materials, 27.2 (1991) 169-185.

[55] Y.N. Shebeko, A.V. Ivanov, T.M. Dmitrieva, Methods of calculation of lower concentration limits of combustion of gases and vapors in air, The Soviet Chemical Industry, 15.3 (1983) 311-314.

[56] L.I. Nuzdha, M.A. Glinkin, E.E. Rafales-Lamarka, N.F. Tyupalo, A system for determining the upper explosive limit, The Soviet Chemical Industry, 11.4 (1979) 209-212.

[57] M.S. High, R.P. Danner, Prediction of upper flammability limit by a group contribution method, Industrial & Engineering Chemistry, 26.7 (1987) 1395-1399.

[58] S. Kondo, Y. Urano, K. Tokuhashi, A. Takahashi, K. Tanaka, Prediction of flammability of gases by using F-number analysis, Journal of Hazardous Materials, A82 (2001) 113-128.

[59] S. Kondo, A. Takahashi, K. Tokuhashi, Experimental exploration of discrepancies in F-number correlation of flammability limits, Journal of Hazardous Materials, A100 (2003) 27-36.

[60] S. Kondo, A. Takahashi, K. Tokuhashi, A. Sekiya, RF number as a new index for assessing combustion hazard of flammable gases, Journal of Hazardous Materials, A93 (2002) 259-267.

[61] F. Gharagheizi, Quantitative structure-property relationship for prediction of the lower flammability limit of pure compounds, Energy Fuels, 22 (2008) 3037-3039.

[62] F. Gharagheizi, Prediction of upper flammability limit percent of pure compounds from their molecular structures, Journal of Hazardous Materials, 167 (2009) 507–510.

[63] H. Le Chatelier, Estimation of firedamp by flammability limits, Annales des Mines, 19.8 (1891) 388-395.

[64] S. Kondo, K. Takizawa, A. Takahashi, K. Tokuhashi, Extended Le Chatelier's formula for carbon dioxide dilution effect on flammability limits, Journal of Hazardous Materials, A138 (2006) 1-8.

[65] S. Kondo, K. Takizawa, A. Takahashi, K. Tokuhashi, Extended Le Chatelier's formula and nitrogen dilution effect on the flammability limits Fire Safety Journal, 41.5 (2006) 406-417.

[66] S. Kondo, K. Takizawa, A. Takahashi, K. Tokuhashi, A. Sekiya, Flammability limits of five selected compounds each mixed with HFC-125, Fire Safety Journal, 44.2 (2009) 192-197.

[67] F. Zhao, W.J. Rogers, M.S. Mannan, Calculated flame temperature (CFT) modeling of fuel mixture lower flammability limits, Journal of Hazardous Materials, 174 (2010) 416–423.

[68] K.J. Liekhus, I.A. Zlochower, K.L. Cashdollar, S.M. Djordjevic, C.A. Loehr, Flammability of gas mixtures containing volatile organic compounds and hydrogen, Journal of Loss Prevention in the Process Industries, 13 (2000) 377-384.

[69] W.K. Wong, Measurement of flammability in a closed cylindrical vessel with thermal criterion, Ph. D. dissertation, Department of Chemical Engineering, Texas A&M University, (2006).

[70] D.S. Burgess, A.L. Furno, J.M. Kuchta, K.E. Mura, Flammability of mixed gases, Report of Investigations RI-8709, Bureau of Mines, Pittsburgh, PA, (1982).

[71] C.V. Mashuga, Determination of the combustion behavior for pure components and mixtures using a 20 L sphere, Ph. D. dissertation, Department of Chemical Engineering, Michigan Technological University, (1999).

[72] F. Zhao, W.J. Rogers, M.S. Mannan, Experimental measurement and numerical analysis of binary hydrocarbon mixture flammability limits, Process Safety and Environmental Protection, 87 (2009) 94-104.

[73] I. Wierzba, G.A. Karim, H. Cheng, The flammability of rich gaseous fuel mixtures including those containing propane in air, Journal of Hazardous Materials, 20 (1988) 303-312.

[74] D.M. Himmelblau, Basic Principles and Calculations in Chemical Engineering, Prentice Hall PTR, NJ, (2004).

[75] M.G. Zabetakis, S. Lambiris, G.S. Scott, Flame temperature of limit mixture. In: seventh Symposium (international) on Combustion, The Combustion Institute, Pittsburgh, PA, (1959) 484-487.

[76] C.C Chen, H.J. Liaw, T.C. Wang, C.Y. Lin, Carbon dioxide dilution effect on flammability limits for hydrocarbons, Journal of Hazardous Materials, 163 (2009) 795-803.

[77] C.C. Chen, T.C. Wang, H.J. Liaw, H.C. Chen, Nitrogen dilution effect on the flammability limits for hydrocarbons, Journal of Hazardous Materials, 166 (2009) 880-890.

[78] R. Chang, Chemistry, 9th ed., in: Thermochemistry, McGraw-Hill Inc., New York, (2007).

[79] D.A. Crowl, Understanding explosions, Center for Chemical Process Safety, AICHE, New York, (2003).

[80] C.V. Mashuga, D.A. Crowl, Derivation of Le Chatelier's mixing rule for flammable limits, Process Safety Progress, 19 (2000) 112-117.

[81] D. Drysdale, An introduction to fire dynamics, John Wiley and Sons, New York, (1985).

[82] ASHRAE, Designation and safety classification of refrigerants, ANSI/ASHRAE Standard 34-2007, Atlanta, GA, (2007).

[83] S. Kondo, K. Takizawa, A. Takahashi, K. Tokuhashi, J. Mizukado, A. Sekiya, Flammability limits of olefinic and saturated fluoro-compounds, Journal of Hazardous Materials, 171 (2009) 613–618.

[84] Y.A. Cengel, M.A. Boles, Thermodynamics: an Engineering Approach, 5th ed., McGraw-Hill Inc., New York, (2006).

[85] B. Martel and K. Cassidy, Chemical Risk Analysis: A Practical Handbook, Kogan Page Science, London, (2004).

[86] B. Hanley, A model for the calculation and verification of closed cup flash points for nulticomponent mixtures, Process Safety Progress, 17 (1998) 86-97.

[87] J.E. Hustad, Experimental studies of lower flammability limits of gases and mixtures of gases at elevated temperatures, Combustion and Flame, 17 (1988) 283-294.

[88] B. Lewis, G. Von Elbe, Combustion, Flames and Explosions of Gases, Academic Press, New York, (1987).

[89] F.J. Weinberg, The significance of reactions of low activation energies to the mechanism of combustion, Proceedings of Royal Society A (London), 230 (1955) 331-342.

[90] C.K. Westbrook, Chemical kinetics of hydrocarbon ignition in practical combustion systems, In Proceedings of the 28th International Symposium on Combustion, Edinburgh, UK, (2000) 1563-1577.

[91] R.D. Coffee, Cool flames and autoignitions: two oxidation processes, Journal of Loss Prevention, 13 (1980) 13-74.

[92] B. Vanderstraeten, D. Tuerlinckx, J. Berghmans, S. Vliegen, E. Van't Oost, B. Smit, Experimental study of the pressure and temperature dependence on the upper flammability limit of methane/air mixtures, Journal of Hazardous Materials, 56.3 (1997) 237-246.

[93] H. Wang, T.O. Hahn, C.J. Sung, C.K. Law, Detailed oxidation kinetics and flame inhibition effects of choloromethane, Combustion Flame, 105.N3 (1996) 291-307.

[94] K. Holtappels, V. Schroeder, A. Kobiera, P. Wolanski, M. Braithwaite, H.J. Pasman, Gas explosion safety characteristics and anomalies at unusual conditions,

In Proceedings of the 12th International Symposium on Loss Prevention and Safety Promotion in the Process Industries, Edinburgh, UK, (2007).

[95] R.A. Strehlow, Combustion Fundamentals, McGraw-Hill Inc., New York, (1984).

[96] C.K. Law, F.N. Egolfopoulos, A kinetic criterion of flammability limits: the C-H-O-inert system, Proceedings of the Combustion Institute, 23 (1990) 413–421.

[97] M. Goethals, B. Vanderstraeten, J. Berghmans, G. De Smedt, S. Vliegen, E. Van't Oost , Experimental study of the flammability limits of toluene–air mixtures at elevated pressure and temperature, Journal of Hazardous Materials, 70 (1999) 93-104.

[98] D.A. Crowl, Y.D. Jo, A Method for determining the flammable limits of gases in a spherical vessel, Process Safety Progress, 28 (2009) 227-236.

VITA

Name: Fuman Zhao

Address: Mary Kay O'Connor Process Safety Center, Division
Artie McFerrin Department of Chemical Engineering
Texas A&M University
College Station, TX 77843-3136

E-mail Address: zhaofuman@neo.tamu.edu

Education: B.S., Chemical Engineering, 1998
University of Tianjin, China

M.S. Environmental Engineering, 2006
Texas A&M University

M.S. Chemical Engineering, 2008
Texas A&M University

Ph. D. Chemical Engineering, 2011
Texas A&M University